

**Erosion and Stream sedimentation due to pipeline
construction in laterite soils
- Madagascar -**



Hasina Harivelo Andriamanamihaja Rakoto
Department of Civil Engineering and Applied Mechanics
McGill University, Montreal

December 2013

A thesis submitted to McGill University in partial fulfillment of the requirements
for the degree of Master of Engineering
©Hasina Harivelo Andriamanamihaja Rakoto, 2013

Abstract

Madagascar - Ambatovy region, AMBATOVOY Project - Sherritt International.

The Ambatovy Project, a mine for nickel and cobalt ore located in the centre of the country, required the construction of a slurry pipeline to transport the ore 220 km to be processed on the east coast. The pipeline and its maintenance road traverses primary forests, the sensitive Torotorofotsy Wetlands and include 172 stream crossings in sensitive laterite soils. The restoration and rehabilitation of the cut and fill geotechnical works and stream crossings is important technical works within the environmental portfolio and for project cost reductions.

The surface water erosion of the soil and the associated stream sedimentation are studied. These processes are classified based on the characteristics of the vegetation/land use, the slopes and the type of laterite soil. Three representative sites are chosen for a detailed study using field observations and field measurements (TSS in streams). These results are compared to numerical modeling results using RUSLE (Revised Universal Soil Loss Equation model) for surface erosion within GeoWEPP (Geo-spatial interface for Water Erosion Prediction Project), a USGS (US Geological Survey) –LESAM (Landscape-based Environmental System Analysis & Modeling) model which conducts continuous and process-based simulations of small watersheds, for soil erosion and sedimentation.

At the three selected sites, the use of GeoWEPP as a tool to explore possible mitigation measures using geotechnical engineering methods combined with revegetation is investigated and discussed. The results of these studies will be used to suggest measures to mitigate environmental impacts associated with the pipeline construction for the Ambatovy Project.

Résumé

Madagascar – région d’Ambatovy, Projet AMBATOVY - Sherritt International.

Le Projet Ambatovy, une mine de nickel et cobalt située au centre de l’île, a requiert la construction d’un pipeline de pulpe pour pouvoir transporter le minerai sur 220kms, pour pouvoir être acheminé et transformé sur la côte Est. Le pipeline et son réseau routier de maintenance traverse des forêts primaires, la sensible région du marais de Torotorofotsy et incluant 172 cours d’eau sensibles reposant sur le sol latéritique. La restauration et la réhabilitation des tranchées de remblai et déblai grâce aux travaux géotechniques sont d’importants travaux techniques pour les cours d’eaux notamment au niveau de l’impact environnemental et jouant sur la réduction des couts du projet.

Le phénomène de l’érosion de surface au niveau des cours d’eau et la sédimentation des rivières y associée ont été étudiés. Les processus sont classés sur base des caractéristiques de la végétation, de la pente et du type de sol latéritique. Trois sites représentatifs sont choisis aux fins d’une étude détaillée avec usage des données et observations de terrain (MES dans les rivières). Ces résultats sont par la suite comparés aux résultats avec usage des modèles numériques utilisant RUSLE (Revised Universal Soil Loss Equation model) pour l’érosion de surface dans GeoWEPP (Geo-spatial interface for Water Erosion Prediction Project), un modèle provenant de USGS (US Geological Survey) –LESAM (Landscape-based Environmental System Analysis & Modeling) qui conduit notamment des simulations en mode continu et sous base de processus pour les petits bassins versants, concernant l’érosion et la sédimentation.

Au niveau de ces trois sites sélectionnés, l’utilisation de GeoWEPP comme utile de prédiction et de « design » des mesures de mitigation possibles par usage de solutions d’ingénierie géotechnique combinée à la re-végétalisation ont pu être étudiés et comparés. Les résultats de ces études pourront être utilisés en tant que suggestion de mesures de mitigation des impacts environnementaux relatifs à la construction du pipeline du Projet Ambatovy.

Acknowledgements

The success of this study required the help of various individuals. Without them, the research would have been impossible and I might not meet my objectives in doing this study. I want to give gratitude to the following people for their invaluable help and support throughout its development:

To Jesus Christ, our Lord and Savior, for giving the wisdom, strength, support and knowledge in exploring things; for the guidance is helping surpass all the trials that the researchers encountered and for giving determination to pursue their studies and to make this study possible;

Special thanks to Dr Susan Gaskin, my understanding adviser, who was always there during the process of this thesis giving some advice and ideas to accomplish and improve this thesis; to her patience. Who was abundantly helpful and offered invaluable assistance, support and guidance. With your collaboration, my dreams become reality. From my heart, thank you.

To Dr Benoit Courcelles, for giving thoughts and ideas for improvement of the study;

To the Ambatovy Project for the necessary data and equipment used for this project. Many thanks to the personnel for their continuous help, especially to the Environment Department.

To my parents, for giving support and encouragement to pursue their study, for giving love;

To Feno, I love you.

Table of contents

Abstract	ii
Résumé	iii
Acknowledgements.....	iv
Table of contents	v
List of figures.....	viii
List of tables.....	x
Abbreviations.....	xi
Chapter 1. Introduction	1
Chapter 2. Literature review.....	6
2.1 Water erosion processes.....	6
2.2 Laterite soils.....	11
2.3 Sedimentation models.....	12
Chapter 3. Site presentation.....	19
3.1 General overview of the pipeline of Ambatovy Project	19
3.1.1 Land use	21
3.1.2 Topography	21
3.1.3 Geology and soil	22
3.1.4 Hydrology	23
3.1.5 The influence of social patterns on biodiversity	24
3.2 Representative sites characteristics.....	25
3.2.1 Category 1: Metamorphic rock, primary forest, steep mountain zone with steep slope	25
3.2.2 Category 2: Metamorphic rock, primary forest, steep mountain zone with gentle slope.....	26
3.2.3 Category 3: Granitic and gneiss rocks, primary forest, steep mountain zone	27
3.2.4 Category 4: Granitic and gneiss rocks, partial primary forest, steep mountain zone	27
3.2.5 Category 5: Granitic and gneiss rocks, partial primary forest, steep mountain zone with gentle slope.....	28
3.2.6 Category 6: Granitic and gneiss rocks, completely deforested area, semi-flat zone with gentle slope.....	28
3.2.7 Category 7: Granitic and gneiss rocks, completely deforested area, flat zone	29
Chapter 4. Methods.....	31
4.1 Criteria for selection of representative field study sites	31
4.2 Description of the three representative field sites.....	31
4.2.1 1st field site: Near the Ambatovy mine area.....	31
4.2.2 The second field site: midway along the pipeline	35

4.2.3	The third field site: near the plant site.....	39
4.3	<i>Methodology for sedimentation and sediment transport rates</i>	43
4.4	<i>Detailed description of the methods</i>	44
4.4.1	Field estimation of sediment load in streams.....	45
4.4.1.1	Measurement of TSS and analysis of data to get average TSS values.....	45
4.4.1.2	Sediment property measurements.....	46
4.4.1.3	Estimation of water discharge.....	48
4.4.1.4	Calculation of wash load transport rates (annual estimate from field data).....	52
4.4.2	Estimation of sediment loads calculated using GeoWEPP.....	53
4.4.2.1	GeoWEPP (Water Erosion Prediction Project).....	53
4.4.2.2	Model selection criteria and comparison.....	54
4.4.2.3	GeoWepp and Wepp Models parameter estimation and processing.....	56
4.4.2.4	Design of mitigation measures or alternative design for the field sites using GeoWEPP.....	60
Chapter 5.	Data analysis, results and discussion	61
5.1	<i>Data analysis</i>	61
5.2	<i>Field estimation of Sediment loads</i>	62
5.3	<i>Water discharge calculations</i>	67
5.3.1	Discharge estimated by the reference station method.....	68
5.3.2	Second methodology: Manning's equation.....	73
5.4	<i>Calculation of wash load transport rates (annual estimate) with the field data</i>	76
5.5	<i>Wash load using a full year hydrograph</i>	78
5.5.1	Modeling with GeoWepp.....	83
5.5.1.1	First field site: Ambatovy mine.....	83
5.5.1.2	The second field site: midway along the pipeline.....	85
5.5.1.3	The third field site: near the plant site.....	87
5.5.1.4	Detailed analysis of sedimentation rates at the field sites.....	89
Chapter 6.	Analysis and discussions	91
Chapter 7.	Mitigation measures	98
7.1.1	Risk evaluation.....	98
7.1.2	Mitigation procedures already executed by the Ambatovy Project during the construction phase.....	98
7.1.2.1	For the stream areas.....	98
7.1.2.2	For the upstream areas of the watersheds:.....	99
7.1.3	Mitigations designed using GeoWEPP.....	100
7.1.3.1	First field site mitigation proposal.....	100
7.1.3.2	Second field site mitigation proposal.....	101
7.1.3.3	Third field site mitigation proposal.....	102
7.1.3.4	Summary report of the GeoWEPP sedimentation simulations for the mitigative proposals.....	103
Chapter 8.	Conclusion	105

REFERENCES	107
APPENDIXES	112
I. Appendix A	112
II. Appendix B: Ambatovy standards for TSS	116
• Laboratory procedures for the TSS estimation	119
III. Appendix D: Models details	120
III.1. HSPF details	120
III.1.1. Data requirements	122
III.2. GeoWEPP details	123
III.3. SWAT (Soil and Water Assessment Tool) details	124
IV. Appendix E:	128
IV.1. Soil's characteristics	128
IV.2. Cross- section pictures	128
V. Appendix F.....	130
V.1. Sedimentation of the first field site	130
V.2. Sedimentation of the second field site	131
V.3. Sedimentation of the third field site	132

List of figures

Figure 1. Sheet erosion on the pipeline route in Ambatovy, in the vicinity of the mine, 2009	8
Figure 2. Example of interrill erosion process along the pipeline route of Ambatovy	9
Figure 3. Example of rill erosion in the pipeline route of Ambatovy, 2009.	9
Figure 4. Example of gully erosion process along the pipeline route of Ambatovy, 2010.....	10
Figure 5. Example of land slide in a typical hill in Madagascar.....	10
Figure 6. Ambatovy Project situation map	20
Figure 7. The pipeline route from the mine to the plant site area	21
Figure 8. Monthly average rainfall for Moramanga and the port at Toamasina region.....	24
Figure 9. Bank stabilization	26
Figure 10. Stream crossing using a culvert.....	26
Figure 11. A stream crossing from the fifth category.	29
Figure 12. A watershed of the seventh category	30
Figure 13. A stream with its infrastructure for the seventh category.....	30
Figure 14. First field site localisation	32
Figure 15. The beginning of deforestation around the village of Berano.	33
Figure 16. The geomorphology and the vegetation of the first field site.	33
Figure 17. The first field site's particle size distribution.....	34
Figure 18. The second field site study location.	36
Figure 19. (a). Aerial photo of the second field site. View from the top	37
Figure 19. (b) . Aerial photo of the second field site. View for the north.	37
Figure 20. Pipeline route around the field site two.	38
Figure 21. Soil particle distribution of the second field site.	39
Figure 22: The third field site location	40
Figure 23. Third field site: near the coastal region.....	41
Figure 24. A view near the watershed outlet of field site three during the construction phase.....	42
Figure 25. Particle size distribution of the third field site	43
Figure 26. Stream gauging and weather station at the first field site near the mine.....	51
Figure 27. Stream gauging and weather station at the third field site near the plant	52
Figure 28. TSS and turbidity values for the Ambatovy mine site case	64
Figure 29. TSS and turbidity correlation for the 1 st study case	64
Figure 30. TSS and turbidity values for the 2 nd study case, RoW 08-09.	65
Figure 31. TSS and turbidity correlation for the 2nd study case.....	66
Figure 32. TSS and turbidity values for the 3 rd study case, RoW 13-14.....	67
Figure 33. TSS and turbidity correlation for the 3rd study case	67
Figure 34. Water discharges for the first field site	70
Figure 35.a) Annual average water discharges	71
Figure 35.b) Total monthly discharges.....	71
Figure 36. Water discharges for the second field site	71
Figure 37. a) Annual average water discharge	72
Figure 37. b) total monthly discharges	72
Figure 38. Water discharges for the third field site.....	72
Figure 39. a) Annual average water discharges	73
Figure 39. b) Total monthly discharges.....	73

Figure 40. TSS values versus Water discharge values for the first field site.	79
Figure 41. TSS values versus water discharges for the second field site.....	79
Figure 42. TSS values and water discharges for the third field site.	80
Figure 43. Monthly wash load data for each field site.	81
Figure 44. Daily wash load data for the three field sites.	82
Figure 45. The vegetation cover and DEM of the first field site.	84
Figure 46. Simulation results for the Ambatovy mine field site	85
Figure 47. The vegetation cover and DEM of the second field site study.....	86
Figure 48. Simulation results for the second field site	87
Figure 49. DEM and vegetation cover of the third field site.....	88
Figure 50. Simulation results for the third field site.....	89
Figure 51. Graphical presentation of average discharge values at the three field sites using the three methods.	92
Figure 52. Example of mitigation done for large width channel and sensitive streams.....	99
Figure 53. Simulation results after the mitigation process for the first field site	101
Figure 54. Simulation results after the mitigation proposal for the second field site.....	102
Figure 55. Simulation results after the mitigation process for the third field site	103
Figure 56. From Chaudhry, 2008.....	128
Figure 57. From the 1st field site	128
Figure 58. From Chaudhry, 2008.....	129
Figure 59. From the 3rd field site	129
Figure 60. From Chaudhry... ..	129
Figure 61. From the 2nd field site.....	129

List of tables

Table 1. Annual average rainfall data for the plant site and the mine	24
Table 2. Water quality parameters at field site one during the construction phase.....	35
Table 3. Water quality parameters for site 2 in the central region of the pipeline.....	39
Table 4. Water quality parameters for site 3 near the coast.....	43
Table 5. Land use and elevation range comparison of the main catchments to its sub-catchments	68
Table 6. Water discharge by using the reference station methodology	69
Table 7. Calculated gradients with different lengths for each field case.	74
Table 8. Water discharge calculations using the Manning’s equation.....	75
Table 9. Annual Average wash load rates estimated from the field data.....	76
Table 10. Estimation of the sedimentation rates for each site.....	82
Table 11. Average water discharge through the 2 methodologies	82
Table 12. GeoWEPP reports of erosion loss parameters for the 3 cases of study.....	89
Table 13. Average water discharge through the 4 methodologies	91
Table 14. Comparison of the difference of each method from the average value.....	92
Table 15: A comparison of the sedimentation rates estimated using field data and GeoWEPP	94
Table 16. The different kind of risks related to the parameters of slope, vegetation and sensitivity	98
Table 17. GeoWEPP simulation reports of erosion loss parameters after mitigation proposals.....	104
Table 18. 1 st site physical hydrology parameters data sampling results.....	112
Table 19. 1 st site physical hydrology parameters data sampling results: TSS and turbidity	112
Table 20. 2 nd site physical hydrology parameters data sampling results: TSS and turbidity	113
Table 21. 2 nd site physical hydrology parameters data sampling results: TSS and turbidity	113
Table 22. 3 rd site physical hydrology parameters data sampling results	114
Table 23. 3 rd site physical hydrology parameters data sampling results: TSS and turbidity	114
Table 24. Wash load calculations from the full year hydrograph	114
Table 25. Wash load calculations from the full year hydrograph	128
Table 26. Wash load calculations from the full year hydrograph	130
Table 27. Wash load calculations from the full year hydrograph	131
Table 28. Wash load calculations from the full year hydrograph	132

Abbreviations

A:	area of the cross section [m^2]
Ca :	concentration
d :	sediment particle diameter [mm]
D :	Water depth [m]
Ea:	amount of evapotranspiration on day i [mm H ₂ O]
g:	Gravitational acceleration, 9.81 [m/s^2]
n:	Manning coefficient
Q:	water discharge [m^3/s]
Q _{bv} :	water discharge of the area of study [m^3/s]
Q _{gw} :	amount of return flow on day i [mm H ₂ O]
q _r :	specific water discharge [$m^3/s/km^2$]
R:	hydraulic radius [m]
R ² :	coefficient of correlation
R _{day} :	amount of precipitation on day i [mm H ₂ O]
S:	longitudinal channel slope [m/m]
S :	Energy slope [m/m]
S _{BV} :	watershed area for the study [km^2]
t :	time [days]
T:	Temperature [°C]
W _{seep} :	water amount entering the vadose zone from the soil profile on day i [mm H ₂ O]
X :	Rate of suspended sediment transport [g/l]
AMBATOVOY:	Name of the project from Sherritt International Company in Ambatovy region, Madagascar
AnnAGPS :	Agricultural Non-Point Source Pollution model

ASCII:	American Standard Code for Information Interchange
BOD:	Biochemical Oxygen Demand
CLIGEN:	stochastic weather generator for USA regions used in WEPP
CREAMS:	Chemical, Runoff and Erosion from Agricultural Management Systems model
DEM:	Digitalized Elevation Model
EPA:	US Environmental Protection Agency
EPIC:	Erosion Productivity Impact Calculator
EUROHARP:	European Harmonised Procedures for quantification of nutrient losses from diffuse sources (EU project)
EUROSEM:	European Soil Erosion Model
FTM:	Foiben-Taosarintanin'I Madagasikara
GeoWEPP:	Geo-spatial interface for WEPP
GIS:	Geographic Information System
GLEAMS:	Groundwater Loading Effects of Agricultural Management Systems model
GPS:	Global Positioning System
HSPF:	Hydrological Simulation Program—Fortran model
KINEROS2:	KINEmatic runoff and EROSIon model
LESAM:	Landscape-based Environmental System Analysis & Modeling
Mukey:	Soil file type for USA used in some USGS data
MUSLE:	Modified Universal Soil Loss Equation model
NTU:	Nephelometric Turbidity Unit
ONE:	Office National pour l'Environnement (Madagascar)
ORP:	Oxydation reduction potential
ORSTOM:	Office de la recherche scientifique et technique outre-mer
PESERA:	Pan-European Soil Erosion Risk Assessment model
ppm:	parts per million
PRISM:	Parameter-elevation Regressions on Independent Slopes Model

Rock:Climate : data base of meteorological data of USA

RoW: Right of Way

RUSLE: Revised Universal Soil Loss Equation model

SPEROS: Soil Properties and Erosion model

SWAT: Soil and Water Assessment Tool

SW_t : final soil water content [mm H₂O]

SW_0 : initial soil water content on day i [mm H₂O]

TDS: Total Dissolved Sediment [mg/l]

TIN: Triangular Irregular Networks

TSS: Total Suspended Solids [mg/l]

USDA: US Department of Agriculture

USGS: US Geological Survey

UTM: Universal Transverse Mercator

Chapter 1. Introduction

Soil-erosion and sediment-deposition have long been among the major environmental problems affecting the ecosystems and habitats of forests and rivers. Erosion issues are predominantly due to forest clearance, changes in the vegetation or climate change. When soil erosion takes place, irreversible processes happen in the watershed such as the sedimentation of the rivers, the decrease in infiltration of rainfall, the reduction of the protective cover of the vegetation resulting in drought conditions, increased aridity and finally a progression to a desert-like climate. These processes are the similar in all parts of the world independent of the type of vegetation and the type of the soil. Fortunately, some countries, but not all, have more opportunities to change or modify the processes and to prevent or reduce the problems due to the type of soils, due to the strength of their economy and due to the involvement of their population.

For decades, scientists and researchers have investigated this problem, trying to understand the phenomenon and to develop solutions to reduce the erosion processes. The US Department of Interior and the Agricultural Sector have thoroughly examined the different kinds of erosion processes and the resulting sedimentation, and have developed predictive empirical equations and models. Many countries, from China to Australia, have also studied the problem in a similar manner. Governments, institutions and international agencies have also provided support and resources to reduce the problems through environmental programs and actions which have been widely implemented across the world.

Madagascar, a very beautiful island with a wide range of endemic species, also experiences erosion and sedimentation problems. As far as Madagascar is concerned, erosion-issues are related to the economic development of the country. Unfortunately, Madagascar is a poor country. For the Malagasy people, the main source of livelihood, for a large majority of the population, is agriculture. Vanilla and litchis are the main export crops. However, Malagasy farmers have to address the endemic character of their ecosystem. Most of the fauna and flora

are endemic, and a great variety of species have been declared at risk due to deforestation and soil- erosion problems resulting in part from agriculture.

The erosion problem in Madagascar has also been declared unique due to the process of lavakisation, i.e. the soil-erosion is due to lavaka. “Lavaka” is a Malagasy word which means hole, and the “lavakisation” process means erosion producing large holes, a process endemic to Madagascar. The process of “lavakisation” is specific to laterite soils in the southern hemisphere and in a tropical climate.

Earlier studies on Malagasy soil-erosion have prompted international environmental Institutions to elaborate programs to help both the economy and the people, and also to reduce the impacts of erosion and sedimentation. In addition, these programs will help the country to fight against climate change and to aid in carbon sequestration.

The Eastern region of Madagascar, where the weather is very wet and the rainfall is abundant, supports perennial and green forests. The forests and the rivers also abound with endemic species. However, currently, due to deforestation, this perennial forest is being reduced and both the habitat and the species within this habitat are becoming endangered. The sedimentation in the rivers is greater than the natural rate, cyclones are becoming more intense and therefore more destructive for the entire ecosystem due to the accompanying floods; the vegetation, a green and perennial forest, is being replaced by a fifth year forest with bushes and grass; the endemic species have been disappearing and being replaced by exotic species. These problems are taking place in Madagascar because of economic problems, lack of communication and corruption with the net result being forest clearance and the resulting physical problem of soil erosion.

Nevertheless, there are still some regions of the green forests which are intact and actions are required to protect them for a better future. Help is needed for this paradise-like country.

From one point of views, because Madagascar is a poor country, the establishment of the Ambatovy Project, an international nickel-cobalt mining project, should be a good help for the

economy and for the people. Ambatovy is being established in the Eastern region of Madagascar, from the Moramanga region to the Toamasina region, and the development of the project requires one open mine, an ore processing plant site, and a pipeline 228 km long to transport the ore from the mine to the plant.

Ambatovy approached the mine project with the development of programs to address challenges and to implement concrete actions in terms of engineering, the environment and to fulfill their social duties. The environmental actions started with baseline studies undertaken before the beginning of the project. These responsibilities have been executed in three main areas: the mine, the pipeline area and the plant site.

This study focuses on the pipeline, 228 km long, which traverses different ecosystems, and where the environment is already changing ecologically and anthropologically. Three different field sites, representing a range of environmental impact through a range of vegetation type, slope, geotechnical properties, soil type and precipitation, will be investigated and discussed, in terms of the erosion and sedimentation problems.

The aim of the study is to understand the erosion processes in the Eastern regions of the island of Madagascar and to find mitigation solutions to reduce the erosion processes. For each field site, estimations of sedimentation and erosion processes have been developed using two different methods:

- The first methodology estimates sedimentation rates using field data. Field measurements of TSS combined with an estimation of water discharge provide an estimate of the sedimentation rate in the catchment.
- The second methodology uses the GeoWEPP model to estimate the sediment load supplied to the water course based on land characteristics (vegetation, geotechnical properties of the soil and catchment slope;
- Lastly GeoWEPP is explored as a tool to design remediation and mitigation options. Its usefulness as a tool is discussed as are the possible options, which include alternative vegetation in some areas of the sub-catchments, modification of slopes associated with

the geotechnical engineering required and finally - if required – modification of the soil or use of geo-engineering materials.

For each representative field site, the data used were collected before the beginning of this research study. This data includes the weather data and the in-situ field data of total suspended solids. The other parameters required to characterize the site, such as the geotechnical properties of the soil, the type of soil and the vegetation cover, were obtained from previous studies. The literature has been surveyed to establish existing knowledge about data collection, environmental regulations, environmental processes and erosion processes in other countries.

Physically based models are important because they are an effective approach to provide good estimates where field data is scarce. Empirical equations developed in the northern hemisphere must be applied with caution in the southern hemisphere where few field studies have been done to validate the equations. Therefore, for Madagascar physically based models are postulated to provide better estimates than empirical models.

The physically based model GeoWEPP has been chosen, from among the different models, as it may be able to represent forested areas as a land use and it has been previously applied in tropical regions having with laterite soils. GeoWEPP was assessed as being the most appropriate model, after consideration of other models and their capabilities, which are also presented.

The GeoWEPP model is also explored as a possible tool to recommend possible mitigation solutions for the future, an important aim for each representative field site.

The remainder of the report is organized into 5 sections.

Chapter 2 presents the literature review of the erosion processes, the laterite soils and the sedimentation models. Chapter 3 describes the site, in terms of its geography, topology, soils, regional hydrology and hydrological parameters, land uses and vegetation. The next section, Chapter 4, presents the methods including the criteria for selection of representative field study sites, a description of the three representative field sites and a detailed description of the methods. Chapter 5 discusses the data analysis and presents the results. Chapter 6 provides a

discussion of the results. Chapter 7 presents possible solutions to mitigate the erosion and sedimentation in the field sites. Lastly Chapter 8 summarizes the conclusions from the research

Chapter 2. Literature review

This literature review explores the three dominant themes of the research: water erosion processes, laterite soils and soil erosion models. These three themes, related to each other, needed to be considered for the field site of the Ambatovy Mine Project in Madagascar. The review covers erosion processes in general, erosion processes in Madagascar and reviews similar studies in lateritic soils. In addition, physically based models of erosion processes will be also reviewed.

2.1 Water erosion processes

Erosion by water is the most important components of basin soil erosion. Soil erosion dynamics (or mechanics) are the processes resulting in the erosion or movement of soil in the downslope direction. Understanding them is key for the prevention of soil and water loss and development of physical models used to design actions to reduce soil erosion.

Natural processes such as the production of soil occur at an alarmingly slower rate than the rate at which soil can be lost. It is estimated that over 3 billion metric tons of soil are eroded from our fields and pastures each year by water erosion alone (NSERL, 2002).

When fertile soil is removed, the organic matter which is important for plant and crop-growth is also lost (Hodges, 1995). The organic matter in soil increases water infiltration, moisture retention and erosion resistance. It plays an important role in the soil's physical structure and for the establishment of a microclimate. It is a source of nutrients for the plants. Without this soil, plants and crops would not survive. The effect is compounded as a reduction in the vegetation cover will expose the soil more to the detrimental effects of wind and water erosion. In agriculture conservation tillage is used to control sheet and rill erosion. In addition, vegetated waterways can be very important in small watersheds in which water flows from hill slopes to concentrate in natural drainage ways which otherwise can cause significant gullying (NSERL, 2002).

The main variable affecting water erosion is precipitation in the form of rainfall or snowfall (NSERL, 2002). Precipitation is part of the hydrologic cycle in which moisture in the atmosphere condenses and falls to earth as rain (or snow). Precipitation creates runoff when the rainfall rate exceeds the infiltration rate or when the ground is saturated. In addition, when the runoff is intense, especially when the overland flow is intense, the soil has a low infiltration rate. When there is poor aggregate stability or poor vegetative cover, the sediments are detached from the soil and the erosion phenomenon starts (NSERL, 2002).

Rain, the most common form of precipitation, can be very destructive when the raindrops strike bare soil. With impacts of over 32 km/hr, raindrops splash grains of soil into the air and can also wash out seeds (NSERL, 2002). As water accumulates on the surface of the soil, it will start to flow downhill as overland flow or surface runoff. The overland flow then carries away the detached soil, and may detach additional soil particles or sediments which can be deposited elsewhere. This is called *sheet erosion* (NSERL, 2002). Figure 1 presents an example of sheet erosion on the pipeline route in the vicinity of the mine area.

When overland flow is concentrated, it results in erosion processes called *gully erosion* (NSERL, 2002). Very severe types of erosion by water are landslides, which are initiated when the soil becomes fully saturated resulting in a lower effective shear stress and slope failure (FAO, 1991).

Precipitation mainly generates sheet and gully erosion (KERSTÉZ, Hungarian Geographical Bulletin, 2009). Sheet erosion removes a fairly uniform layer of soil in thin layers by the forces of both the raindrops and the runoff. This erosive process can cover large areas of sloping land and go unnoticed for quite some time. Either soil deposition at the bottom of a slope, or the presence of light - colored subsoil appearing on the surface permits its recognition. If it is unnoticed, sheet erosion will gradually remove the topsoil, the nutrients and the organic matter, which are important to agriculture and eventually lead to unproductive soil (NSERL).



Figure 1. Sheet erosion on the pipeline route in Ambatovy, in the vicinity of the mine, 2009

Interrill flows also produce the removal of a fairly uniform layer of soil on a multitude of relatively small areas by raindrops which strike exposed soil and detach the soil particles and splash them into the air and into shallow runoff (Gentile, 2002). It appears that the raindrops striking these shallow flows can enhance the flow's turbulence and help to transport more of the detached sediment to a nearby rill or flow concentration. The deposit of interrill sediment to the rill channels is a function of the slope, vegetative cover, soil surface erodibility and surface roughness (NSERL, 2002). Figure 2 shows an example of interrill erosion on the pipeline route.



Figure 2. Example of interrill erosion process along the pipeline route of Ambatovy.

Rill erosion is the removal of soil particles by concentrated water running through little streamlets, or channels which are less than 300mm depth (NSERL, 2002). Soil particle detachment in a rill occurs due to concentrated runoff. If the process of detachment continues or the surface runoff increases, rills may become wider and deeper (NSERL, 2002). Rill erosion is one of the most common forms of erosion, as shown in Figure 3.



Figure 3. Example of rill erosion in the pipeline route of Ambatovy, 2009.

Channel erosion is the largest concentration of the flow into a flow path for water for surface runoff which leaves a field or a watershed (Smith, 2005). The resulting waterways from the channel erosion may be permanent or may be tilled across. Erosion in channels is mostly caused by downward scour due to flow shear stress. Channel erosion is the first stage in development of a classical gully .

Classical gully erosion is an advanced stage of channel erosion, defined as when the channel erosion is too large and too deep, to cross (NSERL, 2002). After a rainfall event, this type of channel can carry large amounts of water and deposit eroded material and particles at the foot of the gully (NSERL, 2002). Figure 4 shows an example of gully erosion in the middle section of the pipeline route.



Figure 4. Example of gully erosion process along the pipeline route of Ambatovy, 2010.

When the underlying layers of soil are saturated and more erodible than the other layers, landslides and mass failures occur (NSERL, 2002). The water infiltrating from the surface can saturate the soil reducing the effective shear stress and enabling the outer layer of soil to slide downslope (Thiebes, 2012). The gravitational forces cause the mass to slide rapidly to the foot of the hill or the bottom of the gully. Figure 5 presents an example of a land slide.



Figure 5. Example of land slide in a typical hill in Madagascar.

2.2 Laterite soils

The word laterite is used widely in the literature to describe soils in tropical and subtropical regions of the world. This general term is often used to describe a range of morphological, physical and chemical states. Laterite formations involve the redistribution and concentration of sesquioxides in the soil profile (Sherman,1949). They are classified as "Ultisols" and "oxisols" in the classification system of the Department of Agriculture U.S. (United States Department of Agriculture, USDA) (Whitmore T.J., 1975).

Laterite soils are the result of intense weathering in tropical and sub-tropical climate regions, (Gidigas, 1972, 1976). The properties of these soils are quite different from the soils of temperate and cold regions. The dissimilarities are particularly pronounced for the soil's geotechnical properties.

Laterite soils are specific soils known to be difficult to rehabilitate and to manage after the execution of civil engineering works (Achankeng, 2003). Studies of the geotechnical properties of laterite soil reveal the following properties:

- Low compressibility or even incompressibility, despite the existence of high consolidation pressure and the non-influence of clay regarding the soil's compressibility. (Mahalinga-lyer, 1994).
- Fair shear strength in the compacted state and a high angle of shear resistance. Thus, the lateritic soil has a high density, a good interlocking at the macro-level and a bonding micro-structure due to the sesquioxide coating and the micro-voids. (Mahalinga-lyer, 1994).
- Good drainage (Arulanandan, 1968).
- Good effective cohesion intercepts. The cohesion parameter, explained by the edge to face flocculation, is also due to potassium ion bonding, to drying or to natural cementation by carbonates and iron compounds. (Lambe and Kikuchi, 1960).
- The above geotechnical properties are not sensitive to remoulding. (Lumb, 1966).

As described in USDA (1975), by Aubert G. (1954) and Maignien (1966), the term laterite soil is indicative of:

- materials which are rich in iron oxides and / or aluminum
- soft mottled clays which could irreversibly change into shells or become armor hardened when exposed to alternating humidity and drought
- concretions or nodules in a matrix of consolidated and unconsolidated materials
- a combination of physical and chemical phenomena due to extreme alteration of the bedrock.

Laterite soils can be used for base / sub-base construction because they are easy to manipulate for the road surface. For the pavement structure, the behavior of laterite soils is dependent on the particle-size distribution, the nature and the strength of the gravel particles (pisoliths), the degree of compaction and the environmental conditions. (Fossberg 1963, Remillon 1955).

According to Ackroyd (1963, 1967) and Vallerga (1969), the stability of laterite soil depends on factors such as the content of sesquioxides, the limit slope related to the rate of sesquioxides, the surface of unsaturated soil in the slope section, the depth of moisture and the degree of weathering. From these factors, they state that it is conceivable to estimate the soil surface that could be affected by water erosion processes.

2.3 Sedimentation models

Various approaches and equations for risk assessment or predictive evaluation of soil erosion by water are available in the literature. For example, the universal soil loss equation (USLE) was developed to assess soil erosion by water. (Wischmeier and Smith, 1960). Soil erosion data were collected from 8000 communities in 36 regions in 21 states in the US, and were analyzed and assessed for the range of factors contributing to soil erosion.

USLE predicts the long-term average annual rate of erosion on a field slope based on rainfall pattern, soil type, topography, crop system, and management practices. The implementation of USLE relies on a survey of slope surface. Subsequently over 10 years, more comprehensive

research on soil erosion by water was conducted. By including additional data and incorporating recent research results, the USLE methodology has been improved and therefore, a modified version of USLE has been presented. In the new version, MUSLE (Modified Universal Soil Loss Equation model), soil erosion can be predicted more accurately (Yoder and Lown, 1995). Furthermore, based on the basic idea of the USLE approach, a predictive equation is constructed. To generalize the application, the slope factor was changed to a regional factor to represent regional topography. This was validated in a soil erosion study in the Three Gorges region of the Yangtze River.

With the integration and application of statistical approaches and georeferential information system (GIS) techniques, specific quantitative models, which can assess and predict the soil erosion, are available. Moreover, using remote sensing (RS) data a quantitative method based on GIS is widely applied. In the early 1980s, the implementation of such methods used to establish a prediction model for soil erosion in each sub-area of a study area in China and therefore, permit the prediction of the trend of soil erosion for the whole area. (Lin, 1980).

It should be noted that soil erosion is a complex process influenced by many factors and investigators face great challenges in quantifying the relationships between soil erosion and its influence factors. Currently quantification of soil erosion is a process requiring complex and unstructured decisions. As a result, an integrated and systematic approach should be implemented. Although there is an understanding of the physical processes by which soil erosion takes place, many models have been established- based on either empirical approaches or statistical methods, and therefore significant uncertainty in the predictive simulations could result, particularly when applied to other climatic/geologic regions.

For risk assessment using models of soil erosion, standard modeling techniques including model calibration, model validation, and model refinement, can be incorporated to facilitate the reduction of the model uncertainty by using observed field data of soil erosion. A framework for risk assessment of soil erosion by water using an integrated and systematic approach has been implemented by Wu (2007).

Physical models have been developed and tested to predict the effects of rainfall erosion. Modeling is an important instrument for erosion scenario assessment (Moehansyah et al, 2004). Erosion and sediment yield can be assessed with the use of two main types of models: empirical and physically based models.

The first group of models is established based on the recognition and calculation of relationships between parameters. These relationships must be statistically important.

Physically based models consist of a description of the processes involved described using mathematical equations and considering the laws of conservation of momentum, energy and mass (Morgan, 2005).

The USLE⁺ (Wischmeier and Smith, 1978), RUSLE (Revised Universal Soil Loss Equation model - Renard et al., 1991), MUSLE are models based on a single event basis, which means a simulation for just one period or event. EPIC (stands for Erosion-Productivity Impact Calculator- Williams, 1985) is a lumped model assuming, a spatially homogeneous uniform hillslope. Nevertheless, it is possible to apply EPIC models to more complex terrain (e.g. Foster and Wischmeier, 1974; Desmet and Govers, 1996). GLEAMS and CREAMS (Chemical, Runoff and Erosion from Agricultural Management Systems model, Knisel, 1991) are both field-scale models that assume that a linked system of interrill and channel elements adequately represents the area of erosion.

The more recent WEPP (Flanagan et al., 2001), KINEROS2 (KINEmatic runoff and EROsion model - Smith et al., 1995) and EUROSEM (European Soil Erosion Model - Morgan et al., 1998) are models which adopt a similar element-based scheme. In terms of process descriptions, the models evolved from rainfall based erosion prediction, via Soil Conservation Service Curve-Number-based runoff estimations, to a more physically based water balance approach.

With the emergence of computing power and GIS capabilities, spatially distributed catchment models have been developed with simulation of the runoff and erosion dynamics of larger and more complex catchments. The potential advantages of these models are the possibility of the identification of source and sink areas of water, sediment and associated chemicals within a

catchment. Soil conservation measurements could be designed to prevent the problem whenever it occurs, for example to minimize the runoff, to mitigate the increase in the sediment discharge and chemicals which leave the catchment.

The models mentioned above are adapted to the catchment scale by increasing the number of elements and using a combination of special elements such as channels and ponds, whereas models such LISEM (De Roo et al., 1996; Jetten and De Roo, 2001), EROSION 3D (Schmidt et al., 1999), ANSWERS (Beasley et al., 1980), TOPMODEL (Beven and Freer, 2001) and MIKE-SHE (Refsgaard and Storm, 1995) are based on a regular grid of equal-sized raster cells.

All the cited models are based on a water and sediment balance that produces runoff and (suspended) sediment for each spatial element, which is then routed towards the outlet using a kinematic wave routine. Although, in principle, this approach allows one to provide the user with a distributed image of the runoff and erosion, the models are mostly used to calculate the discharge and soil loss from a catchment at only one point: the outlet. The majority of results reported in the literature are outlet based, where both simulated hydrographs and sedigraphs are compared to measured data, or the models are used to predict future events. Likewise, the majority of the models' tests and sensitivity analyses deal with the outlet-based data only (Jetten et al., 2003).

There are surprisingly few studies that compare simulated erosion patterns with observed erosion patterns. This is not only true for soil erosion models: Beven (2002, 2006) states that there are also very few validations of distributed predictions against distributed measurements in runoff, subsurface flow and groundwater modeling. (Jetten et al., 2003).

At the same time, many researchers report the phenomenon of "predicting the correct result for the wrong reasons", the prediction of acceptable soil loss and discharge with an incorrect (sometimes completely wrong) pattern of the source and sink areas (e.g. see Jetten et al., 1996; Takken et al., 1999, Favis-Mortlock et al., 2000, Beven 2009). Although field information on

erosion sources and sinks is often relatively easy to obtain by mapping erosion and sedimentation phenomena, it is rarely used in calibration exercises to improve the models. The usefulness of such data is shown by Desmet et al. (1999) and Vandaele et al. (1997), who show by an analysis of field data, digital terrain models and aerial photographs that the locations of ephemeral gullies can be predicted with simple, relief-based criteria. Improvement of distributed model results has been realized by incorporating agricultural features such as tillage direction, wheel tracks and field boundaries (e.g. see Souch'ere et al., 1998; Takken et al., 2001; Moussa et al., 2002).

Physically based models, such as EROSION 3D (Schmidt et al., 1999), EUROSEM (Morgan et al., 1998), SMODERP (Holý et al., 1989) and SHETRAN (Ewen et al., 2000), are usually applied to small areas (10^1 – 10^2 sq. km). The study area is usually divided into regular grid cells and soil erosion processes caused by extreme storm runoff events are modeled as a series of numerically solved partial differential equations. Detailed and spatially accurate simulations can be used to design and test technical anti-erosion measures (Z. Kliment et al., 2008). However, these models become less convenient with the increase in size of the study area because computation time increases and numerous field and laboratory measurements of input parameters (such as physical soil properties) are required. Most of these models (e.g. EROSION 3D) can only simulate single rainfall-runoff events.

In larger catchment areas, hydrological processes, such as subsurface flow or sediment deposition in river channels, are important and are often not considered. In addition, many physically based models can only be purchased as commercial software. In medium-sized areas (10^2 – 10^4 sq. km) semi-empirical models are often applied combining physically based and empirically-derived simulation algorithms (Borah and Bera, 2003). These are often referred to as conceptual models (Beven, 2001) and enable continuous long-term predictions of runoff, soil erosion, sediment transport and other hydrological processes in larger river basins and their subareas. Examples of conceptual erosion models include AnnAGNPS (Binger and Theurer, 2003), HSPF (Hydrological Simulation Program FORTRAN - Bicknell et al., 2001), Pesera (Pan-

European Soil Erosion Risk Assessment model - Gobin and Govers, 2003) and SWAT (Soil and Water Assessment Tool -Arnold et al., 1998).

AnnAGNPS (Binger and Theurer, 2003) and SWAT (Arnold et al., 2001) are frequently used, free models and are linked to a GIS system. The main goal of these two models is to predict the impact of land management practices on water, sediment and nutrient yields in large river basins. The models can be used to simulate a period of several years with a daily time step. Both models have a GIS interface that makes data preprocessing and visualization easy and are available as public domain software. Various studies describe the results of sensitivity analyses, calibrations, validations and applications of SWAT in many parts of the world including several medium-sized river basins in Germany (Pfennig, 2003, Pohlert et al., 2005, Krysanova et al., 2007). In the Czech Republic SWAT was tested in the Želivka river basin as part of project EUROHARP (European Harmonised Procedures - Grizzetti and Bouraoui, 2005). AnnAGNPS has been tested mainly in the USA (Das et al., 2006).

Ultimately there are some fundamental limits to the degree of accuracy that erosion models may achieve; this problem is probably rather more important for minor to moderate events than for large erosion events. However, the simulation of large events poses specific problems as well. More complex, physically based models do not necessarily perform better than lumped, regression-based models, mainly because input errors increase with increasing model complexity.

What constitutes a good model has been discussed. Quinton (1997) suggests an iterative, stepwise approach in calibrating a model, whereby the 'fitness' of the model, for a specific purpose, may increase when more data and effort are added. Models should always be carefully calibrated for a given area before being used for predictions. This calibration should not only focus on outlet data. The model's capability to represent the processes occurring within the catchment can be much better assessed whenever the spatial pattern of erosion and deposition, as they are observed within the catchment, are also used. (Jetten et al., 2003)

The physically based models which could be suitable for the study are SWAT, GeoWEPP and EROSION 3D. These models respond to the specifications required for the study area and have also been used before in many case studies. (Zdeněk Kliment, 2007; Hebel 1997; Ketsela, 2009; A. Landi, 2011; Chris S. Renschler, 2003). They are also compatible with the Arc-GIS software and with specific graphical interfaces. Detailed descriptions of the three models will be presented in the methodology and one model will be selected for the study.

Chapter 3. Site presentation

3.1 General overview of the pipeline of Ambatovy Project

Madagascar, the 2nd largest island in the world, is located near the southeast of Africa. The Ambatovy mine is located in the middle of the island in the region of Moramanga, approximately 120 km from Antananarivo, the main city of Madagascar. The pipeline route of the Ambatovy project traverses the eastern region of Madagascar, from the forested area of Mantadia to the coastal region of Toamasina. The route is located between the following coordinates in UTM, zone 39S (Universal Transverse Mercator), (216 978m, 7 913 233m) to (318 344m, 7 979 699m)

Social investigations undertaken along the pipeline route in 2011 identify 2000 households living in the vicinity of the pipeline area, and they are concentrated in the vicinity of the watercourse crossings.

The ore slurry pipeline begins in the mountains in the north of Moramanga, traverses the Torotorofotsy Marsh, crosses some abrupt valleys and granite outcrops, and continues its route through rolling hills until it arrives in the coastal dunes along the east coast of Madagascar near Toamasina.

Five main watersheds and their main rivers have been identified along the pipeline route. In the western section of the pipeline, the main tributary river is the Sahatandra River, which is supplied by the Firikana River originating from the mine and having several additional tributary creeks. The Sahatandra River and Firikana River are parallel to the pipeline route from the outlet of the Torotorofotsy Marsh until the Sahatandra itself arrives at the village of Tanambao, situated near the Beforona Commune. The pipeline then crosses creeks and streams until it reaches the Rianila River, midway along the pipeline and near the Ambatovola commune. The Rianila River, one of whose tributaries is the Sahatandra River, is one of the main rivers of Madagascar. The pipeline crosses the Rianila River at Anivorano and then continues its route through the north-east of the island, until it crosses two tributaries of the Rianila River, which

are the Sahanavo and the Morongolo. The pipeline finally arrives at the watershed of the Ivondro River in the coastal area of Toamasina, which is another large and main watershed of Madagascar.

The location of the Ambatovy project is presented below in Figure 6 and the pipeline route from the mine to the plant area is shown in Figure 7.



Figure 6. Ambatovy Project situation map

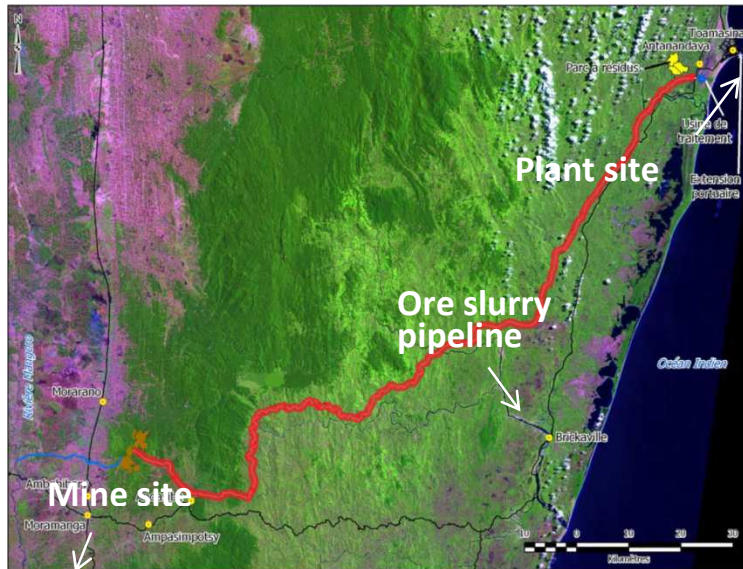


Figure 7. The pipeline route from the mine to the plant site area

The characteristics of the land crossed by the pipeline route will be described below in terms of the land use, the topology, the geology and the soil, the hydrology and the influence of social patterns on biodiversity.

3.1.1 Land use

The selected pipeline route has been chosen to cross some inaccessible /complex areas like the western portion of the Ankeniheny-Zahamena forest corridor. The dominant vegetation is the tavy, which is a combination of cleared forest and stunted trees. The second most common type of vegetation is the degraded forest composed of exploited forest invaded by exotic species. The primary forest, also known as the perennial forest, is the third type of vegetation, which is mostly found around the mine site and in the Ankeniheny-Zahamena forest corridor. It is a tropical forest, which may have been partially exploited, but in which the unexploited areas still have the characteristics of the primary forest.

3.1.2 Topography

The topography of the watersheds around the pipeline route is characterized by steep mountains and valleys from the mine to the Anivorano region; then the mountain formation continues with lower hills until it reaches the flat coastal region of Toamasina. The altitude of

the mountains along the pipeline varies from 1100m to 5m. 60% of the mountains have a slope from 0 to 40%. 20% have slopes higher than 40% and are to be found particularly in the area of the mine to the Fanovana region.

3.1.3 Geology and soil

A large intrusive gneissic formation, known as the complex of Antampombato, probably dating from the Cretaceous era, intersects the ground and dominates the geological environment of the Ambatovy pipeline. The complex is located on the remains of a plateau known as the Massif of Antampombato. This plateau, composed of a horst structure, is bordered to the east and west by two graben structures. The plateau is situated at an elevation of approximately 1100m above the sea level, while the graben structures and the depressions thus formed are found at 900m elevation. The grabens are filled with 40 - 70 m of recent alluvial sediments. (Melluso, 2005).

Since the deposits outcrop on a raised ridge, the lateritic soils have been submitted to an intense climate due to the tropical conditions prevailing in Madagascar. Laterite soil is defined as a soil developed by the process of laterisation, which involves leaching out of silica and alkali, and the increase of hydrated iron and aluminium oxides. The resulting layer of laterite / limonite has an average thickness of 50 meters (Melluso, 2005).

The laterite soils can be divided into three specific zones: the ferralitic carapace area, the ferralite- limonite section and the saprolite zone.

- The shell is a ferralitic surface layer forming a crust several meters thick, which is very hard, like a rock, and which covers the upper reservoir.
- Under the ferralitic carapace, the ferralite-limonite zone, a reddish brown clay-like layer which contains most of the economic ore, is created. This layer has an average thickness of 40 meters. The ferralite-limonite ore is considered the primary layer since it is enriched in nickel and cobalt due to the preferential removal (natural leaching) of the other elements, in particular magnesium and silicon. (Mandimbiharison, 2002)

- The saprolite layer is a transition zone where the rock is neither unaltered rock nor rock completely altered into a clay-like ferralite. In this area, the alteration occurs along fractures, giving the saprolite an irregular or mottled texture. (EIE Ambatovy, 2006).

3.1.4 Hydrology

In Madagascar, the seasons are not really apparent. Two seasons are considered as the winter and the summer. The winter is judged as a soft one, with the lowest temperatures reaching 3 °C. In some regions of the island, rain falls during the colder winter. In the summer season, the temperatures reach 25 to 30 °C and much rain falls in the evenings. The cyclone-season occurs during the summer. The return period of the dry and wet seasons affects the water level in the rivers and can affect the erosion process itself.

The driest period of the year is September-October and the rainfall distribution during the rainy season has one peak in January-February. During the rainy season, the precipitation occurs mainly as short heavy showers (averaging about 0.1 mm/min for about 30 to 150 min) between sunny periods.

The weather data used for the study have been taken from a weather station at the Ambatovy mine and at the ore processing plant site at Toamasina. The data have been collected every 30min from 2004 to 2010. Table 1 below presents the annual rainfall data along the pipeline site from 1928 to 2002 for the mine area, and from 1948 to 2004 for the plant site area.

Figure 8 below is presents the monthly average rainfall for the Moramanga region and for the port of Toamasina.

In the study area, the mean annual rainfall during the period 1928 to 2010 ranges from in excess of 2756.9mm (1956) in the mine area to less than 226mm (1934) in the area of the ore processing plant site at the eastern end of the pipeline (Andriamanamihaja, 2007; ORSTOM, 1993).

The temperatures corresponding to the precipitation data set indicate a mean daily temperature of 19.6°C and average maximal and minimal temperatures of 22.4 °C and 16 °C respectively.

Table 1. Annual average rainfall data for the plant site and the mine

Region	Rainfall [mm]	Period of years
Mine	1468	1928-2002
Plant site	3343	1948-2004

(Ministry of meteorology – Madagascar)

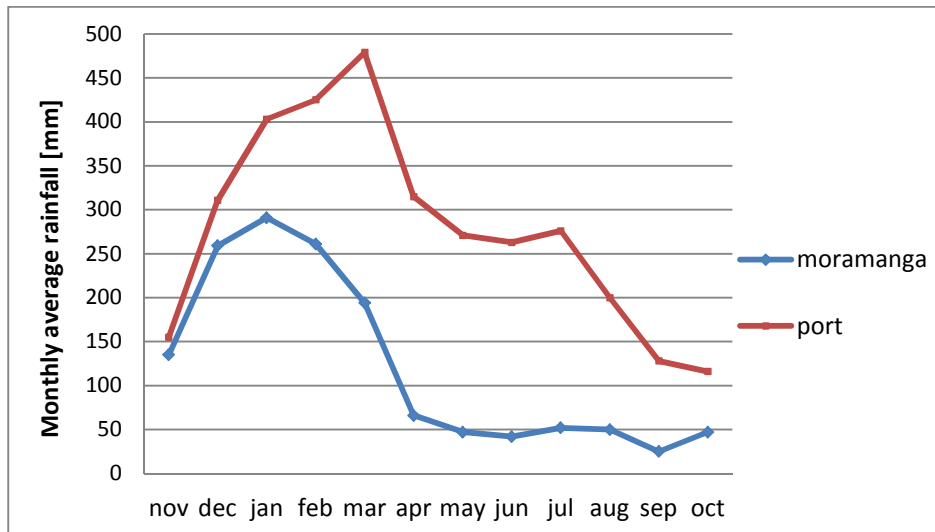


Figure 8. Monthly average rainfall for Moramanga and the port at Toamasina region (EIE Project Ambatovy 2006)

3.1.5 The influence of social patterns on biodiversity

The people living in the vicinity of the pipeline are inhabitants of small villages, with a maximum of 25 households (EIE Ambatovy, 2006). Most of the villages are situated far from a city and the people farm, hunt and fish for a subsistence livelihood. The households practise slash and burn agriculture, as the quality of the soil quickly degrades under cultivation, relocating their villages as they move to stay close to their fields. Once the fields are abandoned, they are not replanted with trees, so their farming contributes to deforestation. Over time this deforestation covers a large area and thus changes the ecosystem and its biodiversity. The only remaining intact primary forests and their ecosystems are in protected areas such as the high mountain areas and remote locations.

These practices affect the biodiversity such that the coastal plains and flatter valleys more suitable to agriculture in the mountains no longer have perennial forests. The three representative field sites chosen represent the range of land use, endemism, habitat integrity and risks present along the pipeline route. To prevent further damage in the higher risk areas (intact perennial forests), it is important to motivate subsequent prevention and mitigation efforts. This is an important objective of the study.

3.2 Representative sites characteristics

Along the pipeline route, the land has been categorized into seven categories according to criteria based on the land use, the slope, the geology and the slope of the river.

There are 458 watercourse crossings, whose catchments have been classified into the seven categories as presented below. Each watercourse is characterized in terms of disturbance due to the natural sediment discharge and due to the construction of the pipeline infrastructure.

This categorization is required for the study of the criteria which can affect the behavior of the catchment and is required to estimate the rate of sediment discharge. The impact of the construction around the crossings and in the catchments results in a large increase in the rate of sediment discharge. The geotechnical works, the cut and fill, the type of bank stabilization, and the choice of the pipeline route, result in an important impact on the runoff and the stream discharge. These need to be considered when implementing modifications to reduce the magnitude of the impact of the erosion and the runoff rates.

For each category, the different types of infrastructure implemented according to the criteria of the upstream environment of the watershed will be presented.

Therefore, this categorization permits a better understanding of the selection of the different sites to study in terms of risks levels.

3.2.1 Category 1: Metamorphic rock, primary forest, steep mountain zone with steep slope

This area is situated around the mine site, where the land use is mostly primary forest undisturbed by deforestation. The geology of the zone is mainly constituted of metamorphic

and laterite rock. The areas with metamorphic rocks are stable and the sediment discharge is normal even with heavy rainstorms. The river can recover to its natural habitat (sedimentation level) in a few hours after an increase in water level. Even on the steep slopes, the area is covered by primary forests, which minimize the runoff and thus the erosion.

Before the construction period, the rate of total suspended solids (TSS) in this zone ranged from 10 to 15 mg/l during a heavy rain and from 2 to 5 mg/l in the dry season. During the construction period, these rates increased to range from 15 to 20 mg/l during a heavy rain and from 5 to 10 mg/l in the dry season, according to the hydrological monitoring executed by Ambatovy team.

The infrastructure implemented in this section depended on the width of the channel; most commonly the channels were of a medium width and the infrastructures implemented were culverts. See Figure 9 and Figure 10 for examples of bank stabilization and a stream crossing using a culvert.



Figure 9. Bank stabilization



Figure 10. Stream crossing using a culvert

3.2.2 Category 2: Metamorphic rock, primary forest, steep mountain zone with gentle slope

This area occurs strictly in the primary forests in the vicinity of large rivers with widths of approximately 5m. This area is situated in the vicinity of the mine site, where the land use is mostly undisturbed primary forest. The geology of the zone is mostly composed of metamorphic

and laterite rocks. This second category is a stable area, with normal sediment discharges, even with heavy rainstorms and the river also recovers its natural habitat after a few hours.

Before the construction period, the rate of TSS in the zone ranged from 10 to 15mg/l during a heavy rain and from 2 to 5 mg/l in the dry season. During the construction period, these TSS rates increased to range from 15 to 25 mg/l during a heavy rain and from 5 to 12 mg/l in the dry season, according to the hydrological monitoring executed by Ambatovy team.

The following four categories of areas are situated not far from the primary forests zones and are in an area unprotected by the government in terms of environment and endemism. These areas are at the stage to become predominantly deforested with "lavaka" and eroded spots. All areas are unprotected and those currently less degraded (due to their remoteness or steep slopes) are in danger of becoming degraded within a relatively short time due to the lack of protection and the increased human pressure.

The other important criterion defining these 4 areas is the geology, which is mainly granitic rocks instead of only metamorphic rocks, with generally less lateritic rock.

3.2.3 Category 3: Granitic and gneiss rocks, primary forest, steep mountain zone

The third category is located in the vicinity of the mine and is composed of granitic and gneiss rocks instead of only metamorphic rocks in the primary forest area. The TSS rates are similar to the two previous categories.

3.2.4 Category 4: Granitic and gneiss rocks, partial primary forest, steep mountain zone

This fourth category is situated near category 3. It is characterized by deforestation and "lavakisation". Geographically, it is positioned in the central section of the pipeline route between the steep forested areas and the deforested flat lands.

The important aspect of this zone is its sensitivity in terms of erosion and runoff. The lavaka are produced by the loss of soil caused by the deforestation and thus the increased runoff. They are mainly situated in the valley zones.

The resulting rate of sedimentation in this section is significant. The grain size distribution is composed of clays, silts, sands and gravel. Most of these sediments are transported to downstream areas as wash load.

Before the construction period, the TSS rate ranged from 15 to 25mg/l during a heavy rain event and from 10 to 15 mg/l in the dry season. During the construction period, the TSS rates have increase to 30 to 40 mg/l during a heavy rain and 20 to 30 mg/l in the dry season.

3.2.5 Category 5: Granitic and gneiss rocks, partial primary forest, steep mountain zone with gentle slope

This category has gentle slopes and large width rivers surrounded by deforestation in areas mostly composed of granitic rocks.

The total disturbance which is mostly due to high sedimentation rates from the upstream zone (category 4) has higher TSS rates in general.

The TSS rates are mainly similar to the values of the fourth category or slightly higher. Before the construction period, the TSS rate ranged from 20 to 30mg/l during a heavy rain event and from 15 to 20 mg/l in the dry season. During the construction period, these TSS rates have increased to 35 to 45 mg/l during a heavy rain event and to 25 to 35 mg/l in the dry season.

Figure 11 below presents a stream crossing classified in this category.

The two last categories (**categories 6 and 7**) are located in the eastern section of the pipeline route, in the coastal zone. The land cover is generally composed of bushes, shrubs and grass and in some areas there remains some coastal vegetation such as Ravinala trees.

3.2.6 Category 6: Granitic and gneiss rocks, completely deforested area, semi-flat zone with gentle slope

This category lies in the flat coastal zone and is surrounded by small gently sloped hills. Nevertheless, the vegetation and the geology remain the same as the fifth category.

The creeks in the area are mainly first order creeks. Usually, the sedimentation in these areas is due to deforestation and the lack of stabilization for the embankments. The TSS rates are high in general, even during the dry season. The particle size distribution is mainly composed of sands with silt. This category has the highest rates of sedimentation and greatest erosion effects.



Figure 11. A stream crossing from the fifth category.

In general, the TSS rate ranges from 50mg/l and up. Before the construction period, the TSS rate was 45 to 50 mg/l during a heavy rain event and 30 to 40 mg/l in the dry season. During the construction period, the TSS rates increased to 45 to 75 mg/l during a heavy rain event and to 40 to 65 mg/l in the dry season.

3.2.7 Category 7: Granitic and gneiss rocks, completely deforested area, flat zone

This category is typical for a coastal area with sediments consisting of sand. The rivers widths are large and the sedimentation is due to the wash load from the upper zones.

The erosion rate is tolerable due to the high level of TSS, considered as natural and normal, in this area. Deforestation and the loss of sensitivity has made the usual TSS levels higher for the past decades. Nevertheless, the area receives the erosion effects and sedimentation from the upper zones, which compounds the high TSS rates.

In general, the TSS rate is 50mg/l or more. Before the construction period, the TSS rate around the zone is 45 to 50 mg/l during a heavy rain event and 30 to 40 mg/l in the dry season. During the construction period, these TSS rates have increased to 45 to 75 mg/l during a heavy rain

event and 40 to 65 mg/l in the dry season. The type of infrastructure implemented in this part of the pipeline route depended on the width of the channel. The most common infrastructure was culverts and bridges with culverts for larger channel widths.

Figures 12 and 13 below present, respectively, an example of the watershed and a stream for the seventh category.



Figure 12. A watershed of the seventh category



Figure 13. A stream with its infrastructure for the seventh category

Chapter 4. Methods

4.1 Criteria for selection of representative field study sites

The construction of the pipeline results in damage to the ecosystem primarily due to the sedimentation caused. Therefore estimating the quantity of sediment washed into the watercourses allows for the identification of damage causing construction methods or designs. The aim is to provide guidelines to allow for future sustainable development and the co-existence of people and endemic species in a watershed.

Three field study sites along the pipeline route of the Ambatovy project, representative of the range of erosion and sedimentation risk, will be investigated by conducting sedimentation and sediment transport studies. For each field site, the key processes will be evaluated according to their particular issues.

These three field sites are located in different sections of the pipeline route representing a range of land use, mean slope, geotechnical properties and climate characteristics. They have been selected for a better understanding of the erosion risk level due to the laterite soil where civil works have been undertaken.

4.2 Description of the three representative field sites

4.2.1 1st field site: Near the Ambatovy mine area

This first site is situated in the vicinity of the Berano village, in the pipeline route section labeled RoW (Right of Way) 01-02. The UTM 39S coordinates of the outlet of the watershed are the following: 219 061 – 7 913 754. The elevation of the impacted watershed ranges from 948m to 1220m. The difference in elevation is 272m. Figure 14 below shows the topography of the watershed, the pipeline route and the location of the water crossing under investigation.

This area is selected primarily for its endemic sensitivity in terms of fish habitat. The main land use is primary forest. Therefore, the water quality of the river is very good having clear water when there is no disturbance. The soil is composed of laterite with clay. The climate has a high

level of precipitation, with frequent rainfall events despite the seasons in the climate of the region.

This area is situated within the protected forest of Mantadia. Therefore, deforestation is forbidden in the surrounding area. The ecosystem is still intact and contains most of its fauna.

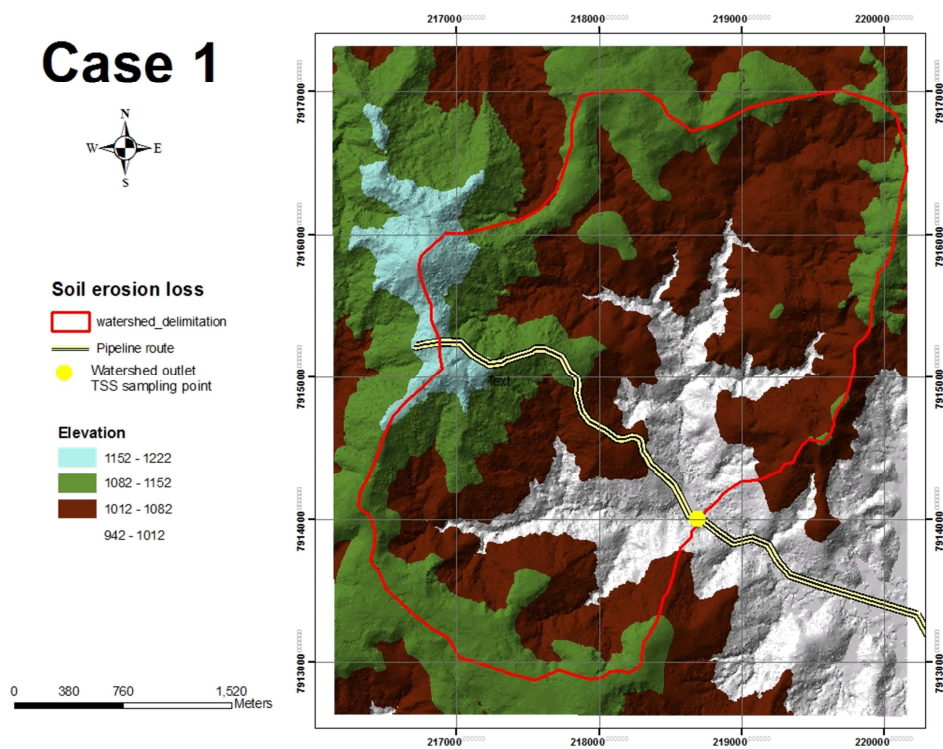


Figure 14. First field site localisation

The following picture in Figure 15 shows the beginning of deforestation around the village of Berano.



Figure 15. The beginning of deforestation around the village of Berano.

Close to the village, there are areas that have been deforested by the slash and burn subsistence agriculture practised by the villagers. These areas are now covered by bushes and non-perennial forests. Nevertheless, almost all of the area is still intact vegetation and is covered with primary forest.

Figure 16 shows the characteristic of the watershed along the pipeline route in the primary forest, during the construction phase and includes the outlet of the first field site.



Figure 16. The geomorphology and the vegetation of the first field site showing the pipeline route and the watershed outlet.

When a rain event occurs in the forested area, the amount of suspended solids in the watercourses remains low and remains at an acceptable level. The vegetation prevents the detachment of soil particles by rill erosion and enables the retention of the soil.

The watershed located in the vicinity of the mine has a 4th order stream which is classified as sensitive due to the endemic habitats that exist within it, particularly for fish. Figure 17 indicates the character of the soil to be clay by plotting the particle size distribution in terms of percent by weight of clay (47%), silt (20%) and sand (33%) (as shown by the red diamond).

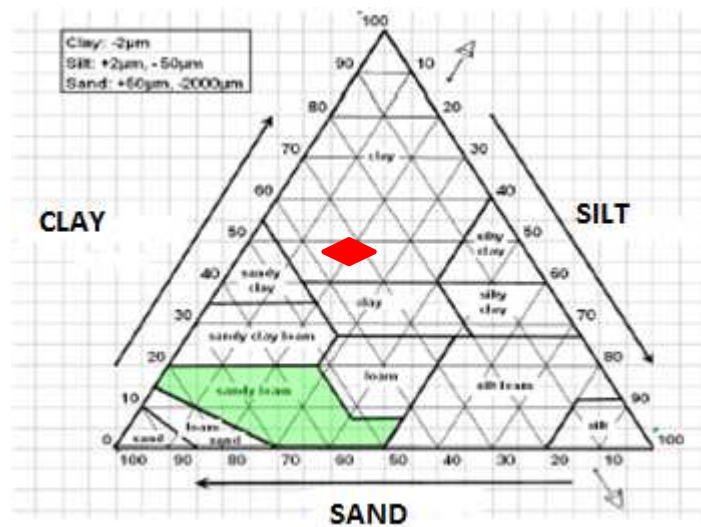


Figure 17. The first field site's particle size distribution

The construction of the pipeline disturbed parts of the forest and hence of the habitat. The pipeline route requires the clearing and leveling of a 25m width line with cuts and fills, which disturbs the forest. In this watershed, the pipeline begins at the highest elevation or the peaks of the watershed and contributes to increased sedimentation in the watercourse below. The increases in TSS levels due to the construction are presented in Table 2. The TSS measurements were taken in situ nominally every three weeks during the period from 2008 to 2013 by the Ambatovy environmental monitoring team. The sampling day could lie within a dry period or after a rain event, at any time of the year. The monitoring of 458 watercourse crossings for the entire pipeline was executed in a three weeks period, and then repeated. (Details of the TSS measurement method are given in Appendix A).

Table 2. Water quality parameters at field site one during the construction phase

Parameter during the construction phase	Minimum value	Maximum value	Average value
<i>TSS [mg/l]</i>	-	338	43.6
<i>Turbidity [Nephelometric Turbidity Unit - NTU]</i>	2.9	392	46.1
<i>pH</i>	6.22	7.74	7.03
<i>Conductivity [μS/cm]</i>	78.3	97.7	87.7
<i>TDS (Total Dissolved Sediment) [parts per million - ppm]</i>	39	48.9	43.9

Note that the climate, the type of soil and the main geotechnical properties of the soils do not change.

4.2.2 The second field site: midway along the pipeline

This second case is located in the central section of the pipeline route, in the section labeled RoW 08-09. The UTM 39S coordinates of the outlet of the watershed are the following: 281 506 – 7 921 073. The elevation of the watershed ranges from 24m to 132m, resulting in an elevation difference within the watershed of 108m.

Figure 18 shows the watershed, the pipeline route and the location of the watercourse sampling.

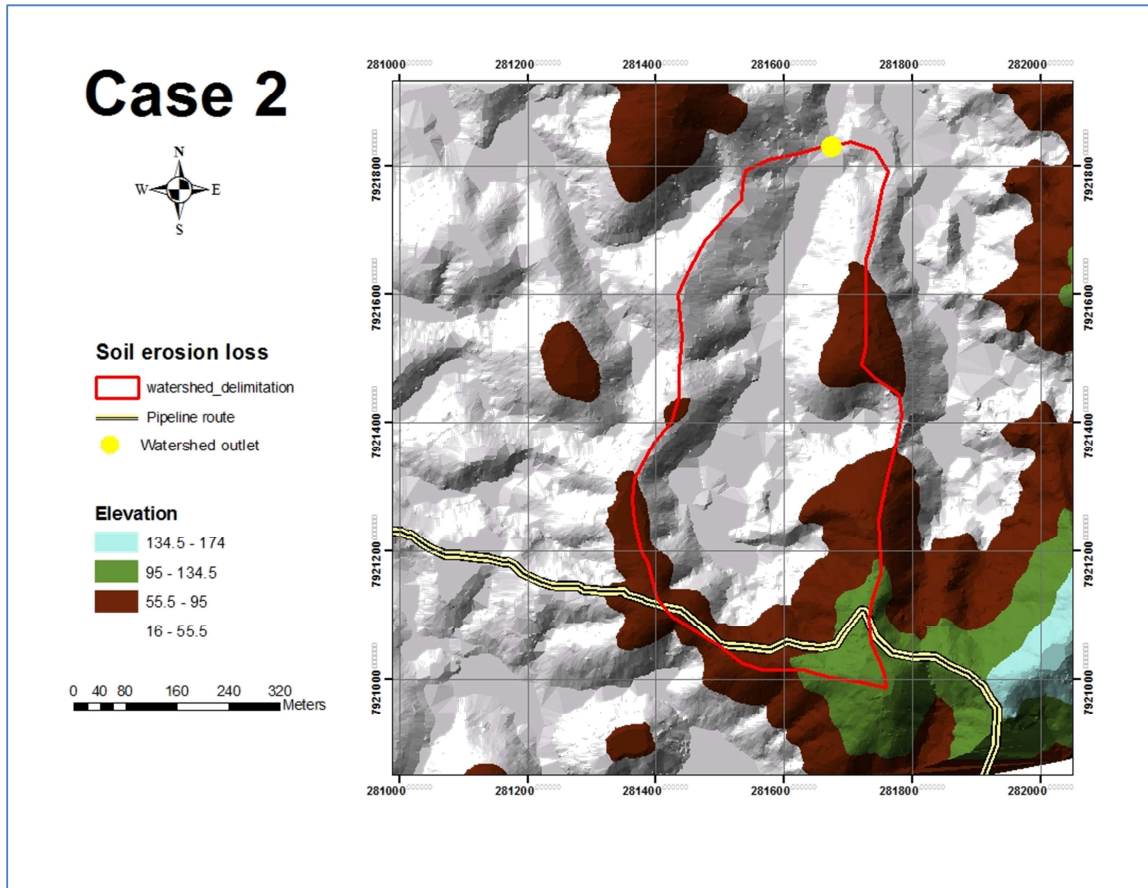


Figure 18. The second field site study location.

Figure 19 a) and b) are aerial views of the watershed showing the extent of the deforestation and the resulting vegetation composed of bushes and non-perennial forests.

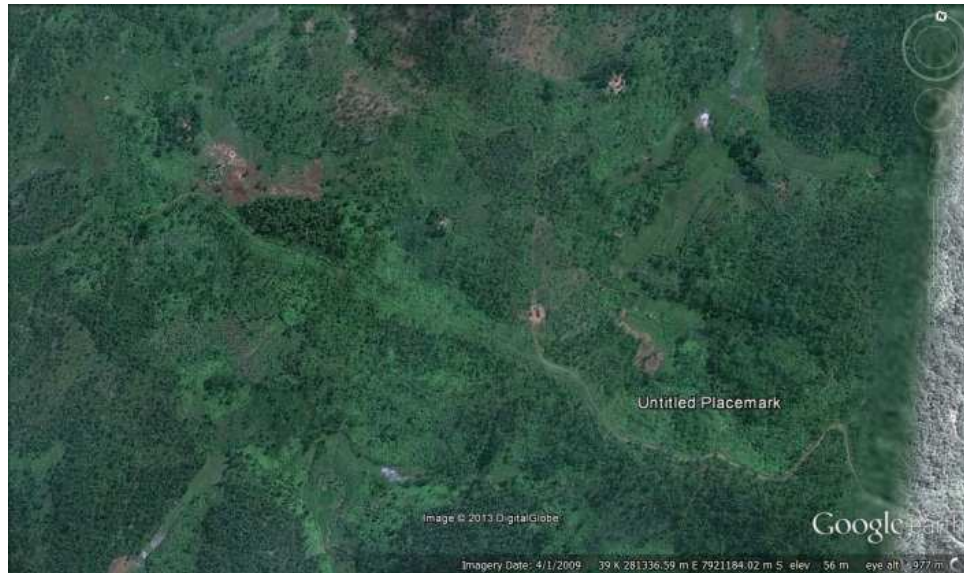


Figure 19. (a). Aerial photo of the second field site. View from the top

Figure 20a is a top view for the field site two. Of note is the vegetation consisting of bush and scrubs, with little forest area remaining. The pipeline route, which was a trail for the villagers before the start of the construction, is also noticeable in the south eastern region. Some areas were already subject to erosion before the pipeline construction.



Figure 19. (b) . Aerial photo of the second field site. View for the north.

Figure 19b shows the watershed viewed from the northern region, close to the outlet of the watershed. The difference in the elevation is especially important as it shows a natural cut from the top of the watershed. Erosion processes were already occurring before the beginning of the construction. Figure 20 below shows the construction of the route in progress.



Figure 20. Pipeline route around the field site two.

Field site two is located in the eastern region of the country, where the climate is warm with high temperatures and a high level of humidity. From this position along the pipeline route, the character of the land is changing from high mountains to flat coastal plains. Therefore, the type of vegetation is also changing with only small patches of perennial forests decreasing in extent and the vegetation increasingly composed of shrubs and bushes. The geology of the soil is lateritic with equal parts of clay, silt and sand.

The slash and burn agriculture and burning of the forests for charcoal have caused the deforestation. This has resulted in a change in the fish habitat, resulting in a loss of endemic species and their replacement with exotic species. The level of suspended solids in the watercourses is higher than in the forested areas, even on dry days. The vegetation cover also includes rice fields.

Table 3 presents the levels of suspended solids during the construction phase measured at the watercourse crossing of the field study site.

Table 3. Water quality parameters for site 2 in the central region of the pipeline

Parameter during the construction phase	Minimum value	Maximum value	Average value
<i>TSS [mg/l]</i>	5.3	22	7.03
<i>Turbidity [NTU]</i>	7.9	44.6	14.4
<i>pH</i>	6.43	6.65	6.51
<i>Conductivity [μS/cm]</i>	32.2	36.4	34.8
<i>TDS [ppm]</i>	16.1	18.1	17.4

Figure 21 presents the soil particle size distribution of the second field site in terms of percent by weight of clay (40%), silt (40%) and sand (20%) (as shown by the red diamond).

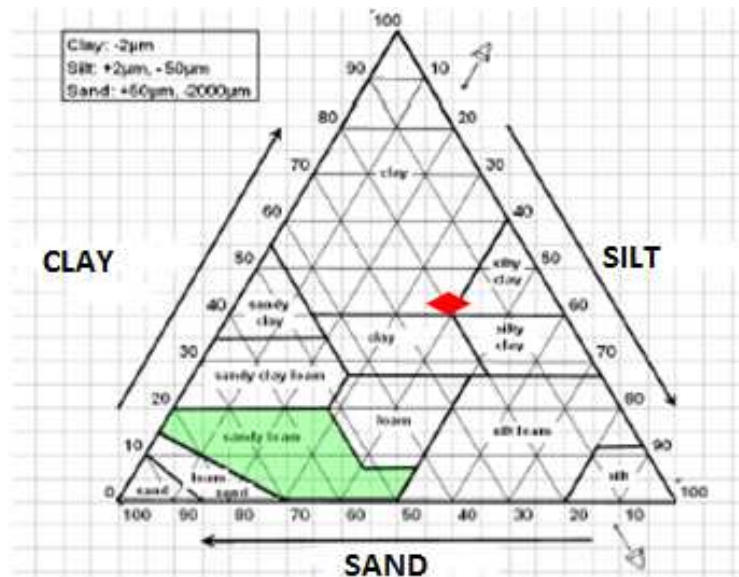


Figure 21. Soil particle distribution of the second field site.

4.2.3 The third field site: near the plant site

This third field site is located in the vicinity of the village of Ambarimilambana, at the pipeline route section labeled RoW 13-14, which is near the plant site at the coast. The UTM 39S coordinates of the outlet of the watershed are 303 850 – 7 962 659. The elevation of the site is

ranges from 72m to 128m, resulting in a maximum elevation difference of 56m. Figure 22 shows the watershed, the pipeline route and the watershed outlet.

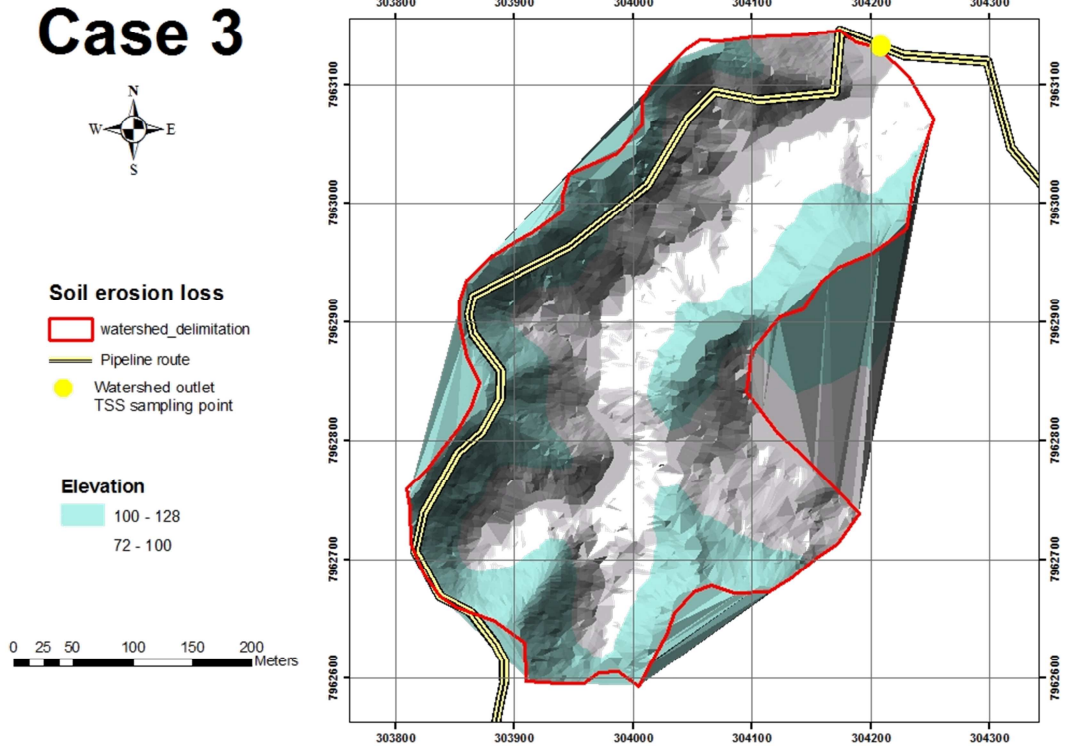


Figure 22: The third field site location

The third field site is located in the eastern coastal region in the coastal plains (without high mountains). The geology is composed of lateritic and sandy soils. The climate is very warm with rainfall events every day which are more intense during the winter season. The vegetation consists of shrubs without any forested areas or patches. Deforestation is complete resulting in an ecosystem composed mainly of exotic species.

Figure 23 shows an aerial view of the watershed from which both the vegetation and the pipeline route are seen. It is a small watershed, completely deforested and with the vegetation being only bushes even before the construction of the pipeline. Figure 24 shows the site after the construction and after the revegetation phase. Erosion in the area is clearly visible. The

vegetation that remains of bush and grasses is the result of human activity, subsistence slash and burn agriculture and charcoal burning, on this sensitive tropical forest on lateritic soils. The impoverishment of the land has caused the villagers to move to another area where forest is still present for their own survival.



Figure 23: Third field site: near the coastal region

This third site was chosen due to the change in the watershed at the higher elevations from the construction of the pipeline route along its upper limits. A view of the route is shown in Figure 24.



Figure 24. A view near the watershed outlet of field site three during the construction phase.

The TSS levels here are high due to the existing disturbance in the watershed and are similar to similar surrounding watersheds. Table 4 shows the water quality parameters measured at the outlet of the watershed during the construction phase. Due to the existing degradation of the area, the increase in the disturbance during the construction phase is low.

Table 4. Water quality parameters for site 3 near the coast

Parameter during the construction phase	Minimum value	Maximum value	Average value
<i>TSS [mg/l]</i>	2.18	30	11.8
<i>Turbidity [NTU]</i>	2.41	58.3	18.3
<i>pH</i>	5.83	6.67	6.38
<i>Conductivity [$\mu\text{S/cm}$]</i>	49.7	58.4	54.7
<i>TDS [ppm]</i>	24.8	28	27.3

The type of soil has been identified as a between a sandy clay and a sandy clay loam with the following particle size distribution of clay (34%), silt (2%) and sand (64%) as shown in Figure 25.

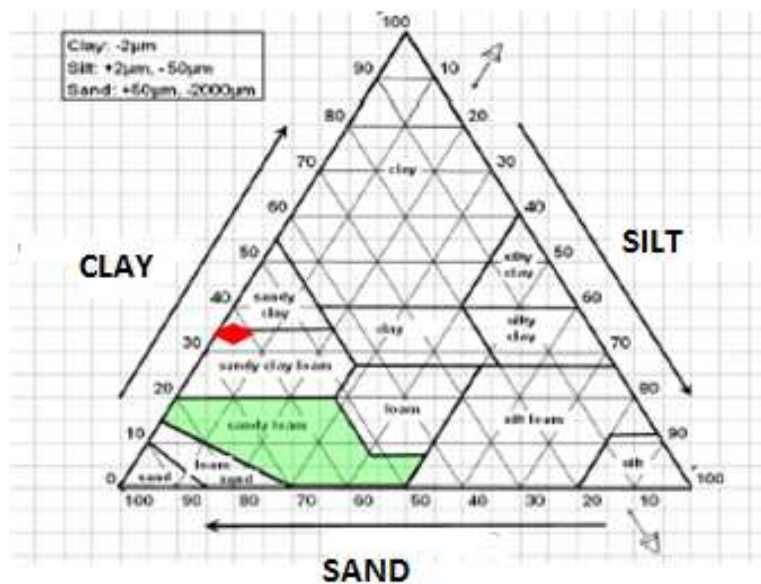


Figure 25. Particle size distribution of the third field site

4.3 Methodology for sedimentation and sediment transport rates

The objectives of the study are first to determine the sedimentation in the watercourses due to surface erosion processes occurring as a result of the civil works undertaken on the laterite soils, to construct the slurry pipeline for the Ambatovy project and second to propose mitigation measures or alternative designs that will lower the sedimentation rates.

Two methods will be used to provide an estimate of the sedimentation occurring in the watercourses. First, field estimates of sedimentation rates are obtained from suspended sediment transport rates from field measurements of TSS combined with an estimation of the water discharge. Second, GeoWEPP is used to estimate the sediment load supplied to the water course based on the daily precipitation record and land characteristics. Due to data scarcity, all these methods require reasonable assumptions to be made.

The methodology was implemented in the following steps.

1. Field estimation of suspended sediment load in streams:
 - a) Measurement of TSS and analysis of data to get average TSS values
 - b) Estimation of water discharge:
 - i) Water discharge estimated as proportional to that of a similar gauged catchment – the reference station method (average annual estimate and full year hydrograph estimate).
 - ii) Water discharge estimated using Manning’s equation with slope and geometry (R, A, P), and Manning’s n estimated from a digital elevation model and site visits (average annual estimate).
2. Estimation of suspended sediment (wash load) transport rates using field data. Field measurements of TSS combined with an estimation of water discharge provide an estimate of the sedimentation rate in the catchment
3. Estimation of sediment loads estimated with GeoWEPP using a daily precipitation record and land use defined (annual estimate based on daily time steps).
4. Design of mitigation measures or alternative designs for the field study sites using GeoWEPP.

4.4 Detailed description of the methods

Each step of the methodology is described in detail below.

4.4.1 Field estimation of sediment load in streams

The sedimentation is estimated from field measurements of TSS and an estimation of the discharge. First, a sedimentation rate determined from an estimated TSS corresponding to the annual average discharge and the average annual discharge will be presented. This provides an estimate of the total sediment transported through the measurement section in a year. Then a more detailed calculation is made using a full year daily hydrograph with corresponding TSS determined from a relationship estimated between TSS and discharge at each site.

4.4.1.1 Measurement of TSS and analysis of data to get average TSS values

The Ambatovy Project's environmental department was required to undertake a monitoring program to record the effect of the pipeline construction on the watercourses. Both the physical hydrology and the suspended sediment in the streams were measured. A baseline study at two selected sites (at the mine and the plant site) was made before the construction phase began. Additional sites along the pipeline route were sampled once the construction phase began and access to these sites was possible. One mid-pipeline site was selected for study (second field site). Sampling at the sites was done nominally every three weeks over a period of a full day and thus represent measurements taken under a random range of weather conditions, and hence of water levels and discharges. The weather conditions ranged from dry, to rain, to cyclones and the water levels range from low water levels to flood levels. Missing data resulted when a cyclone caused lack of access to a site.

Both the first field site at the mine and the third site close to the plant (at the coast) were monitored prior to and during the construction phase. In situ measurements were made, at the stream crossing locations noted in Figures 14, 15, 17 and 23 for turbidity, pH, conductivity and temperature. TSS was determined once the Ambatovy laboratory had been established and was functional, starting in July 2008. TSS was determined from 1.5 L water samples collected from both upstream and downstream of the stream crossing. These water samples were also analyzed for pH and conductivity. Data was gathered for a 3 year period from 2008 to 2011.

At the second field site in the central section of the pipeline, access was only possible by road once the construction survey started and, the pipeline route opened up access to previously

inaccessible regions. In situ measurements were made at the site noted in Figure 19 for pH, turbidity, conductivity and TDS. Again 1.5 L water samples were collected for determination of TSS and confirmation of in situ pH and conductivity.

The Ambatovy laboratories were used both to determine TSS and to check and confirm the results of the in situ testing performed in the field surveys. There are two laboratories, one at the mine and another at the plant site. The pipeline team used the laboratory closest to the pipeline sector under survey. The middle sector was using both of the laboratories.

The laboratory is equipped with instruments to determine TSS, using the methodology detailed below. The laboratory is also equipped with a balance, an oven, a pH meter, a turbidity meter and a fridge. Demineralized water is used in the laboratory.

4.4.1.2 Sediment property measurements

4.4.1.2.1 Suspended sediments

The in situ field measurements made in the stream were the turbidity, pH, conductivity and TDS. In addition, the water samples collected at the sites were processed in the environmental laboratories of the Ambatovy Project. The samples were analyzed for TSS, pH, turbidity, conductivity and TDS. These analyses were used to confirm the in situ measurements. Once the field sampling campaign was completed, the samples were stored in a cool place until processed.

4.4.1.2.2 The Total Suspended Solids (TSS)

Standard procedures were established and followed for obtaining the TSS of a sample. These had the approval of the Ministry of Environment of Madagascar and the “Office National pour l’Environnement” or ONE, which is the government section in charge of the environmental regulations. The procedures were developed based on references from the Canadian and American protocols (EPA- Environmental Protection Agency).

The steps that form the standard procedure are provided in Appendix B.

4.4.1.2.3 Turbidity

The measurement of the turbidity in a stream followed the standard procedures approved by the Ministry of Environment of Madagascar and ONE and were developed based on the Canadian and American protocols (EPA).

A 2100P Hach Portable Turbidity Meter was used in situ to measure the turbidity of a stream. The samples were collected in a vial, which was then wiped, dried and shaken before being placed in the turbidity meter. Three measurements of each sample were made and recorded.

In cases where the turbidity measurements were detected to be higher than the standards from the established protocol of the portable meter, a sample was taken for analysis in laboratory. These samples provided validation of the in situ measurements.

The 2100P Hach Portable Turbidity Meter conforms to the design criteria specified by the US EPA Method 180.1. It uses the nephelometric principle to determine turbidity and the components of its optical system are a tungsten-filament lamp, a 90° detector to monitor scattered light and a transmitted light detector. It is a model with the range, accuracy and resolution of many laboratory instruments. The instrument's microprocessor computes the ratio of the signals from the 90° and transmitted light detectors. This ratio technique accounts for interferences from color and/or light absorbing materials (such as activated carbon) and compensates for fluctuations in lamp intensity. Therefore, long-term calibration stability is provided. Stray light is minimized by the optical design which permits an increase in the measurement accuracy.

As it is a portable turbidity meter, it is provided with Stabilized formazin standards for calibration. Turbidity from 0.01 to 1000 NTU can be measured in automatic range mode with automatic decimal point placement. The accuracy of the measurements is $\pm 2\%$ of reading plus stray light from 0 – 1000 NTU. The contribution of error is not significant for these measurements.

4.4.1.2.4 In situ field measurements of water quality parameters

A multi physical parameter portable meter was used for the field for measurement of pH, conductivity and TDS. The meter conforms to the design criteria of the EPA. The instruments used were Hach - MP Series portable devices and the MP-4, MP-6 and MP-6p handheld meters. They could test for pH, ORP (Oxydation reduction potential), conductivity, resistivity, TDS, mineral/salt concentration and temperature. The measurements are performed by electrode sensors with a reading accuracy of $\pm 1\%$ or better.

4.4.1.3 Estimation of water discharge

4.4.1.3.1 1st methodology: water discharge estimated as a proportion of gauged drainage basin based on area (average annual estimate)

The average annual water discharge was estimated using the reference station method. The principle of the method is to select a gauged catchment having the same hydrological and terrain parameters as the study catchment. It is assumed that the water discharge in the study catchment is in proportion to the ratio of the catchment areas as the same hydrological processes as assumed to occur. This method will be used both for the average annual estimate and for the yearly hydrograph estimate. The watershed characteristics of the reference stations will be compared to those of the field sites (in terms of elevation range and land use) and therewith the similarity of their hydrological processes and the accuracy of the estimate will be discussed.

The closest hydrometric station having a long period of observation (90 years) of annual water discharge was identified. The hydrometric stations used were the Rianila and Ivondro stations, which are ORSTOM (Office de la Recherche Scientifique et Technique Outre-Mer) stations. From these data, the water discharge for a given period (day, month, year) associated with the reference station is calculated according to:

$$q_r = \frac{Q_r}{S_r} \quad (1)$$

where r: reference

q_r : specific water discharge of the referenced station [$\text{m}^3/\text{s}/\text{km}^2$]

Q_r : referenced water discharge [m^3/s]

S_r : watershed area of the referenced station [km^2]

This provides the discharge per unit area, which can be multiplied by the area of the study catchment as:

$$Q_{BV} = q_r \cdot S_{BV} \quad (2)$$

where Q_{bv} : water discharge of the area of study [m^3/s]

q_r : specific water discharge [$\text{m}^3/\text{s}/\text{km}^2$]

S_{BV} : watershed area for the study [km^2]

4.4.1.3.2 2nd methodology: Water discharge determined from Manning's equation with slope and geometry (R, A, P) and Manning n estimated from digital elevation model and site visits (average annual estimate)

A second method of estimating discharge consists of estimating the water discharge using the Manning's equation:

$$Q = \frac{1}{n} \cdot A \cdot R^{2/3} \cdot S^{1/2} \quad (3)$$

With: Q : water discharge [m^3/s]

A : area of the cross section [m^2]

R : hydraulic radius [m]

S : longitudinal channel slope [m/m]

Slopes were estimated from the DEM developed using Lidar and satellite data. It was assumed that that flow is routed consecutively from one upstream cell to only one downstream cell, thus creating a channel that is one cell wide (FERENCEVIC & ASHMORE, 2012). The slope will be determined over 3 different lengths as presented in the results section.

The cross-section area, and hydraulic radius was measured on site with 3 different measurements and the average was determined.

The Manning's n coefficient has been established visually according to the table from Chow (1959).

4.4.1.3.3 Weather stations for precipitation data

Two weather stations, one at the Ambatovy mine site and one at the plant site in Toamasina, were used to collect 30 min data on rainfall, temperature, wind, humidity, pressure and solar radiation.

The weather stations were replaced in 2006, so data was collected at the old station from 2004 to 2006 and then with the new station from 2006 to the present, at both the mine and the plant site.

The stream gauging stations located near the mine was placed at the outlet of the mine watershed and the gauging station near the plant site placed in the Ivondro River.

Figure 26 and figure 27 show the weather and gauging stations at the first field site at the mine and for the third field site, near the plant, respectively.

Case 1

Weather and stream gauging stations

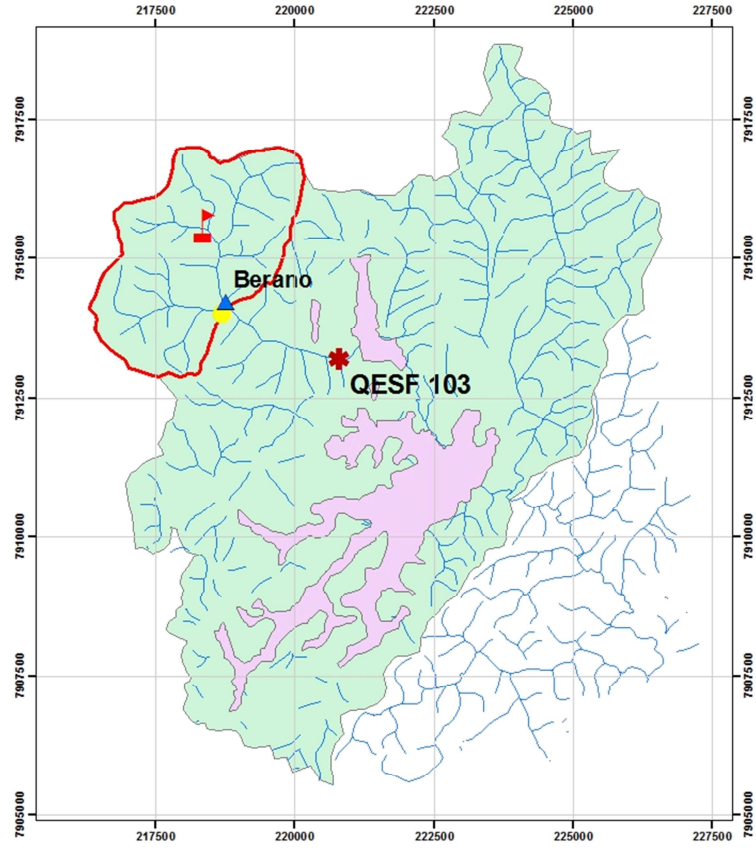


Figure 26. Stream gauging and weather station at the first field site near the mine

Case 3 Stream gauging and weather stations

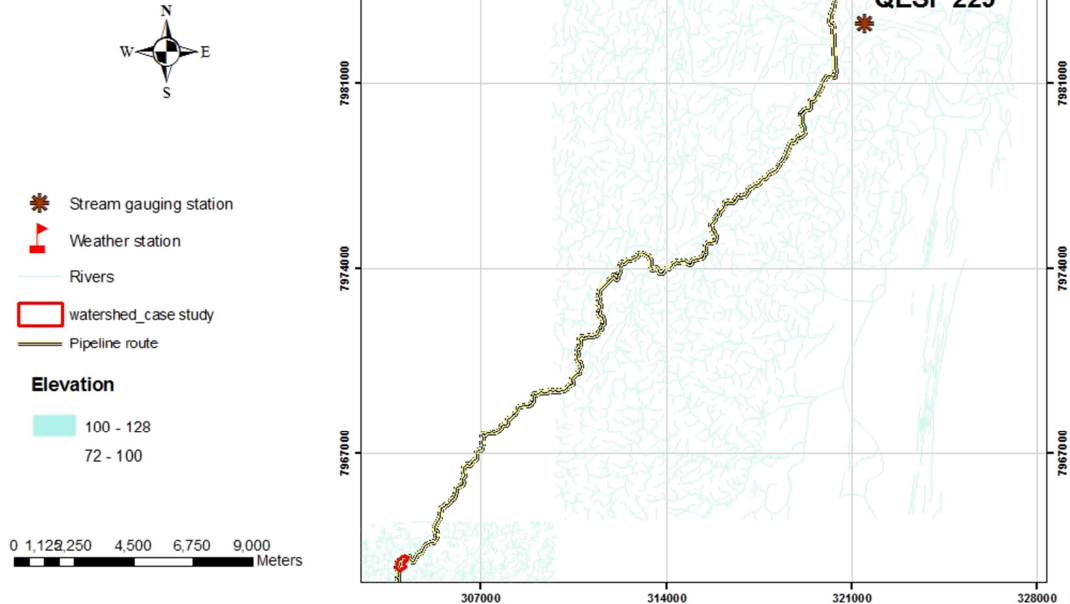


Figure 27. Stream gauging and weather station at the third field site near the plant

4.4.1.4 Calculation of wash load transport rates (annual estimate from field data)

The wash load is estimated from field measurements of TSS multiplied by the water discharge. First a rough estimate is made using the TSS corresponding to the annual average discharge (from a relationship determined at each site) and the average annual discharge (calculated by reference station method and using Manning’s equation). Second a more detailed calculation is made using the full year daily hydrograph (using the reference station method) and the TSS that corresponds to the discharge, from a relationship determined at each site between measured TSS and discharge.

4.4.2 Estimation of sediment loads calculated using GeoWEPP (annual estimate based on daily time steps).

4.4.2.1 GeoWEPP (Water Erosion Prediction Project)

The Water Erosion Prediction Project (**WEPP**) is a physically based model, for erosion simulation, built on the fundamentals of hydrology, plant science, hydraulics, and erosion mechanics. The model was developed by an interagency team of scientists to replace the Universal Soil Loss Equation (USLE) and has been widely used in the United States and the world. WEPP requires four inputs which are climate, topography, soil, and management (vegetation) and provides estimates of the water balance (surface runoff, subsurface flow, and evapotranspiration), soil detachment and deposition at points along the slope, sediment delivery, and vegetation growth. The WEPP model has been improved continuously since its public delivery in 1995, and is applicable for a variety of areas (cropland, rangeland management, forestry, fisheries, and surface coal mining).

WEPP is a process-based model that allows for continuous simulation of small watersheds and hillslope profiles used to assess various soil and water conservation management options for agricultural, rangeland, and forest sites. The Geo-spatial interface for WEPP (GeoWEPP) makes use of digital geo-referenced information such as Digital Elevation Models (DEM) and topographical maps to derive and prepare valid model input parameters and defaults. Site-specific soil and water conservation planning can be done for a small watershed with a single soil type and a category of land use for each sub-catchment. The integration of orthophotos, the soil surveys, the land use maps, climate data, and precision farming data as well as multiple soils and land uses within each sub-catchment is currently under development. The goal of the GeoWEPP project is to provide a series of interfaces for users with different levels of GIS knowledge that uses these different data sources in a standard format either provided by GIS users, by precision farmers with Global Positioning Systems (GPS) databases and/or through accessing commonly readily available U.S. nationwide data sets.

WEPP is available for a wide range of geographic and management conditions and can predict the spatial and temporal distributions of soil detachment and deposition on an event or

continuous basis at both small (hillslopes, roads, small parcels) and large (watershed) scales. Hillslope applications of the model can simulate a single profile having various distributions of soil, vegetation, and plant/management conditions. In WEPP watershed applications, multiple hillslopes, channels, and impoundments can be linked together, and runoff and sediment yield from the entire catchment predicted.

4.4.2.2 Model selection criteria and comparison

The models CENTURY (Parton et al., 1987) and AnnAGNPS (Binger and Theurer, 2003) will not be used because they were developed for both large and small agricultural areas.

Although SWAT is an agricultural model, it has been applied in many parts of the world with different land covers, with adequate and valuable results. SWAT enables some continuous long-term predictions of runoff, soil erosion, sediment transport and other hydrological processes in larger river basins and their subareas. Because the area of study is situated in partially forested mountains, valleys and hills with shrubs, slope is an important variable to consider for improved results. SWAT is not suitable for the study as it is more focused on agricultural assessment. A detailed description of SWAT is provided in Appendix D.

EUROSEM (Morgan et al., 1998), PESERA (Gobin and Govers, 2004), EUROHARP (Grizzetti and Bouraoui, 2005), SPEROS (Soil Properties and Erosion model - Van Oost et al., 2003) are calibrated for specific European areas, and thus have not been developed specifically for or validated for tropical areas, having tropical forests, different precipitation regimes and different soil types.

HSPF is also an agricultural model, using long term rainfall and other meteorological and hydrological parameters and provides a continuous assessment. Therefore, HSPF was not convenient for the study as it requires the monitoring of many meteorological parameters. Many of these parameters have not been assessed continuously for the three field sites. More details about HSPF are given in the Appendix D.

The GeoWEPP model will be used for the simulations in this research for the three field sites both to investigate their actual situation and for the examination of mitigation measures. GeoWEPP is the most appropriate model for the study of Madagascar sites because it can be used for both forested and deforested areas. Another good point in using GeoWEPP is the possibility to use the meteorological data of field sites. For the other models, it is not possible to use data from field site of Madagascar.

Both SWAT and GeoWEPP use the USLE and MUSLE equations to predict the amount of soil erosion.

GeoWEPP is a physically based model; it also considers the computation and evaluation of the shear stress of the soil and the geotechnical parameters of the soil such as the interrill and rill erodibility factors, the particle size distribution of the soil, the albedo, the hydraulic conductivity and the soil's initial saturation level.

The meteorological data required is detailed and hence provides a good representation of the erosive forces at the site. The parameters required are precipitation, solar radiation, values of rainfall peak intensity, the maximum and minimum temperatures and the dew point.

In the GeoWEPP simulations, snowmelt parameters are not used as they are not relevant to Madagascar.

At the end of the simulations, the results are grouped into the following sets:

- Soil loss, the sedimentation in the rill and interrill of each hillslope at sub-catchment outlets and the discharge volume.
- The runoff and the sub-runoff volume, the sediment deposition and the sediment yield on each hillslope
- The discharge volume and the sediment yields of each channel and impoundment.

GeoWEPP is also chosen for its capacity to modify the values of parameters such as slope, land use and soil type, which is useful for the examination of possible mitigation measures.

In conclusion, GeoWEPP was selected as it appears to most likely to provide accurate estimate of sediment loss for the study sites on laterite soil in Madagascar. This model has been used

previously in many countries with a range of different land covers for the estimation of soil erosion loss and therefore there is a large database for comparison.

4.4.2.3 GeoWepp and Wepp Models parameter estimation and processing

The modelling of the erosion process of each catchment using GeoWepp requires many parameters.

First the terrain of the catchment is represented as a DEM from Lidar images, maps and parameters related to the geomorphology of the catchment. The maps used and the information they provide are:

- Lidar images of the pipeline route, from the mine to the Plant site in the Toamasina region. These images have a high resolution and provide information in a buffer zone of 1 kilometer, on each side of the pipeline route. These are used to generate contour lines representing the elevation of the catchments with a precision of 1 m.
- Topographic maps from Foibe Tao-tsarintanin'i Madagasikara (FTM) with a scale of 1/10000. Streams locations, elevation lines, villages, roads, forests and lakes are represented in the maps.
- Soil maps from both the FTM and those developed from the data collected as part of the Ambatovy project, the latter data is not publically available. These provide the soil types and their spatial distribution.
- The Lidar images were also used to develop land use and land cover maps for the Ambatovy project. These are more detailed in the vicinity of the mine. This data is not publically available.

ArcGis 9.2 was used to obtain the Triangulated Irregular Network "TIN" and the DEM of the catchments. All the data sets, including the maps and the Lidar images, enabled a detailed spatial understanding of the catchment and allowed for the calculation of required parameters such as the slopes, the depths of the streams, the elevation and the other characteristics of the catchment.

Data on soil and land use were required in the form of ASCII (American Standard Code for Information Interchange) files. These files were generated from the data from the maps and the spatial reference was reported in UTM 39S coordinates. GeoWEPP only uses UTM coordinates.

The land use has been characterized into four types of land cover, below, and is listed in an attribute Table. These characteristics come from the EIA Ambatovy, done by Dynatec Corp, for all areas of the project which include the three areas of the current study. Field surveys and different assessments with many specialists have been executed during the accomplishment of the EIA Ambatovy in 2006 with high confidence as the land use characteristics has been used and verified for the monitoring during the construction phase.

- transitional forest or 5th year forest: this corresponds to a forest transition which evolves into azonal forest and/or zonal forest. They consist of transitional forest zonal / azonal average altitude growing on lateritic outcrops are characterized by tree vegetation canopy of variable height (about 15 m), which is found on the slopes of trays ferralitic armor,
- evergreen forest or zonal forest which is a moist forest of eastern medium altitude, on which species are varied with different strata clay soil zones as the families of Lauraceae, Myrtaceae, Cunoniaceae, Clusiaceae, Euphorbiaceae, Moraceae, Sarcolenaceae, Flacourtiaceae, Rubiaceae, Sterculiaceae, Pandanaceae, Cyatheaceae.
- mixed forest or azonal forest is present on ferralitic soil dominated by sclerophyllous shrubby vegetation whose main families are Lauraceae, Ericaceae, Asteraceae and Sarcolanenaceae.
- shrub land characterized by savannah dotted with plantations of sporadic eucalyptus.

These terms are specifically defined in GeoWEPP from conversion by Topaz with USGS land use types and the current land use characteristics of each watershed, with files in [.txt], [.db], [.rot].

The soil type has also been characterized in a similar manner. For this study only one type of soil is required, a laterite soil. Mukey soil database from USDA's Natural Resources Conservation Service "NRCS", will be used. These data are publically available with prior request.

Geotechnical characteristics of the soil will be required for the WEPP model. These parameters are the rill and interrill erodibility factors, the albedo, the critical shear stress, the estimated proportions of clay, silt and sand of the soil, the effective hydraulic conductivity and the initial saturation level. These parameters will be obtained from the current data and studies previously done by Ambatovy Project, before the construction phase and presented in the Appendix E.

The weather data required is obtained from the two weather stations at the mine and the plant site. The data are first uploaded into the WEPP model and then the data set to be used in simulations is generated in the GeoWEPP model. Rock:Clime file, which can be subsequently modified to reflect the exact parameters of the catchment. Rock:Clime databases are available for the USA and provided by WEPP for the use in GeoWEPP. The following parameters are considered:

- The average monthly precipitation (in),
- the number of wet days of the month,
- the average maximum and minimum temperature (F)
- the average precipitation on wet days (in),
- the probability of wet days following wet day,
- the probability of wet days following dry day,
- the solar radiation (Langley/day)
- the maximum 30 minutes intensity
- the dew point
- the time to peak intensity

The coordinates of the weather station and its elevation are also required for the assessment.

Once all the required parameters have been collected, they are loaded under one specific project name and opened in GeoWEPP. The model automatically generates the streams and creeks of the catchment from the DEM, according to the desired design level of the streams of the catchment, for example for first, second or third order streams, from the data in the DEM.

The simulation requires a weather record of 100 years. If the available weather record is less than this, the program develops the 100 year record from the existing data based on a correlation analysis of the available data. The user can then set the following parameters:

- The number of years for the simulation
- The choice between the two simulation methods,, which are “Watershed” and “Flowpath”.

The watershed method considers each hillslope in the sub-catchment, determines the representative profile of the hillslope and assigns one soil and one land use to the hillslope. GeoWEPP determines the relevant soil and land use for the hillslope from the input data. The simulation runs for each hillslope and the results are compiled. This method reports the amount of sediment leaving each hillslope and being conveyed to the outlet of the catchment.

The Flowpath method focuses on each flowpath within the sub-catchment. The slope considered for the simulation is the slope for the flowpath only. Nevertheless, it also preserves the same process to represent the diversity of the land use and the soil.

After the simulation is run, output reports are generated by GeoWEPP. These include the following data:

- The soil loss, the sedimentation in the rill and interrill of each hillslope and in downstream areas and the water and sediment discharge volume.
- The runoff and the sub-runoff volume of water, the sediment deposition and the sediment yield on each hillslope
- The discharge volume and the sediment yields of each channel and impoundment.

The simulation results will be compared to the data obtained from the field survey and a final assessment will be made.

An additional advantage of GeoWEPP is its capacity, via WEPP, to modify the values of parameters such as slope, land use and soil, to generate some potential scenarios to investigate mitigation solutions for the erosion processes taking place in the field site catchments.

4.4.2.4 Design of mitigation measures or alternative design for the field sites using GeoWEPP

The Ambatovy project has executed some mitigation measures during the construction phase of the mine, the pipeline and the plant site. First, a selection from the mitigation plans will be presented in the results section first.

Secondly, the mitigation measures developed using GeoWEPP, based on an analysis of the existing situation in each field site will be presented. The aim is to use GeoWEPP to correct and minimize the effect of the erosion process by changing the type of vegetation or by changing the slope of the watershed. The final results of this exercise will be presented showing the optimum of all changes for each field site.

Chapter 5. Data analysis, results and discussion

5.1 Data analysis

The erosion of the laterite soils caused damage in downstream areas due to sedimentation in the streams. It was important to estimate the sediment load, both in terms of the sediment supply as wash load and to determine the maximum possible sediment transport rate in the form of suspended load and the resulting bed deposition, and their relationship to precipitation events. Links between sedimentation and hydrological parameters such as precipitation and runoff are determined to aid in the evaluation of mitigation solutions to prevent erosion processes in the future.

The measurement of precipitation allows for an estimation of runoff and therefore of discharge. It is the runoff that causes the sediment supply to the water courses due to surface erosion and the discharge in the streams that transports the sediment load along the streams.

In order to determine the effect of the pipeline construction on sedimentation, the total sediment load in the streams was estimated by monitoring the total suspended solids (TSS) before, during and after the construction of the pipeline along its route. The turbidity was measured both in the field and in the laboratory and its relationship with TSS determined. This provided validation of the TSS measurements.

Bed deposition of sediments was observed visually to qualitatively assess the depth and the quantity of the sediments transported due to the effect of the construction of civil works or of rainy days,. The bed deposition is related function of the hydrological parameters such as precipitation and runoff.

Geo WEPP was investigated as a possible tool to use to estimate the effectiveness of proposed erosion mitigation measures. The implementation of the GeoWEPP model required the measurement of geotechnical parameters of field samples of the laterite soil. The parameters needed in GeoWEPP are the erodibility factor (K), the permeability and the cohesion of the soil. Precipitation data is also required for GeoWEPP. Precipitation data was obtained every 30 min

at the two stations located at the Mine and at the plant site over a 10 year period. The field study sites were located between these two stations, so their data were interpolated to estimate the discharge for each of the three field study sites. The data thus estimated were checked to ensure they provided a realistic representation of the rain repartition in each watershed of study, outliers were removed.

The flow depths were estimated first by using the Lidar images to generate contour lines of the local topography. Lidar images can be used to obtain the values of the elevation even under the bodies of water with an absolute accuracy of 20cm (Davis P.A 2002; USGS 2007). The Lidar data was confirmed by ground truth measurements made at the three field sites. The estimations using Lidar have errors ranging from 20% (site 1), 110% (site 2) and 50% (site three) (note that the higher error occurs for the measurements made at a smaller scale). These geometrical measurements were then ground truthed and the field measurements of the geometry are estimated to have an error of $\pm 10\%$. However this is a low estimate of the error as the stage-discharge relationship is unknown – this could contribute up to 30-50% more error. These values are needed for both for the estimation of suspended sediment transport and for use in GeoWEPP.

Surface flow velocities were measured in situ by means of a simple chronometer. This provides spot checks in straight sections of the streams. Three measurements were made per estimation and the average used. A section was defined every five meters. The average of the estimations gives the final velocity. The velocities are used for the calibration of the GeoWEPP model.

5.2 Field estimation of Sediment loads

The following section presents the results of the estimation of the water discharge and the sedimentation from before the beginning of the construction of the pipeline of the Ambatovy project to the end of the construction. This requires field measurements of TSS, determination of the discharge and calculation of the sediment load from the TSS and the discharge.

Field measurements of total suspended solids (TSS)

The observations presented here are the measured Total Suspended Solids (TSS), the turbidity and the correlation between these two parameters, which provides a validation of the TSS values. During the monitoring campaign, the lowest values are not shown even they are checked in situ every three weeks.

The results are shown and discussed for each field study site.

TSS and turbidity were measured in the field for the first field site near the Ambatovy Mine from August 2008 to March 2013, as shown in Figure 28. The turbidity and the TSS data have a good correlation of $R^2 = 0.98$, Figure 29, providing confidence in the validity of the measurements. The data show that the sedimentation was highest during the construction period, but peaks after the construction period are found during the cyclone season. The highest value of TSS of 338 [mg/l] occurred during the construction period. Civil engineering works under construction during this peak were excavations and cut and fills. To reduce the increase in turbidity in the streams, stabilisation works on the embankments using the geotextiles, filters and rocks were established. During the post construction phase, there was a peak of 164.5 mg/l during the cyclone season in January 2013. This value occurred during the revegetation phase and was the only high value of turbidity during this period of the construction. The data also show that the peaks decreased after the main phase of the construction and the trend is to recover to the pre-construction values during the revegetation phase. Construction at this site lasted from September 2008 to March 2012. For this site, the lowest values are not shown in the monitoring reports and are just checked in situ. The monitoring was focused on the compliance and the attention was spotted on the high values. The full data used in the calculations is provided in the Appendix E and presented in the graphs.

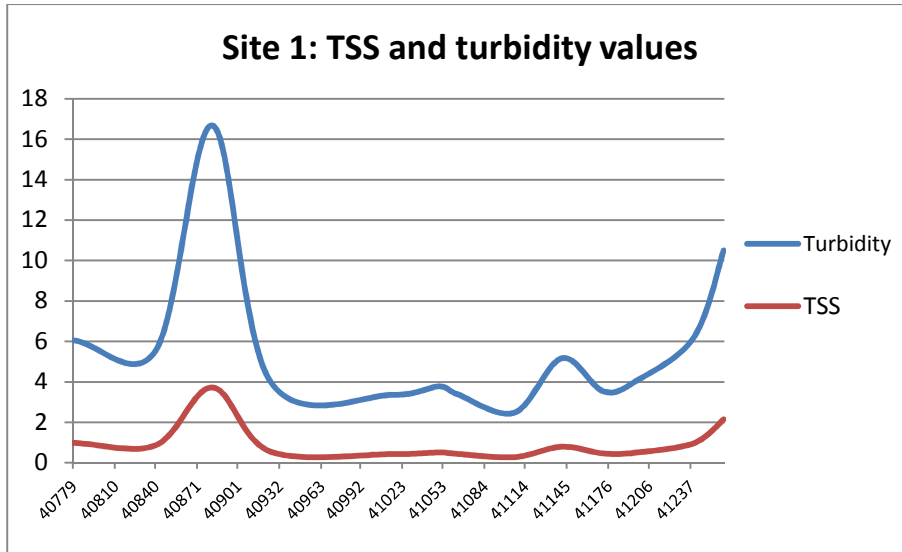


Figure 28. TSS and turbidity values for the Ambatovy mine site case

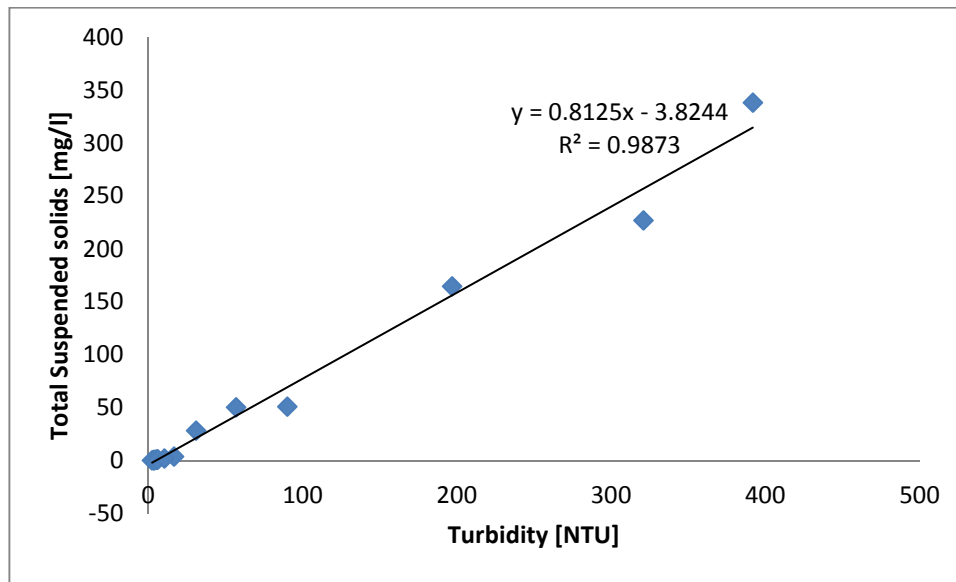


Figure 29. TSS and turbidity correlation for the 1st study case

At the second field study site near Anivorano data was collected from May 2010 to March 2013, shown in Figure 30. The correlation between the turbidity and the total suspended solids was $R^2 = 0.74$, shown in Figure 31, with three TSS values being significantly lower than the trend. Construction at this site started in May 2010 with civil works such as excavations. Construction was finished by March 2012 when the planting of the revegetation was complete. The highest TSS measured of 22 mg/l was within the required norms and as the sample site was situated at

the bottom of a high hillslope, these results are acceptable for the construction phase. During the post construction phase, the higher peaks occur again during the cyclone season between 2010 and 2012. Now, post construction the TSS values during the rainy season are satisfactory as they are similar in magnitude to the values before the beginning of the construction phase, with high values of sedimentation during rainy days but still in the acceptable norms. For this site, during the period between May 2010 to May 2012, just nine values were checked due to the access road difficulty during the construction due to the rain. Nevertheless, efforts were made after for better monitoring after May 2012 because this site has high risk of erosion and sedimentation even after the construction period and during the revegetation phase.

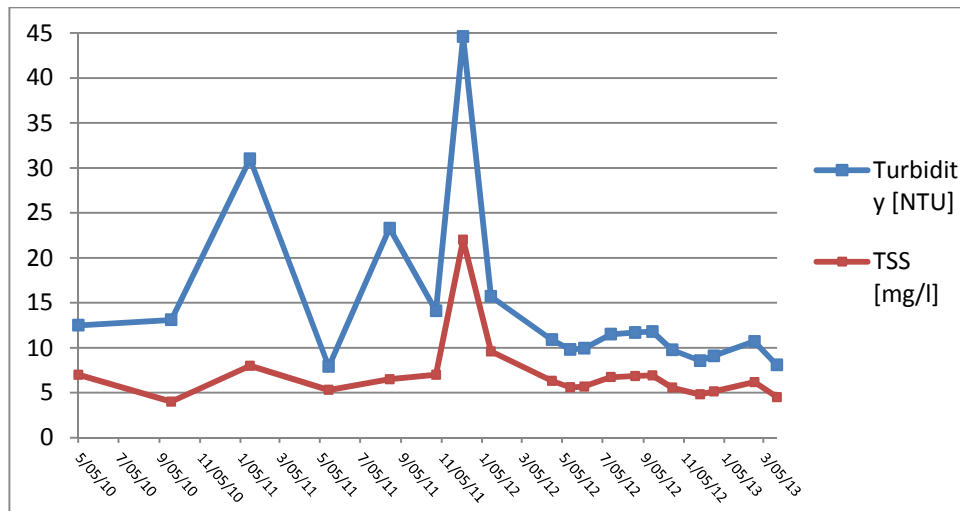


Figure 30. TSS and turbidity values for the 2nd study case, RoW 08-09.

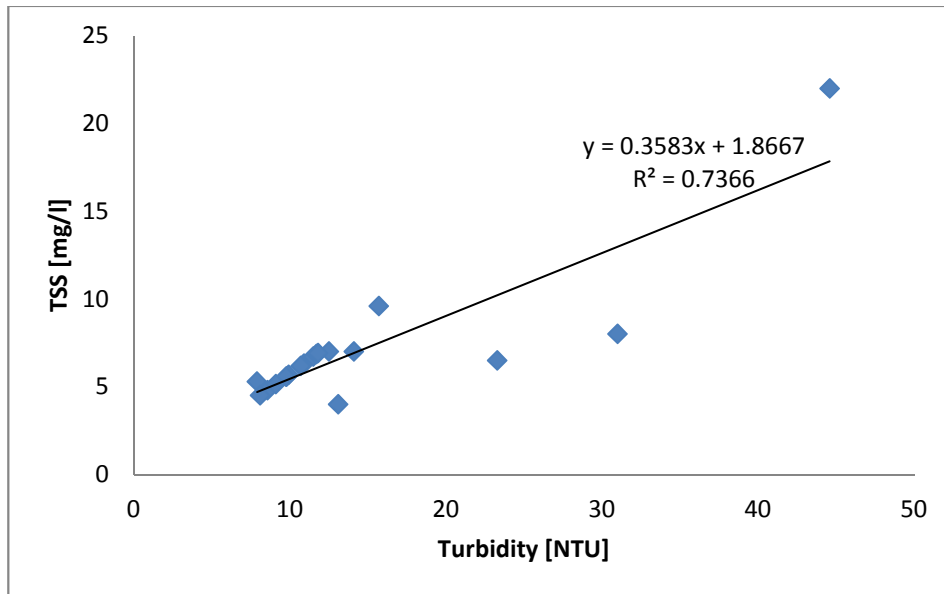


Figure 31. TSS and turbidity correlation for the 2nd study case

At the third study site near the Toamasina region, data was collected from January 2010 to January 2013, Figure 32, and the correlation of the turbidity with the total suspended solids was $R^2=0.98$, Figure 33. At this site construction began in October 2010 consisting of excavation and cut and fills. The highest TSS measured of 45.65 mg/l occurred in 2012, which was post-construction and not during the rainy season. The main activities during the post construction phase are the remediation and re-corrections of the slopes, the stabilization of the embankments and revegetation if needed. This region has a particular climate such that from June to September and in cold weather there is constant drizzle. This would result in saturation of the soil and easier loss of sediment due to surface runoff. The second highest value occurred during the rainy season. The data used for the calculations at this site all fall within the required norms. For this site, the TSS was checked often after the construction for a better compliance and the values were similar to those during the beginning of the construction phase. Data have been monitored nominally every three weeks; nevertheless for many reasons as impossible access road due to cyclones seasons or during the construction phase, there were some times the three weeks period was not respected.

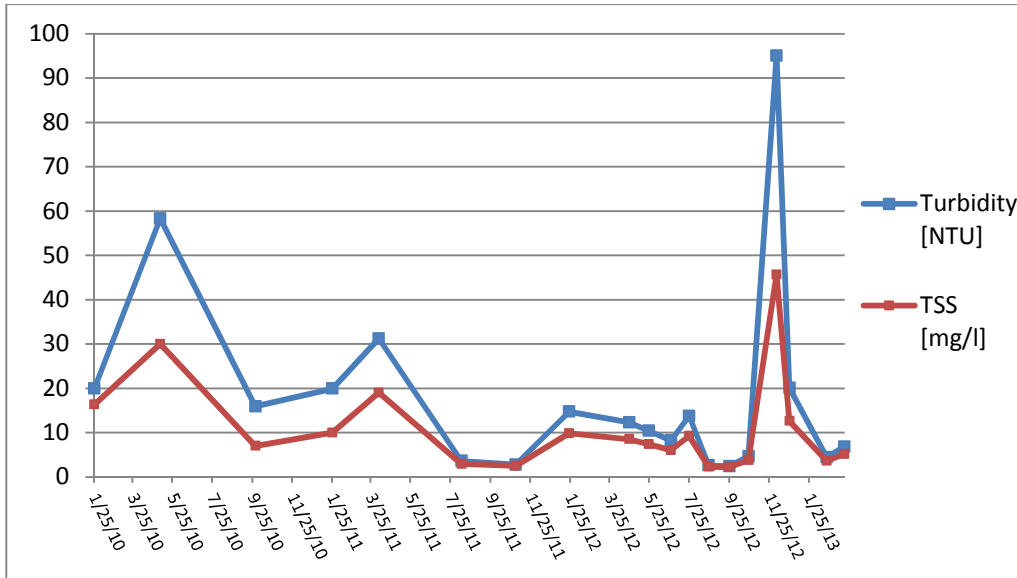


Figure 32. TSS and turbidity values for the 3rd study cas, RoW 13-14.

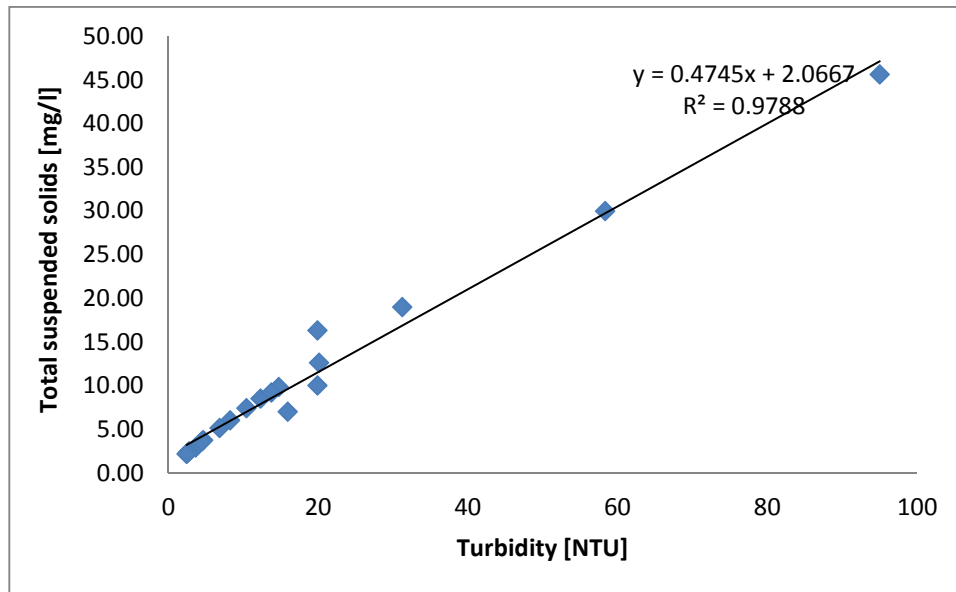


Figure 33. TSS and turbidity correlation for the 3rd study case

5.3 Water discharge calculations

Water discharge estimates at the three field study sites are presented below. The data used in the calculations came from the Ambatovy weather station, the World Meteorology Organization

(ref. Rakoto, 2007), and the document entitled “Fleuves and Rivières de Madagascar” (cf. and Danloux, 1993).

The total discharge over a year period using the daily hydrograph for the full year hydrograph, from 30 min data, which was then averaged and provided as daily data, is estimated using the reference station method. Only the annual average discharge is estimated using Manning’s equation.

5.3.1 Discharge estimated by the reference station method

For the 1st and the 3rd cases, the calculations of the discharges are performed using the data from the reference stations at Ambatovy, Moramanga, Rianila, Toamasina plant and Ivondro ORSTOM weather stations, respectively. The discharge information at these ORSTOM stations is provided normally once per day but increases to 3 times per day during the cyclones. For the 2nd case, the calculations will be completed by interpolating from the two reference stations (from Ambatovy and Toamasina Plant) and verified by checking the coefficient of correlation obtained through the discharge calculations of the two reference stations, using a 50/50 average. The 1st case is a sub-catchment of the Rianila main watershed. The 3rd case is a subcatchment of the Ivondro main watershed. The ORSTOM stations are used to verify the discharge estimations. In terms of elevation range and land use, Table 5 is presented below for comparison of the main catchments to its sub-catchments.

Table 5. Land use and elevation range comparison of the main catchments to its sub-catchments

Case	1 st case	2 nd case	3 rd case
Land use	The same land use as Rianila’s as it is in the main forested part of Madagascar without any access road yet. Rianila’s land use is composed by the dense rain forest	The land use is particularly established between the deforested area and the vegetation of the 3 rd case, with almost transitional forest or 5 th year	The same land use type as Ivondro’s as it is in the flat coastal region. Ivondro’s land use is composed especially by shrubs, grass with marshes in the flat areas (15%).

	(100%).	forest and shrubs.	For the rest, the azonal forest is observed (85%).
Elevation range	Same steep slope of 25m/km (ORSTOM, 1995)	Same steep slope of 25m/km (ORSTOM, 1995)	The same elevation range as Ivondro's as it is in the flat coastal region.

Therefore field site 1 is considered similar to the Ambatovy Moramanga, Rianila station, and field site 3 similar to the Ivondro ORSTOM station. Field site 2 has hillslopes and river slopes similar to Ambatovy Moramanga, Rianila station and vegetation that is partly similar to Ivondro ORSTOM station. Although the hydrological processes are likely to be different from the gauged stations, there is no other alternative and a 50/50 weighted average of the two reference stations is used as this then provides the best estimate. The weighted average used in the reference station method was based on the area of each watershed. Both daily and monthly average data for rain and discharge for the years 2008 to 2013 were available. For the reference station, the data are available as daily data and as thrice daily data for cyclones.

The resulting annual average discharges and the total annual discharge estimated from the daily discharge data are determined for the three study sites as given in Table 6.

Table 6. Water discharge by using the reference station methodology

Case	1st case	2nd case	3rd case
Reference of the station	QESF 103	Interpolation QESF 103 -229	QESF 229
Coordinates of the referenced watershed	220 748 7 913 139	247 040 7 919 593	314 909 7 988 652
Referenced station annual water discharge Q_r [m^3/s] (1)	0.3	69.8	107
Area of referenced station [km^2]	15.1	1910	2560
Area of the watershed of study [km^2]	10.133	0.249	0.141
Corrected area [km^2] (2)	11.81	0.29	0.15
Specific water discharge [$m^3/s/km^2$]	0.013	0.036	0.042
Annual average water discharge	0.204	0.009	0.006

[m ³ /s]			
Total annual discharge from the annual average discharge [m ³ /s]	72.75	3.38	2.15
Total yearly discharges using the full year hydrograph [m ³ /s]	72.8	3.33	2.19

(1)The discharge is the annual average discharge calculated from daily discharge.

(2) The area is corrected from a horizontal projection to the total area by accounting for topographical relief.

The following graphs present the full year discharges for each site, respectively in Figures 34, 36 and 38. The annual average discharge is shown in Figures 35a, 37a and 39a respectively for each site. The full year hydrograph is estimated from the daily data, which is supplied as an average of data recorded every 30min from the weather stations at Ambatovy and Toamasina regions.

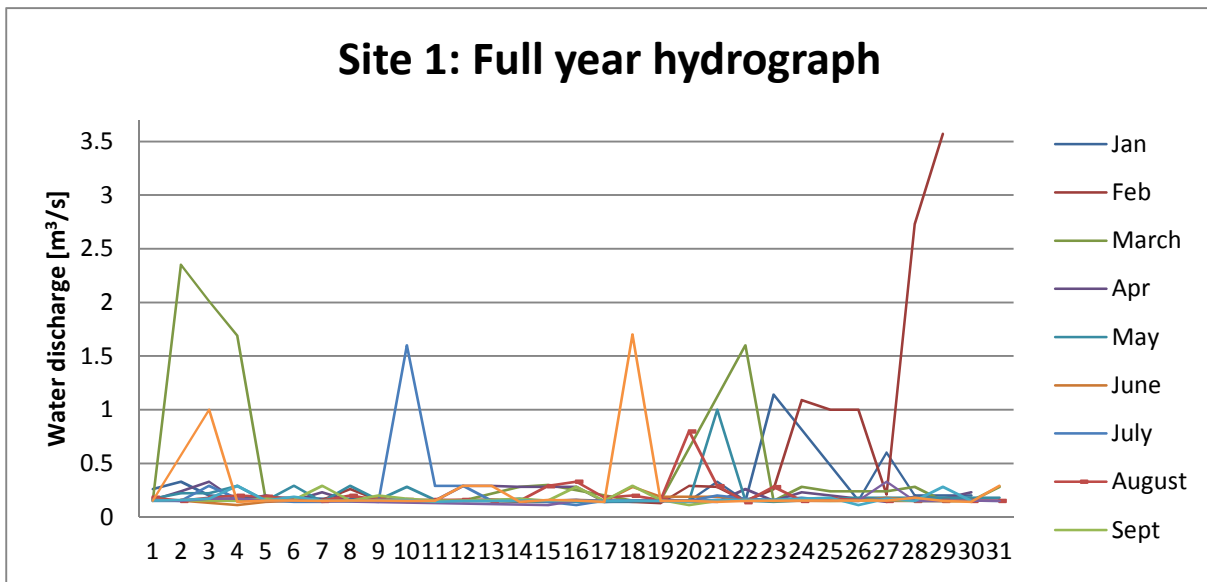


Figure 34. Water discharges for the first field site

The water discharges values for the first field study are established from 0.065[m³/s] to 3.57[m³/s] for year 2012.

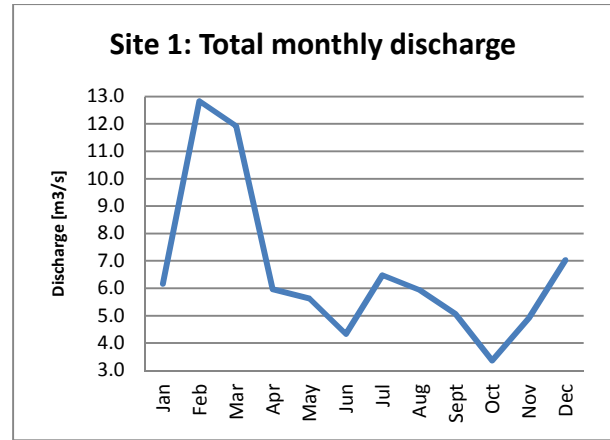
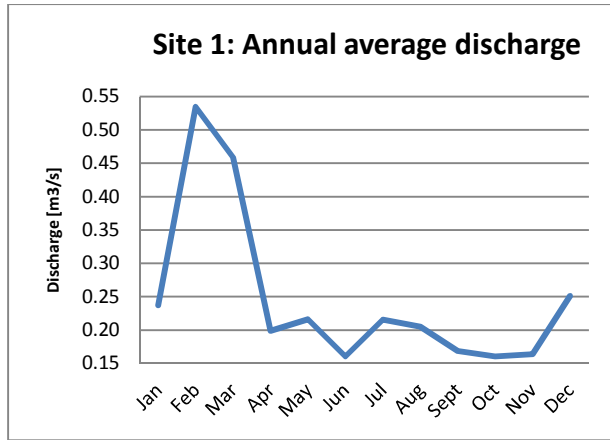


Figure 35.a) Annual average water discharges

b) Total monthly discharges

The water discharges values for the second field study are established from 0.028[m³/s] to 0.085[m³/s] for year 2012.

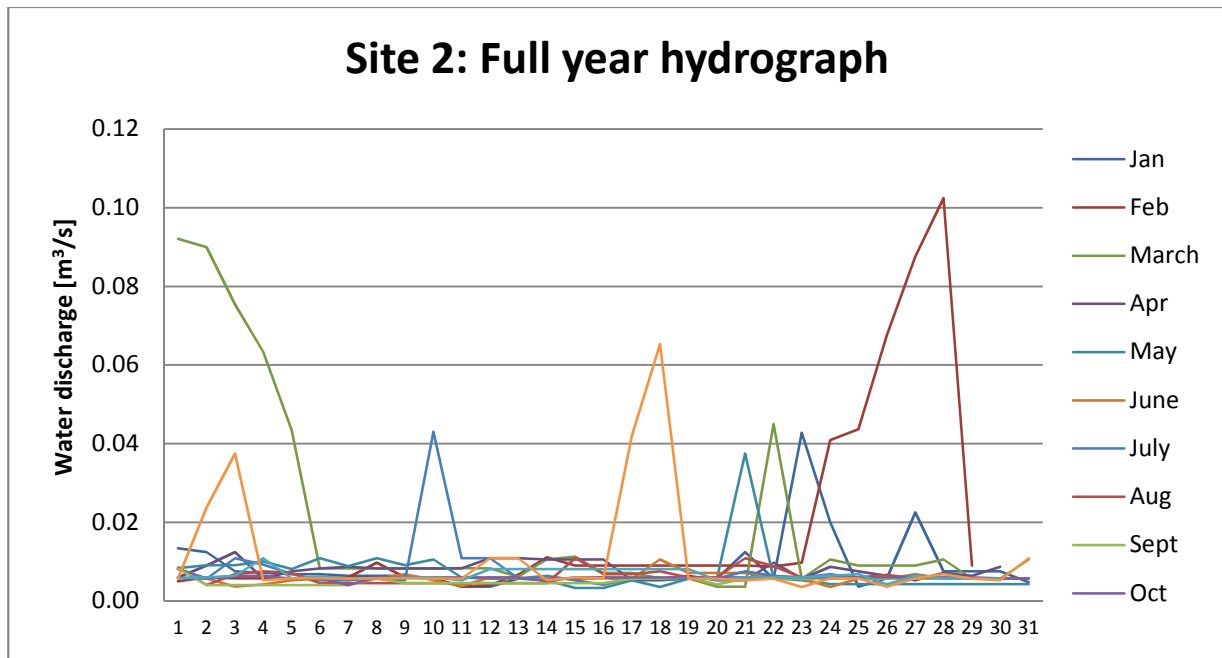


Figure 36. Water discharges for the second field site

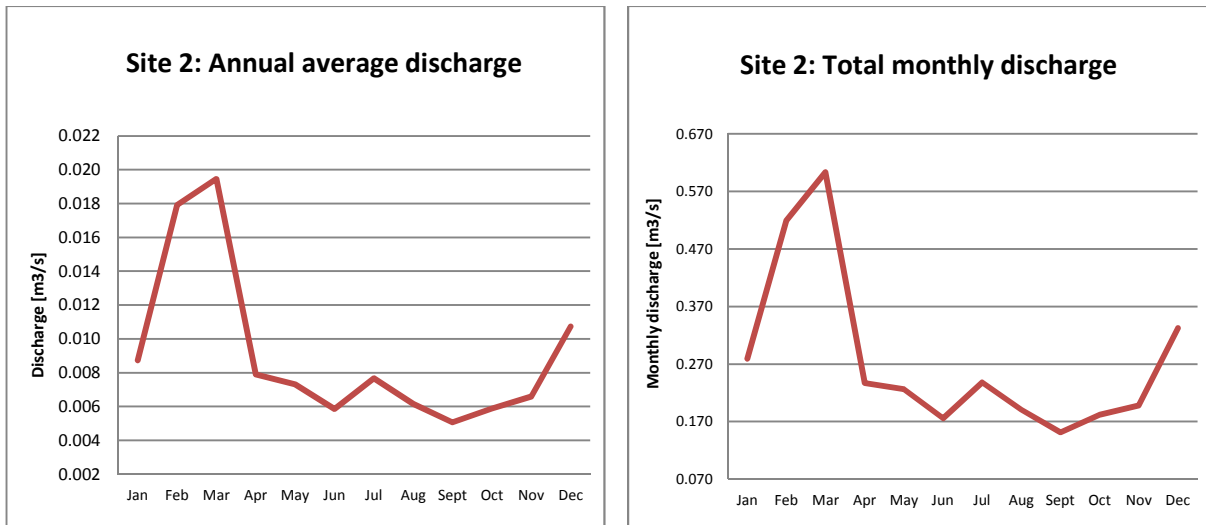


Figure 37 a). Annual average water discharge b) total monthly discharges

The water discharges values for the third field study are established from 0.049[m³/s] to 0.013[m³/s] from 2010 to 2013.

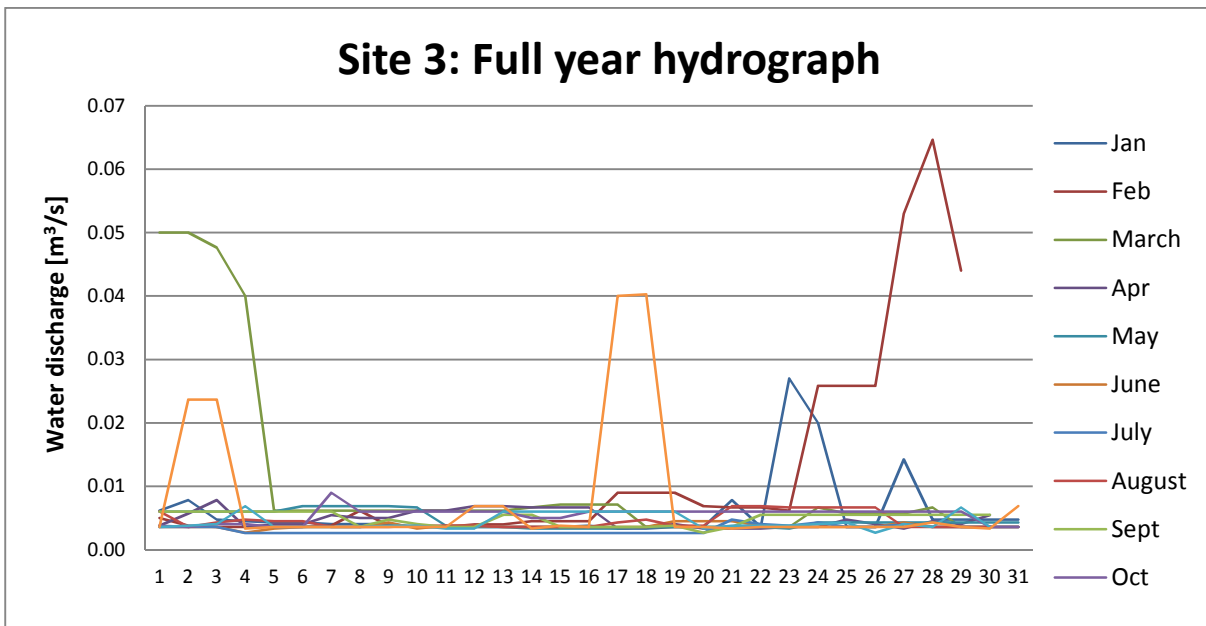


Figure 38. Water discharges for the third field site

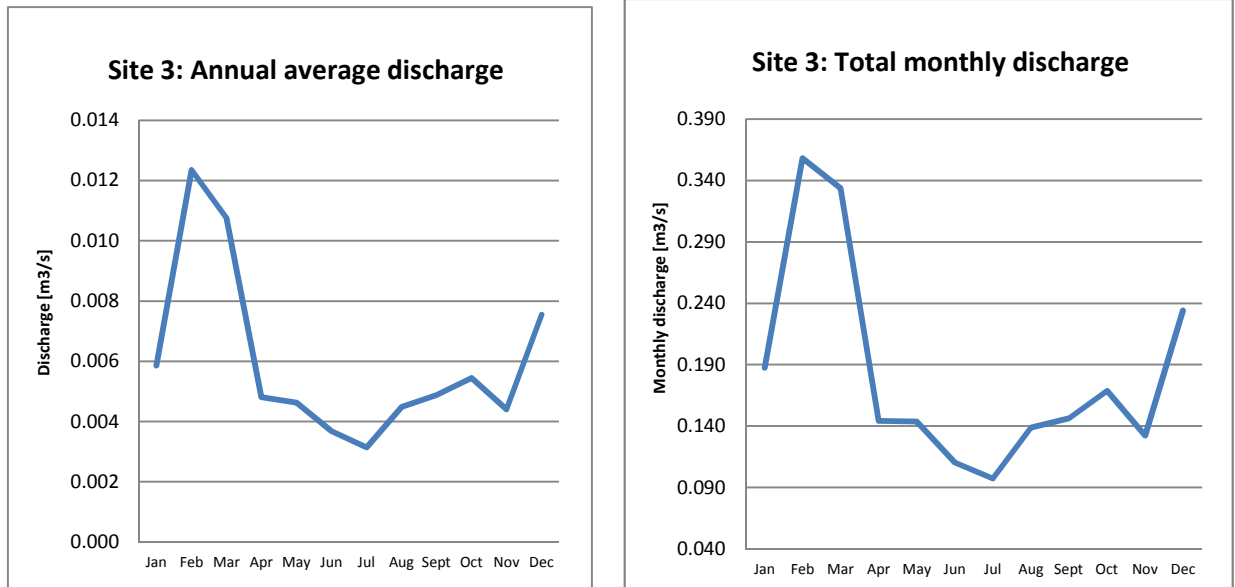


Figure 39 a) Annual average water discharges b) Total monthly discharges

5.3.2 Second methodology: Manning’s equation

Manning’s equation is used to estimate the discharge by estimating the geometrical parameters from the DEM and the Lidar images and then measuring them on the ground. The water discharge is calculated for the three field sites at the outlet of each watershed. Figures 14, 19 and 23 show respectively the outlet for the first, the second and the third field sites. ArcGis was used with the Lidar and the DEM to estimate the longitudinal channel slope, the area of the cross section and the hydraulic radius. Because the resolution of the Lidar images for the study is 16cm, the magnitude of the errors in the estimation of the geometrical parameters is 20% for the area.

The slope was estimated on the assumption that flow is routed consecutively from one upstream cell to only one downstream cell, thus creating a channel that is one cell wide (FERENCEVIC & ASHMORE, 2012). The assessments were done from the bed stream level and measured in meters (elevation) per kilometer (stream drainage). Therefore, the related error of uncertainty is insignificant, around 3%. For the field study sites, the watershed’s slope is assessed as the longest constant section with a constant slope from the top of the watershed to its reach as presented in Table 7.

Table 7. Calculated gradients with different lengths for each field case.

Case Length [m]	1 st case	2 nd case	3 rd case
200 [m]	0.005 ($\pm 1\%$)	0	0.02 ($\pm 2.5\%$)
500 [m]	0.012 ($\pm 1.7\%$)	0.008(± 1.3)	0.024 ($\pm 3\%$)
1000 [m]	0.012($\pm 1.7\%$)	0.0425 ($\pm 5\%$)	0.042 ($\pm 5\%$)
For the entire watershed	Gradient of 0.057 for 3630m	Gradient of 0.06 for 1020m	Gradient of 0.029 for 670m

The cross section area and the hydraulic radius was based on the assumption of a trapezoidal section for each site and the required measurements were undertaken on site. Three different measurements were taken for each field site and the average was determined.

The average water depth was estimated during the TSS monitoring by using a meter or a ruler. The field measurements were done throughout the year, during sunny or rainy days. Therefore, an averaged value of the water depth is presented, based on engineering judgement. The width of the stream section was checked on site but also measured by the satellite images.

The Manning coefficient was estimated based on a visual qualitative description of the river and related to values in the literature (Chow, 1959). The rivers of the field study sites are more or less natural streams with a main channel, even during the pipeline construction phase. The channels are clean, straight, full stage and without rifts or deep pools.

- For the first and the third field study sites, the streams are in lower stages with lower slopes. Some bank protection with a pavement of stones was added along some short lengths of the water course crossing the pipeline. Nevertheless, the stream section where the monitoring and the surveys were executed remains straight and fairly natural. The Manning's n values is estimated to be $n = 0,048$.
- For the second field study site, the stream has the main characteristics similar to the first and the third field study sites (in lower stages with low slope). Nevertheless, from Figure

20a, the stream is shown as weedy with sluggish reaches. It is due to the flatness of the area almost used as a rice field. The Manning's coefficient estimated as $n = 0,075$.

The results are presented in Table 8. The pictures of the cross-section for each site are presented in Appendix E.

As described in the methodology, the geometry was estimated using ArcGIS software on the DEM created using Lidar data and also measured in the field. The width and the depth were measured during the field monitoring.

Table 8. Water discharge calculations using the Manning's equation

<i>Case</i>	<i>1st case</i>	<i>2nd case</i>	<i>3rd case</i>
Manning coefficient n	0.048	0.075	0.048
Area of cross section A [m²]	0.180	0.172	0.017
Hydraulic radius R [m]	0.114	0.066	0.016
Longitudinal slope S [m/m]	0.028	0.0012	0.06
Annual average water discharge Q [m³/s]	0.144	0.009	0.005
Total annual discharge [m³/s]	52.56	3.28	2.08
Estimated error for the area	±12%	±26%	±20
Estimated error for R	7%	18%	15%
Estimated error for Manning's n	10%	10%	10%
Estimated error by using the partial slope	0.8%	1%	3%
Total Estimated error for the discharge	34%	133%	71%

The longitudinal slope was estimated, to best approximate the assumption of uniform flow of Manning's equation, along a reach in which the slope was closest to constant in a reach upstream of the cross-section. Uniform sections for each entire watershed were reviewed using ArcGIS Tool as the Slope, especially around the cross section. Therefore, for the first field site,

the longitudinal slope, as shown in Table 8, was estimated for 1350m reach, 900m for the second field site and 400m for the third field site.

The water discharge is used to determine the field estimates of sedimentation, the averaged sediment transport capacity from the sediment transport equations and the sedimentation from the GeoWEPP model.

5.4 Calculation of wash load transport rates (annual estimate) with the field data

The wash load transport rates estimated from the TSS field data and the annual water discharge give the following results presented in Table 9.

Table 9. Annual Average wash load rates estimated from the field data

Type of water discharge	<i>From Manning's equation</i>			<i>From the reference station</i>		
Case	<i>1st case</i>	<i>2nd case</i>	<i>3rd case</i>	<i>1st case</i>	<i>2nd case</i>	<i>3rd case</i>
Annual average water discharge [m³/s]	0.144	0.009	0.006	0.204	0.009	0.006
Total annual discharge [m³/s]	52.56	3.28	2.08	72.75	3.38	2.15
Annual discharge comparison [%]	27.8%	3%	3.33%	27.8%	3%	3.33%
Average annual TSS rates [mg/l]	1,13	15.79	17.19	1.13	15.79	17.19
Annual wash load rates [Tons/year]	5.15	4.48	3.25	7.27	4.481	3.251

The estimate of sediment discharge has an error which is due to the error in the estimated annual average discharge and an error from the estimated TSS. The estimated error in the discharge using the Manning equation was determined in Table 8 to be 34%, 133% and 71% respectively for sites 1, 2 and 3. The error in the reference station method is not known as discharge was not measured at the outlet of any site. We can assume that it is in the same range as the Manning's equation estimate, i.e between 50% and 130%.

Nevertheless, Ambatovy Project has always monitored the discharges for the respective main watersheds of each site for long time with a certain confidence (EIA Ambatovy, 2006) and with consideration of the references from studies before (Chaperon P., Danloux J., 1993).

Discharge estimated using the reference station method and the Manning's method provide estimates that differ from each other by 27.8%, 3% and 3.33% for sites one to three respectively. This provides sufficient confidence in the discharge values calculated, given the errors and uncertainties in the estimations, estimated at $\pm 34\%$ for the first field site and $\pm 130\%$ for the 2nd and 70% for the 3rd field site.

The TSS rates are the estimation of the annual average values, based on measurements taken over the full year of 2012 for all 3 field sites. The TSS rate includes the peaks and the low values, as the random sampling is assumed to represent the yearly variation in the TSS concentrations and the larger rainfall runoff events move proportionally more sediment than smaller events. During the monitoring, the low values have not been assessed in the laboratory due to budget management. Nevertheless, these low and acceptable values are always monitored in situ and reported.

The TSS rates vary due to the variation in the rainfall intensity and duration. The variation in TSS with discharge is examined below and the TSS corresponding to the average annual discharge is used. As TSS increases with the magnitude of the rain-fall event, then using the average discharge and its corresponding TSS underestimates the sedimentation as the larger rainfall runoff events move proportionally more sediment than smaller events. This bias is examined by calculating the total sedimentation below using the daily hydrograph and the TSS that corresponds to the daily discharge. The rainfall data of Ambatovy and Ivondro weather stations, are examined for the storm hydrographs to give more information about the peaks and the intensity of the rainfall related to its duration.

- The storms events near the mine area close to the first field site increase in intensity by around 50% to 60 per half hour and also reduced at the same rate. The storm hydrograph usually lasts 1h30 min to 2 hours. Therefore, the highest runoff and the wash load estimated during rainfall peaks also will occur in short freshets in the river.
- The storms events near the Ivondro weather station close to the third field site are increase suddenly by 100% to 150% in a half hour for a storm event of one hour duration, with the rain stopping suddenly. Runoff and wash load will also follow is

pattern. This demonstrates that even the daily hydrograph will only be a rough estimate of the sedimentation as discharge varies over a time scale much smaller than a day.

This indicates that even using the full year daily hydrograph will not catch the highest wash load events as they occur in time periods in the order of one hour rather than one day. However, the daily data provides the best available estimate within the study's data constraints.

5.5 Wash load using a full year hydrograph

The water discharges is used to calculate the sedimentation rates, combined with the TSS values by the development of a relationship for each field site using the full year hydrograph. The water discharge, provided as a daily average from data recorded every 30mins, is considered for the following calculations. The year 2012 is chosen.

Therefore, the in situ sedimentation data are collected for the Year 2012. The water discharges related to the in situ data are collected. The relationship between TSS and water discharge is determined and assessed as reasonable based on its correlation coefficient.

Figures 40, 41 and 42 show the TSS values related to the water discharge values for the specific days respectively for each field site. From the results, a relationship between TSS and discharge is established. The bias and the high values have been excluded in order to obtain a better correlation between the data (outliers due to isolated construction activities).

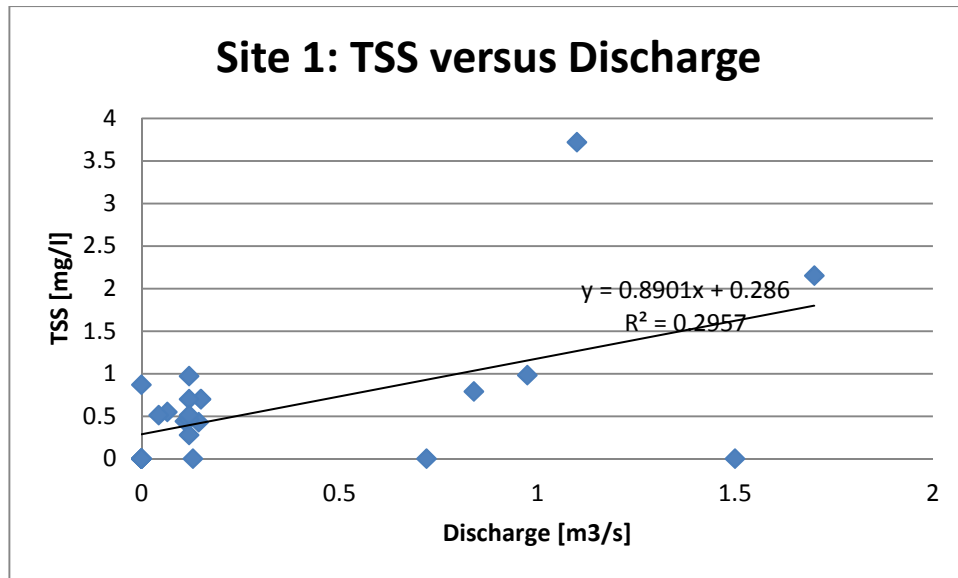


Figure 40. TSS values versus Water discharge values for the first field site.

For the first field study site, the correlation between TSS and the water discharge is equal to $R^2=0.2957$ and the relationship is $TSS [mg/l] = 0.89 \text{ discharge } [m^3/s] + 0.286$.

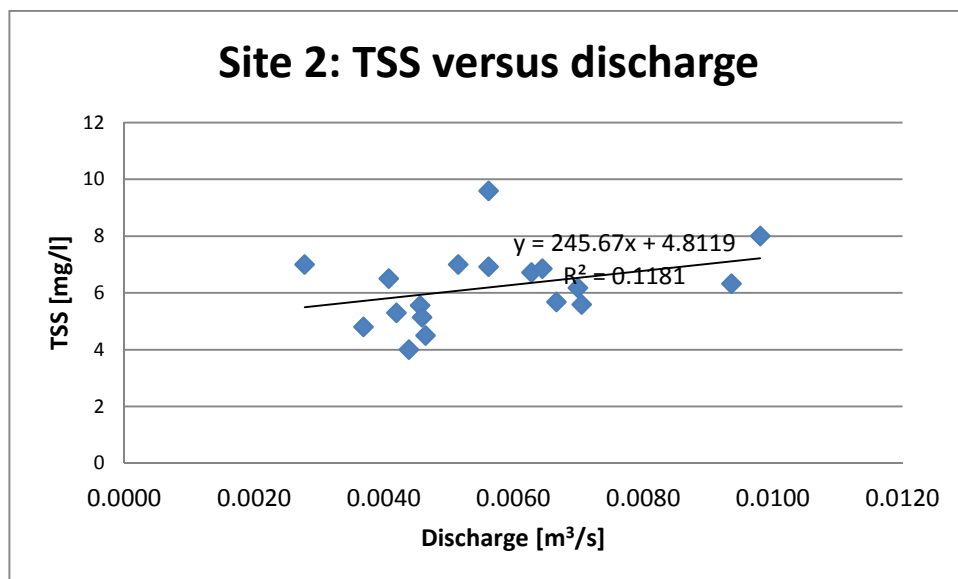


Figure 41. TSS values versus water discharges for the second field site

For the second field study site, the correlation between TSS and the water discharge is equal to $R^2=0.11$ and the relationship is $TSS [mg/l] = 246 \text{ discharge} [m^3/s] + 4.8$.

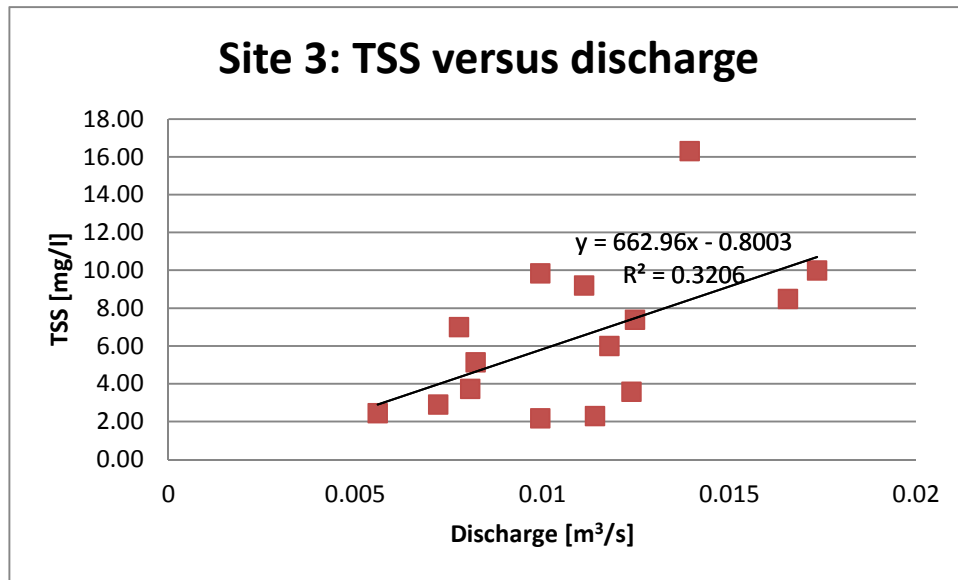


Figure 42. TSS values and water discharges for the third field site.

For the third field study site, the correlation between TSS and the water discharge is equal to $R^2= 0.32$ and the relationship is $TSS [mg/l] = 663 \text{ discharge} [m^3/s] - 0.8$.

Note that these relationships have not been forced through the origin which implies that even at very low flows there is a TSS, particularly for site 2.

These relationships between TSS and discharge indicate that there is very little sedimentation at the first field site (with TSS increasing at only 0.9 times the discharge), a greatly increased amount at the second site (with TSS increasing at 246 times the discharge) and the greatest sedimentation at the third field site (with TSS increasing at 663 times the discharge).

The full year daily hydrograph data of the Year 2012 were presented in Figures 36, 37 and 38. These water discharge values are calculated from the station reference method, using average daily values which were supplied from 30 mins recorded data. Therefore, from the relationship obtained by the relationships between TSS and discharge above for each site, the calculations of the field site estimate of the wash load are therefore established, for a one year long

hydrograph. The annual estimate of wash load is therefore calculated as a total estimate and an average estimate is also presented.

For the each field site, the wash load values for the 2012 year from the daily data are presented in Figure 43. The first graph shows the wash load for a full year hydrograph as a monthly value for each field site. Figure 44 presents the daily wash load for the 2012 year for each field site.

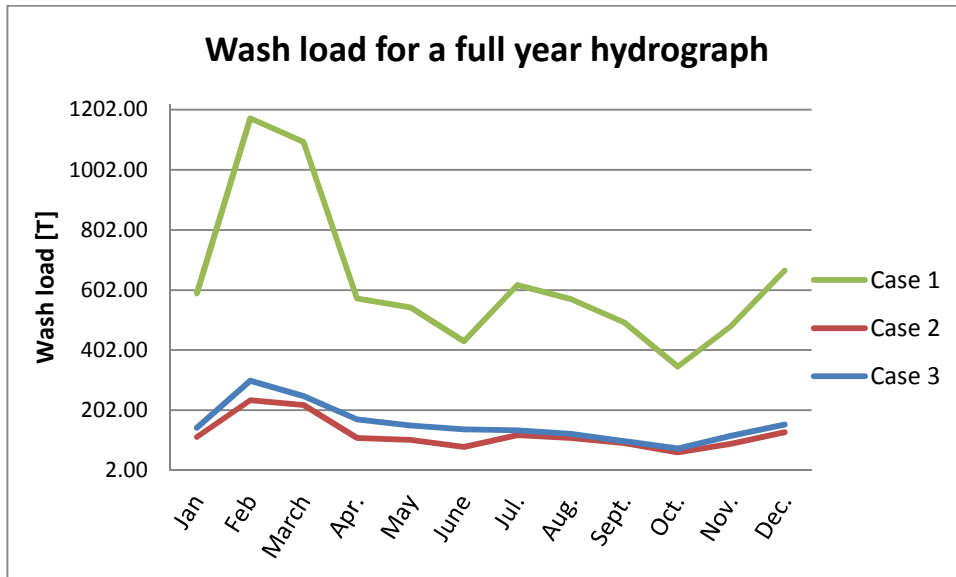


Figure 43. Monthly wash load data for each field site.

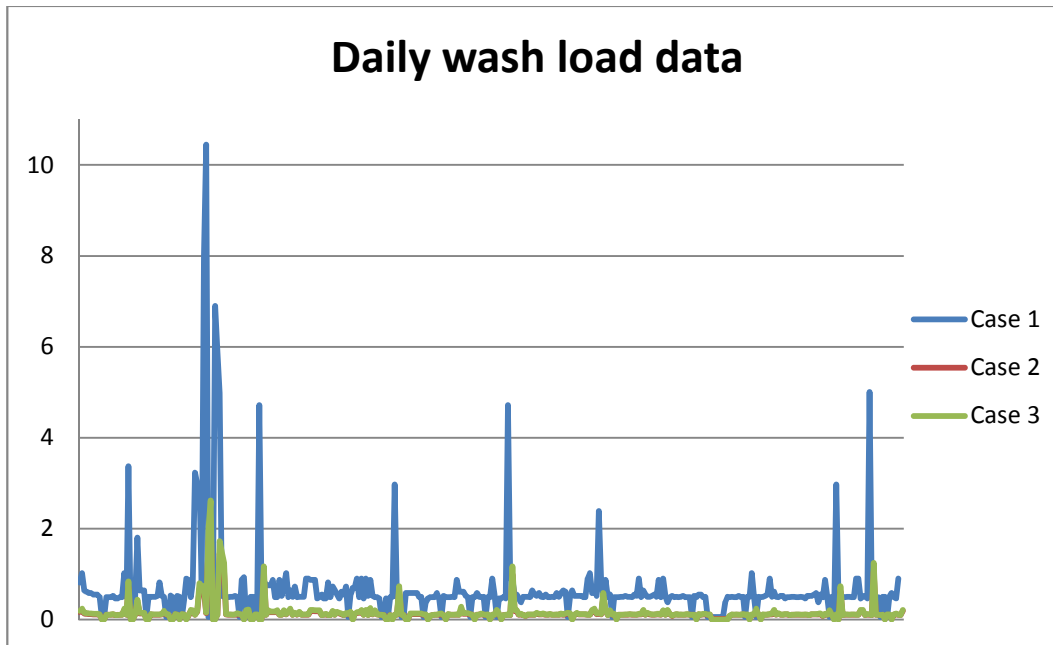


Figure 44. Daily wash load data for the three field sites.

The wash load calculated from the first field study is higher than the two other field study sites.

Table 10 presents the estimation of the sedimentation rates for each site. The appendix F presents the calculations.

Table 10. Estimation of the sedimentation rates for each site

	Case 1	Case 2	Case 3
Average rate of sediment transport X [mg/l]	1.13	15.79	17.19
Average Q [m ³ /s]	0.24	0.01	0.006
Wash load per area [tons/km ² /year]	0.72	11.2	21.66
Wash load per stream length [tons/km/year]	2.35	4.83	4.75

Therefore, these estimates are compared to the average annual sediment discharge according to the following Table 11.

Table 11. Average water discharge through the 2 methodologies

Methodology	<i>Estimation with TSS rates and the annual hydrograph</i>	<i>Average annual sediment discharge (reference station method)</i>

Case	<i>1st case</i>	<i>2nd case</i>	<i>3rd case</i>	<i>1st case</i>	<i>2nd case</i>	<i>3rd case</i>
Annual average water discharge [m³/s]	0.24	0.01	0.006	0.204	0.009	0.006
Annual wash load rates [Tons/year]	36.89	15.60	14.73	7,27	4.481	3.251
Sediment discharge comparison	500%	350%	450%	500%	350%	450%

5.5.1 Modeling with GeoWepp

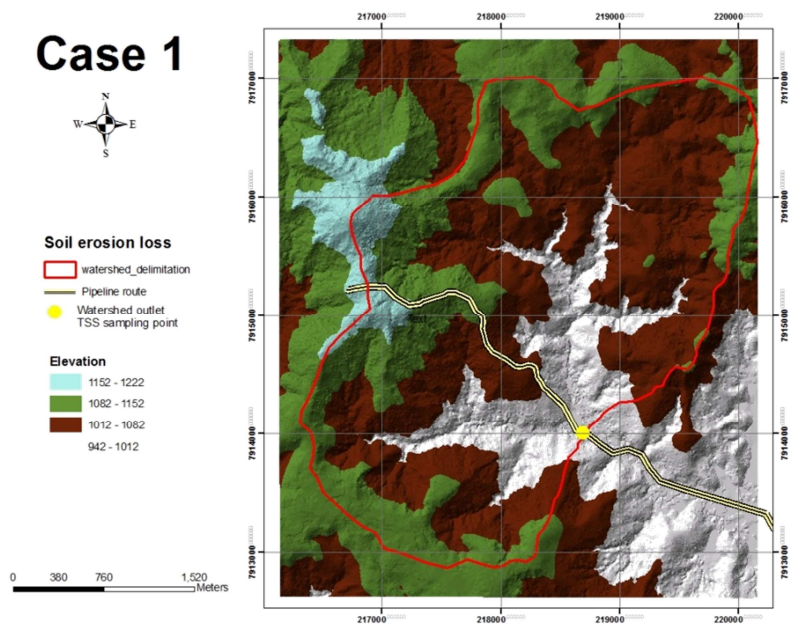
GeoWEPP is applied to simulate the total sediment discharge for each field site using detailed precipitation data, topography, soil and land cover information as described above in the methodology.

Once the input files had been prepared the simulations were run using the Watershed method. The model results are presented below.

5.5.1.1 First field site: Ambatovy mine

The first case near Ambatovy mine was developed and analyzed, of note is its land use which is mainly forest (primary forest) with some deforestation in azonal forest. Reports have been generated from the simulation to calculate the amount of soil loss.

This 1st case represents the lowest rate of soil erosion as the soils are protected by the forest and by bushes in the deforested areas. The topography and the land cover are respectively shown again in the following figures (14 and 45).



As Figure 14. First field site localisation

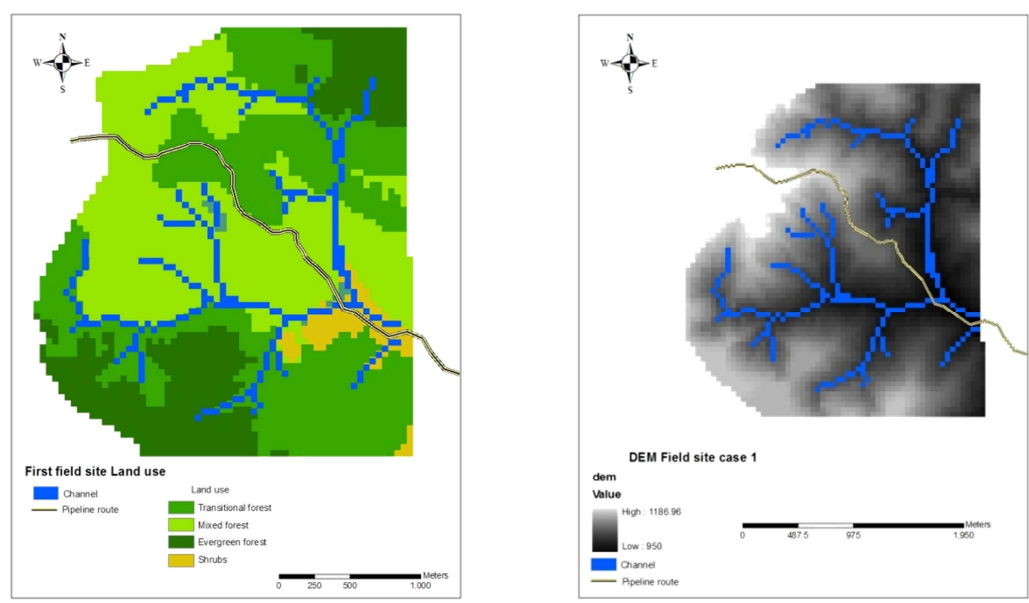


Figure 45. The vegetation cover and DEM of the first field site.

Figure 46 presents the results for the simulation at the first field site in its current state.

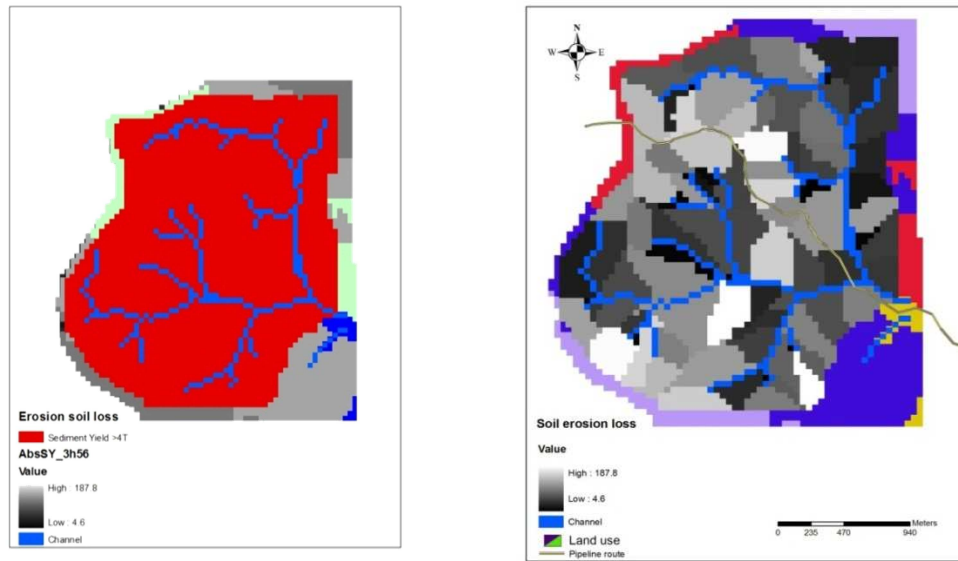
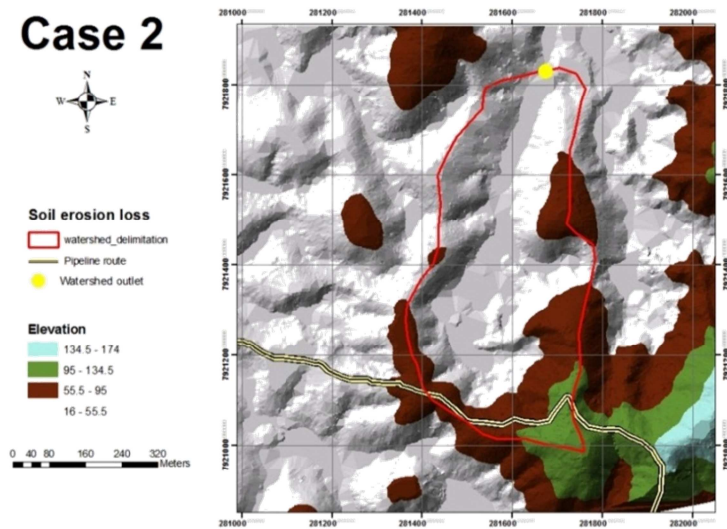


Fig 46. Simulation results for the Ambatovy mine field site a) in terms of the threshold of greater than or less than 4 T/ha/yr and b) in terms of the quantitative amount of soil loss [kg]

5.5.1.2 The second field site: midway along the pipeline

The second simulation shows the highest rate of soil erosion, as the area has been completely deforested with the vegetation reduced to bushes and grasses, which provide minimal erosion protection, while the hill slopes are steep. The land use is almost represented by the azonal forest and the 5th year forest. The topography and the land cover are respectively shown again in the following figures (18 and 47).

Case 2



As Figure 18. The second field site study location.

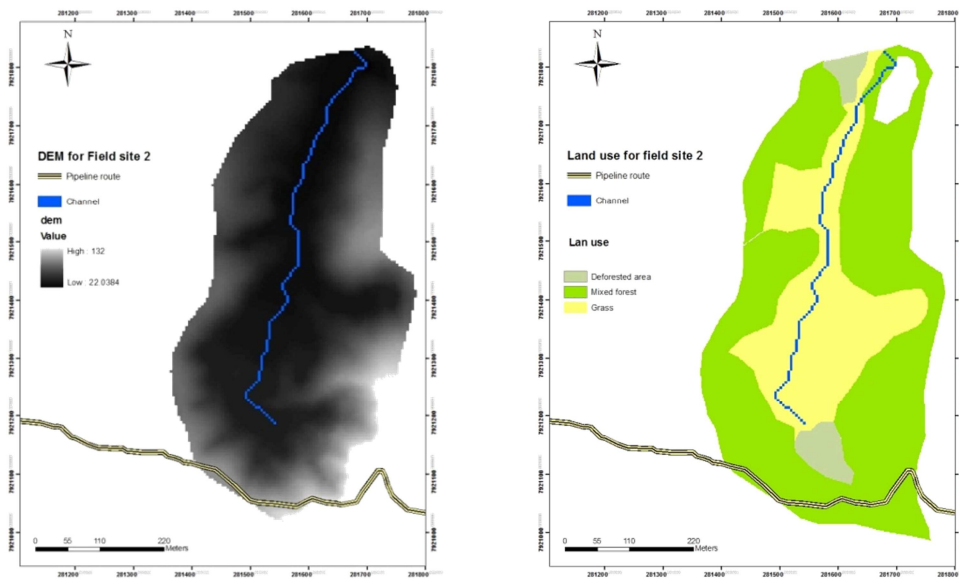


Figure 47. The vegetation cover and DEM of the second field site study

Figure 48 represents the results for the simulation for the field site in its current state.

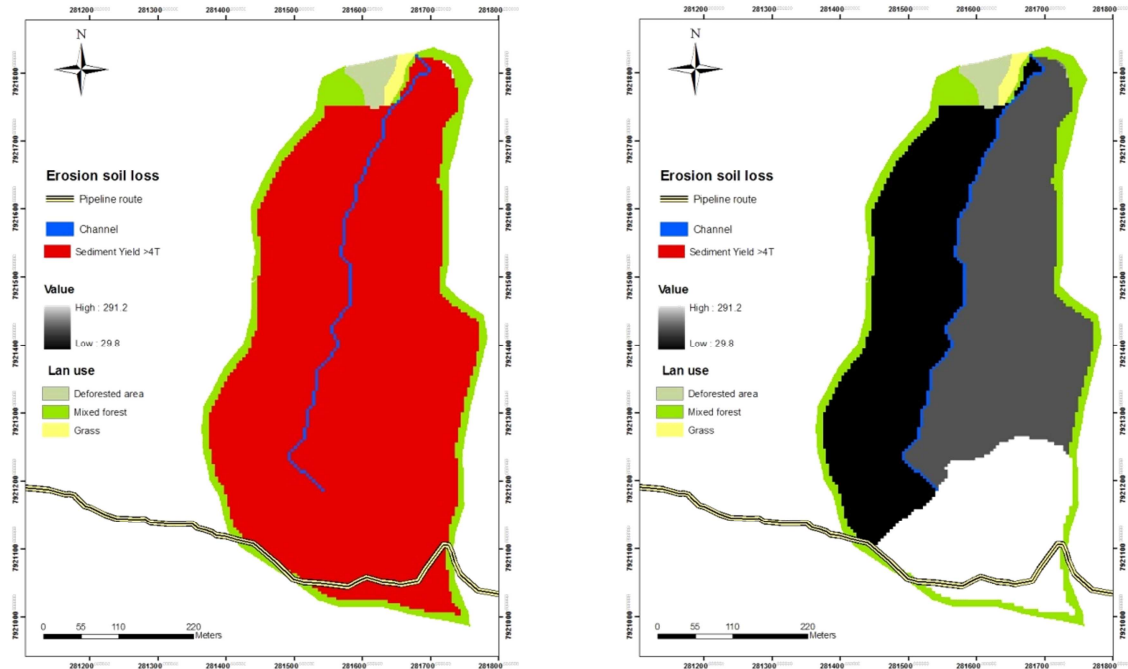
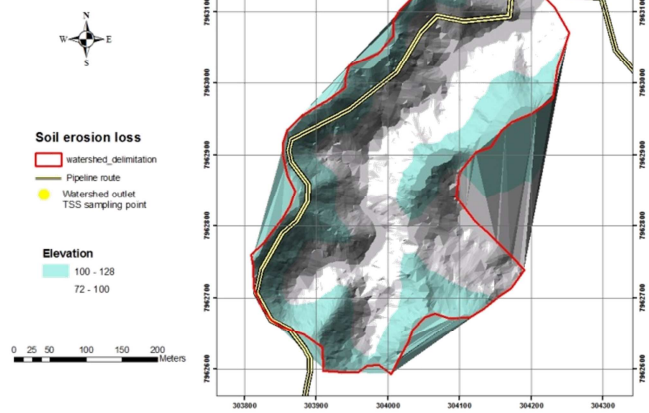


Fig 48. Simulation results for the second field site a) in terms of the threshold of greater than or less than 4 T/ha/yr and b) in terms of the quantitative amount of soil loss [kg]

5.5.1.3 The third field site: near the plant site

The erosion at the third field site is also simulated for its current state. The topography and the land cover are respectively shown again in the following figures (22 and 49). The land use is represented by 5th year forest with azonal forest and shrubs.

Case 3



As Figure 22: The third field site location

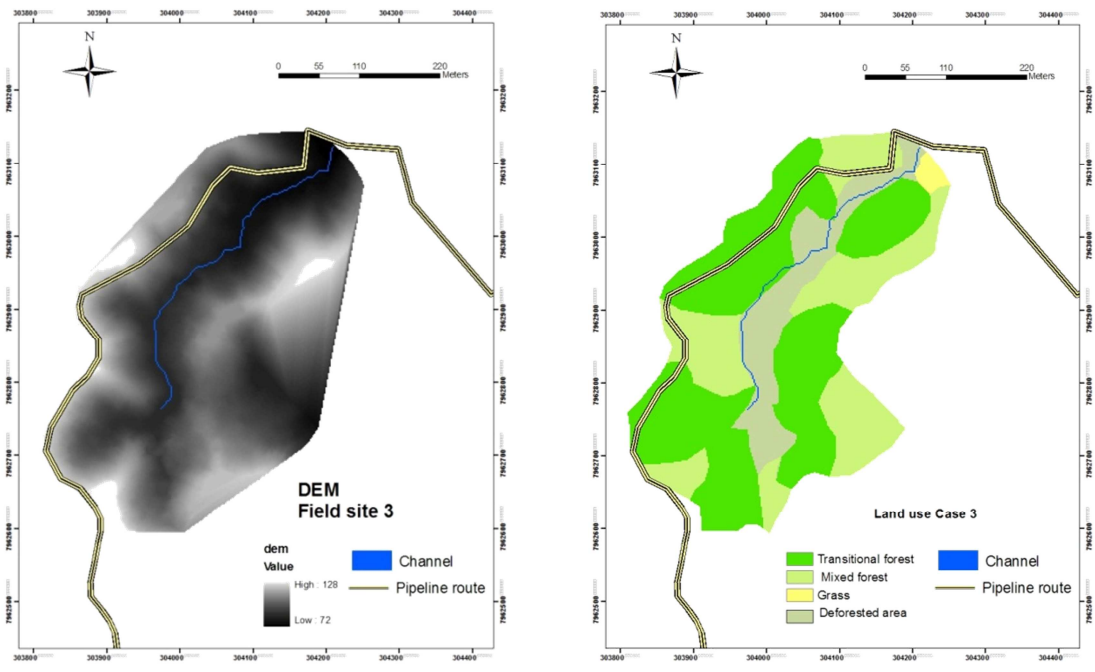


Figure 49. DEM and vegetation cover of the third field site

Figure 50 presents the results.

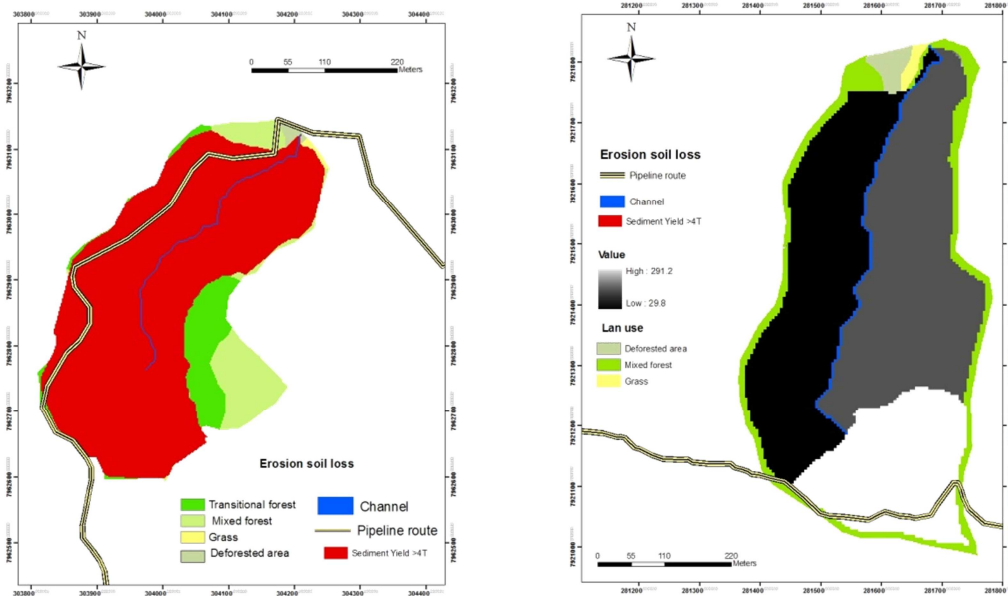


Fig 50. Simulation results for the third field site a) in terms of the threshold of greater than or less than 4 T/ha/yr and b) in terms of the quantitative amount of soil loss [kg]

5.5.1.4 Detailed analysis of sedimentation rates at the field sites

The following section presents the detailed erosion/sedimentation reports generated by GeoWEPP after each simulation. Each report shows the soil loss, the sediment discharge, the runoff, the water discharge and the number of storms and runoff events. The site description parameters of watershed area and soil particle size distribution are also given.

A report of these values are presented below for each field case in Table 12, in its post construction state, i.e before any hypothesized mitigation measures.

Table 12. GeoWEPP reports of erosion loss parameters for the 3 cases of study

WEPP WATERSHED SIMULATION FOR REPRESENTATIVE HILLSLOPES AND CHANNELS			
Case of study	Case 1	Case 2	Case 3
Phase of study : before or after mitigation	Before	Before	Before
Total contributing area to outlet [ha]	489.	21.6	11.6
Avg. Ann. Precipitation volume in contributing area [m^3/yr]	7.26×10^6	320×10^3	172×10^3
Avg. Ann. water discharge from outlet [m^3/yr]	1.71×10^6	81.8×10^3	18.7×10^3
Avg. Ann. sediment discharge from outlet [tonnes/yr]	36 200	165	72.3
Avg. Ann. Sed. delivery per unit area of watershed [T/ha/yr]	74	7.6	6.2

Sediment Delivery Ratio for Watershed	0.303	0.99	1.00
Clay fraction	0.24	0.25	0.30
Silt fraction	0.76	0.70	0.41
Sand fraction	0.003	0.063	0.287
Organic matter fraction	0.019	0.02	0.05
Index of specific surface [m ² /g of total sediment]	61	62.4	88.00
Enrichment ratio of specific surface	0.98	1	1
Number of years of simulation	2	2	2
Number of storms which produce [mm] of rainfall	237	237	237
Number of events which produce [mm] of runoff	64	54	87
Height of runoff [mm]	349	379	160

Chapter 6. Analysis and discussions

The estimation of sedimentation rates in the streams required the estimation of the stream discharge. The discharge was estimated using three different methods: the reference station method, Manning equation with stream geometric properties, initially estimated using LIDAR data and then measured in the field, and GeoWEPP simulations. Each of these methods has its own limitations and uncertainties, which will be discussed below. A comparison of the estimated discharges, shown in Tables 13 and 14 and in Figure 51, using these three methods provides some confidence in the values.

Table 13. Average water discharge through the 4 methodologies

	<i>Manning's equation</i>	<i>GeoWEPP</i>	<i>Reference station as annual average</i>	<i>Reference station as full year hydrograph</i>	<i>Average value</i>
<i>1st case [m³/s]</i>	0.144	0.0541	0.204	0.21	0.161
<i>2nd case [m³/s]</i>	0.009	0.0026	0.009	0.009	0.007
<i>3rd case [m³/s]</i>	0.005	0.0006	0.006	0.006	0.004

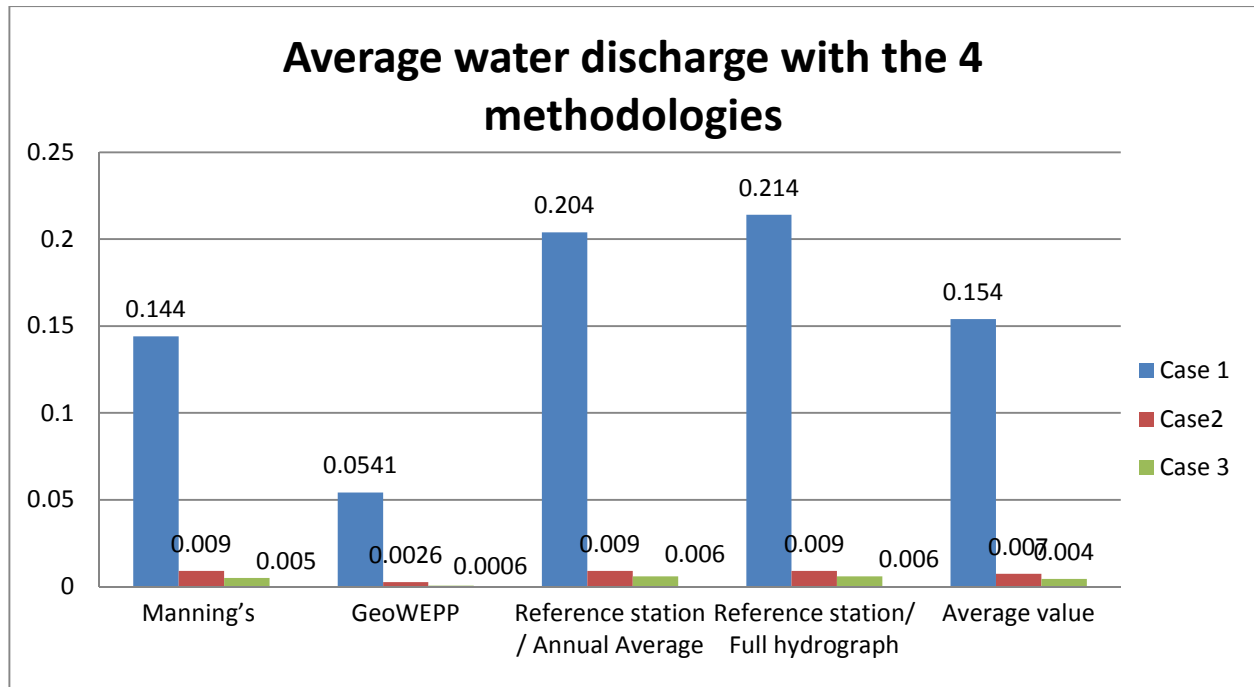


Fig 51. Graphical presentation of average discharge values at the three field sites using the three methods.

Table 14. Comparison of the difference of each method from the average value

	<i>Manning's equation</i>	<i>GeoWEPP</i>	<i>Reference station Annual average</i>	<i>Reference station Full year hydrograph</i>
<i>1st case [%]</i>	-7	-65	+24	+28
<i>2nd case [%]</i>	+18	-65	+18	+18
<i>3rd case [%]</i>	+12	-86	+27	+36

The comparison of the discharges, shown in Table 15, indicates that the GeoWEPP method provides the lowest estimations by between half or a full order of magnitude from the average of the other two estimates except for case three where it is similar in magnitude. The two reference station methods and the Manning's method provide discharge estimations that are fairly close, differing by -7/+26%, +18/+18% and +12/+30% for field sites one, two and three respectively. Therefore the estimated discharge is considered a reasonable estimate with an average error of $\pm 15\%$. This statement for the reference discharges is also reinforced by the average value calculation. Note that the absolute error in discharge is less important for the examination of the effect of mitigation measures as this is a relative comparison of erosion rates.

The reference station method is based on the assumption that the watershed under investigation has the same rainfall-runoff- discharge response as the gauged watershed. This implies that it must have a similar topography, stream network, land cover and soil type. The reference stations used in this study were located close to the first field site and close to the third field site; however it is likely that the spatial variation of land cover will have had differences. For the second field site an interpolation was made based distance from the reference stations. Although this does provide the best available estimate it clearly has limitations as the topography is similar to the first site (steep slopes) while the vegetation is more similar to the third site (regrowth vegetation of bushes and grasses).

The method using the Manning's equation and the stream geometric parameters determined from the DEM produced from the LIDAR data also had sources of uncertainty. The geometric parameters at the outlet were determined from the DEM. Errors estimates were assessed to be around 30% in total with consideration of each parameter. It also required that the "annual average" discharge depth was estimated. This estimation was based on field observations, but is clearly not precise due to difficulties in visually assessing the stream and forming a judgment on what the average depth would be. In addition the slope used in the equation was that measured, based on the section which represent the main watershed with an uniform slope. The stream may not have reached equilibrium slope and a slope measured in the upstream reach would be overestimated.

The water discharges estimations from the reference station method as an annual average and a full year hydrograph present the same trend. The values of the annual average and the full year hydrograph are in the same trend. The annual average discharge was calculated with the annual average water discharge from daily data from their main respective watershed. The water discharges data with the full year hydrograph consider the 30mins recorded data to obtain daily data.

The GeoWEPP simulations estimated the discharge based on a rainfall-runoff process. This relies on reasonably accurate information on the precipitation, the topography, the soil type and the vegetation. There is a limit to the resolution of this data and therefore in the accuracy

of the representation of the processes. The model can be validated by comparison to measured discharge and this will provide an indication of good modelling but not necessarily, as a correct discharge can be obtained from a model with compensating errors.

The sedimentation rates for this study were estimated from field data, from the reference station method and using GeoWEPP. The field data estimate was made on a yearly basis using the calculated average annual discharges from daily discharge and daily hydrograph over a year and then combined with the average annual TSS. The GeoWEPP simulations do try to represent the spatial and intensity variation of the precipitation, hence accounting for the temporal variation of the discharge. A comparison of the sedimentation rates estimated is given in Table 15.

Table 15: A comparison of the sedimentation rates estimated using field data and GeoWEPP

Field site	Field estimation: Manning's Eq.	Reference Station as annual average	Reference Station as full year hydrograph	GeoWEPP
1 st case [tons/yr]	5.6	7.4	36.89	36 200
2 nd case [tons/yr]	4.5	5.0	15.6	165
3 rd case [tons/yr]	3.2	3.8	14.73	72.5
1 st case [tons/ha/yr]	0.005	0.006	0.075	74
2 nd case [tons/ha/yr]	0.16	0.17	0.71	7.6
3 rd case [tons/ha/yr]	0.21	0.25	1.26	6.2

The estimations shown from Manning's equation and the reference station as annual averages have the same magnitude of estimations for the 2nd and 3rd cases. It shows that the full year hydrograph estimates are between 3 and 7 times higher than the average annual estimates, indicating the need for data at some time intervals to be better able to capture the high load events. Note that better than daily data would improve the estimate further. It shows clearly that using the parameters used in this study GeoWEPP is not able to model the sedimentation

for primary forest as the estimation is 3 orders of magnitude higher than that of the full year hydrograph estimation.

The TSS estimates from the annual average present mean values compared to the estimates from the full year hydrograph. As an annual average, the TSS values are therefore averaged and do not represent the TSS in peaks during the storms periods. For the full year hydrograph, the calculation has been established from daily data that was averaged from 30 min data. Note that the outliers are not considered for determination of the relationship between the water discharge and TSS to improve the estimations of each field site. If the outliers had been included in the estimations, the magnitude of the estimate would be 10 times higher than the current estimations for the 1st field site. For the 2nd and 3rd field sites, the estimations would be 3 times higher.

The field determination of the wash load sediment transport, which is the product of the discharge and the TSS, relies on a good estimation of both the discharge and the TSS. The TSS was measured at intervals that were determined by the scheduling of the sample collection and not by the weather (hence random relative to the weather) For a better management in terms of budget and regarding compliance at the same time, the low TSS values were not collected for analysis in laboratory but just checked in situ and recorded. Nevertheless, the calculated average is taking account of the low values as the TSS was assessed based on the discharge values. Therefore the sedimentation rate is approximately assessed as an average of the year from the calculations with Manning's equation and with the two reference stations. The accuracy is limited by the quality of the available data with a best estimate from these 3 methods of around 50-75%.

An investigation of the sedimentation rates per unit area determined from the field estimates show the expected relative difference in erosion rates based on the combination of vegetative cover and land surface slope. Very low sedimentation rates were observed on site at the first field site and this is corroborated by the estimations from the field data. The low sedimentation rates can be explained by the relatively intact primary forest in the watershed. The vegetative cover therefore effectively protects the soil from erosion in spite of the steep slopes. This is

similar to the almost complete lack of wash load found in a river in an undeveloped tropical watershed in Trinidad (Jaramillo, 2007). The sedimentation rates per unit area at sites two and three are similar in magnitude and about 30 times greater than those at the predominantly primary forest watershed. This can be explained by the disturbance of the vegetation in the form of complete deforestation with regrowth of bushes and grasses, which has occurred on a laterite soil. Laterite soils are known to be very sensitive and prone to extreme surface erosion once the vegetative cover has been removed. This is due to the very fine particles sizes in the laterite soils that have no resistance to erosion by raindrops or sheet erosion processes. The difference between the sedimentation rates calculated using the different discharge estimation methods is exactly proportional to the difference in the discharges, whose differences were discussed above.

An investigation of the sedimentation rates estimated using GeoWEPP clearly shows that the vegetation cover is not well represented for forest areas, as at the first field site with the predominantly a primary forest cover the sedimentation rates are extremely high compared to the values obtained from the reference station as a full year hydrograph (3 orders of magnitude higher). This would be expected if the vegetative cover had been disturbed as this watershed has very high land slopes. Therefore estimations of sedimentation rates in areas with intact forests require a validation of the forest vegetation index before reliable estimates can be made. However the result does show that it is extremely important that this watershed is not deforested as this would results in extreme erosion and sedimentation rates in the water courses.

The erosion rates estimated by GeoWEPP for sites two and three are similar to each other, as were the estimates using the field data. However the GeoWEPP estimations are greater than the full year hydrograph estimations by a factor of 10 and 5 for sites two and three, respectively. As there are fewer assumptions, and hence potential of errors, in the field data estimations than in the unvalidated GeoWEPP estimations, we tend to have more confidence in the field data estimations than in the GeoWEPP estimations. However in the following chapter a comparative study on erosion for the purpose of designing the optimal mitigation measures is

done and for this it is assumed that, although the absolute magnitudes of sedimentation rates may have a very large error, the relative erosion will show the correct trend (i.e. either showing an increase or a decrease). Although these estimates will have a high level of uncertainty, they are still being best that can be done with the available data.

Chapter 7. Mitigation measures

7.1.1 Risk evaluation

- The watershed along the pipeline route can be assessed for risk on a scale of low, medium and high, based on the three different criteria of slope, vegetation and land use and biological sensitivity.

Table 16 summarizes the different levels of risk as a function of the characteristics of the areas:

Table 16. The different kind of risks related to the parameters of slope, vegetation and sensitivity

Slope	Vegetation	Biology sensitivity	Risk result
Low and medium	Primary Forest	High	High
High	Primary Forest	High	High
Low and medium	Partially Forest	Low	Low
High	Partially Forest	High	High
Low and medium	Shrubs and bushes	Low	Low
High	Shrubs and bushes	Low	High

The risk result is reflects the impact of erosion on the watershed in terms of biology and geotechnical aspects.

Different measures for lowering the risk level along the pipeline have been applied during the construction phase and are described below.

7.1.2 Mitigation procedures already executed by the Ambatovy Project during the construction phase

7.1.2.1 For the stream areas

Channel sections considered at risk where water course crossings have been established have been stabilized with:

- Rock rip-rap for the sensitive channels with medium and low width
- Sand bags mixed with rocks for low sensitive channels with high and low width

- Rock gabions for large widths of channel for sensitive streams

Figure 52 a sensitive channel with a large width (on a crossing 23 km from Ambatovy mine in the Andasibe, near the mine region).



Fig 52. Example of mitigation done for large width channel and sensitive streams

7.1.2.2 For the upstream areas of the watersheds:

Stabilization was implemented in the watersheds as much as possible where the vegetation had been removed by revegetation with hydro seeds or placement of vetiver, geotextiles, bamboos mats, rocks, woods. Locations where there were large areas of cleared land with low and medium slopes requiring stabilization, hydro seeding was the stabilization of choice and supplemented with replanting of trees in some areas.

In the higher slopes of the areas with high sensitivity, the above cited measures were supplemented with, geotextiles, ripraps, wood and replantation.

7.1.3 Mitigations designed using GeoWEPP

GeoWEPP permits the simulation of some possible mitigation solutions by allowing for the change of the type of land use and/or soil in some specific sub-catchments wherever the amount of sedimentation is really high. The design of potential mitigation solutions was made using the Watershed method. The results of the simulations will be described below.

7.1.3.1 First field site mitigation proposal

For the first field case, the following map presents the results of changing the vegetation type of the sub-catchments with the greatest soil loss. The results show that improving the quality of the vegetation is a potentially effective mitigative measure. The sub-catchments around the pipeline route and around the outlet of the watershed should be highly managed in terms of vegetation to reduce the total soil loss for the entire watershed.

Figure 51 represents the results for the simulation after mitigation purposes for the first field site, which can be compared to Figure 46.

However the proposed mitigation for this case is not valid as GeoWEPP does not accurately calculated the erosion and sedimentation for primary forest areas such as this watershed in Figure 53. This statement was reinforced by the wash load estimations presented above, in Table 15. The hypothetical value of the wash load has been lowered twelve times for the high value represented in the chart. (185 to 15[mg/l]). This hypothetical value provides an illustration of what might be able to be estimated once the forest index values have been validated and calibrated.

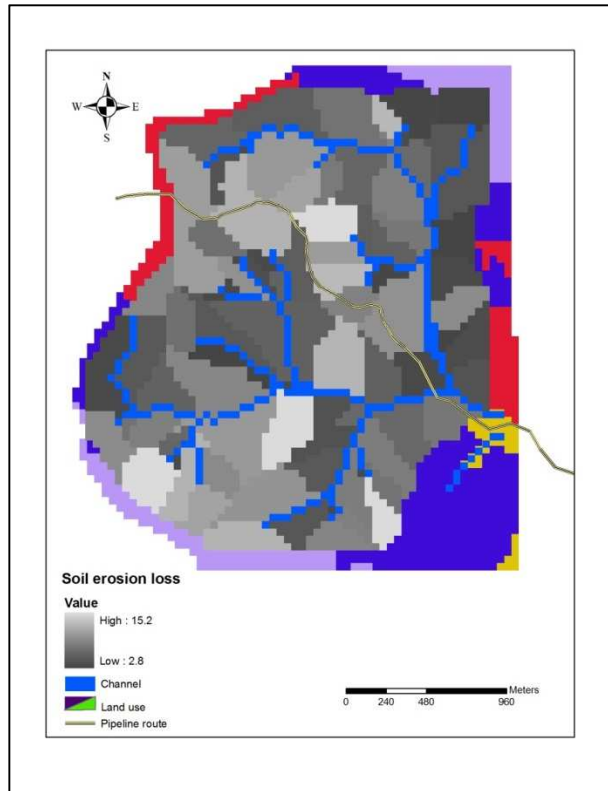


Fig 53. Simulation results after the mitigation process for the first field site

7.1.3.2 Second field site mitigation proposal

The second field case is difficult to propose concrete mitigation actions for due to the steep slope at the top of the watershed. The first simulation of the current situation shows that the soil loss rate is really high. But after going through the various changes in the vegetation, such replanting with a young forest, the results are still complicated to manage and even the rate of high soil loss is still present at the top of the watershed, according to the simulation results. Nevertheless, the simulated soil loss is has decreased at the outlet of the watershed, according to the simulation results presented below.

The optimal mitigation proposal would be to replant the entire area, not only with grass or young forest, but with perennial forest, especially in the steepest zones. However as it is impossible to re-establish a primary forest on laterite soils, in reality it would be crucial to also set up some barriers for the sediments at the bottom of the steepest zone, for instance sediment traps and retaining wall with filters.

Figure 54 presents the results for the simulation after mitigation proposal for the second field site, which can be compared to the results for the current state in Figure 48. The value of the wash load has been lowered sixty times for the high value represented in the chart. (291 to 4.8[mg/l]).

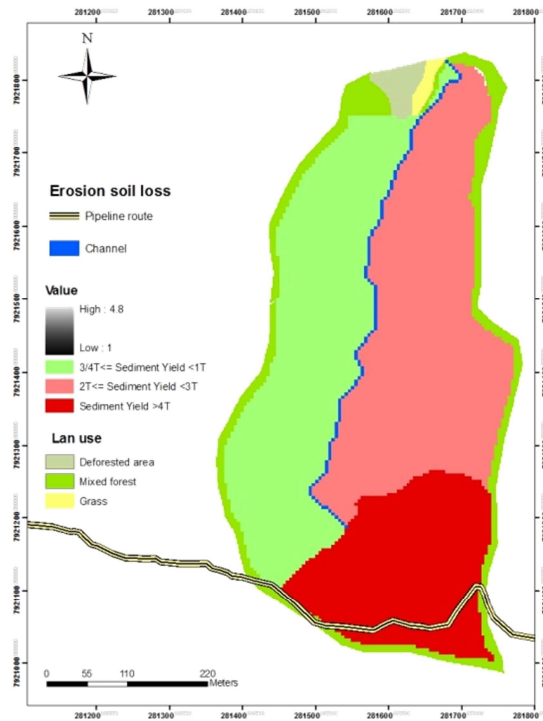


Fig 54. Simulation results after the mitigation proposal for the second field site

7.1.3.3 Third field site mitigation proposal

This site is one of the really feasible projects, with better hope for the future, if the recommendations are correctly applied. Essentially, it is advised to change the type of vegetation in the entire watershed to some young forest, without any modification of the slope, according to the following simulation, presented in Figure 55, which can be compare to the current state shown in Figure 50. The value of the wash load has been lowered 121 times for the high value represented in the chart. (291 to 2.4[mg/l]).

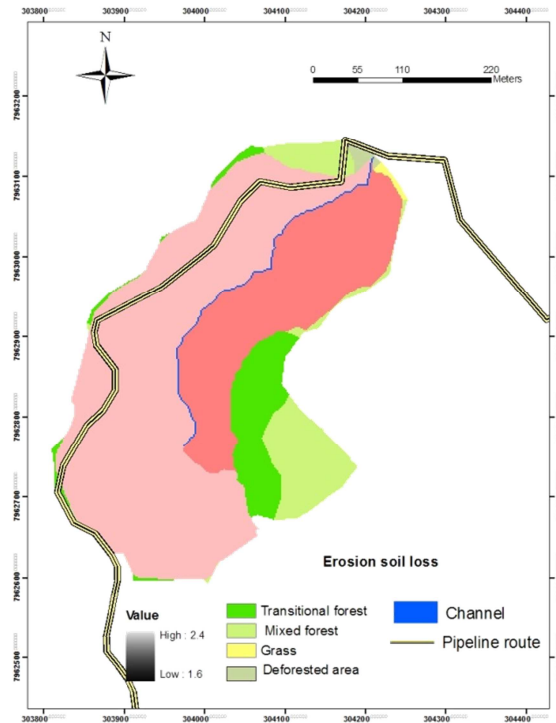


Fig 55. Simulation results after the mitigation process for the third field site

7.1.3.4 Summary report of the GeoWEPP sedimentation simulations for the mitigative proposals

The summary reports for the mitigation proposals for each field site are presented in Table 17.

Table 17. GeoWEPP simulation reports of erosion loss parameters after mitigation proposals

WEPP WATERSHED SIMULATION FOR REPRESENTATIVE HILLSLOPES AND CHANNELS			
Case of study	Case 1	Case 2	Case 3
Phase of study : before or after mitigation	After	After	After
Total contributing area to outlet [ha]	489	21.6	11.6
Avg. Ann. Precipitation volume in contributing area [m ³ /yr]	6.57 x 10 ⁶	320 x 10 ³	172 x 10 ³
Avg. Ann. water discharge from outlet [m ³ /yr]	1.53 x 10 ⁶	75 x 10 ³	18.7 x 10 ³
Avg. Ann. sediment discharge from outlet [tonnes/yr]	6190	136	72.3
Sediment Delivery Ratio for Watershed	0.739	0.992	1.003
Clay fraction	0.239	0.245	0.301
Silt fraction	0.746	0.692	0.411
Sand fraction	0.015	0.063	0.287
Organic matter fraction	0.019	0.02	0.05
Index of specific surface [m ² /g of total sediment]	61.0	62.4	88.0
Number of years of simulation	2	2	2
Number of storms which produce [mm] of rainfall	102	237	237
Number of events which produce [mm] of runoff	56	53	57
Height of runoff [mm]	313	347	373

Chapter 8. Conclusion

The soil loss and sedimentation due to erosion along the pipeline route of Ambatovy Project is a sensitive issue and complex due to different aspects related to the engineering duties: the geotechnical properties of the soil, the environmental considerations and the social compacts. During the construction phase, it was important for Ambatovy to manage the tasks and monitor the sites, and to identify problem area from observations of rainfall events causing very high total suspended. The objective of this research project was to investigate the situation in order to recommend effective and concrete mitigation solutions for the problems of erosion and sedimentation.

In the study, three representative field sites along the pipeline route, having different values of slope, land use, particle size distribution of the soil and its geotechnical properties, rainfall intensity and resulting sedimentation, were chosen. The first field site represents the mine area which is a forested area (predominantly primary forest) with the highest sensitivity of its habitats and ecosystems and having the highest percentage of laterite soil. The second field site represents a partially forested area with mostly fifth year forest cover, with a soil which has the same percentage of laterite-silt-sand. The typical challenge of this case is due to the steep slopes at the top of the watersheds and the required cut and fills from the civil engineering works performed during the construction of the pipeline. The third field site represents a watershed near the coast with a soil having a lower percentage of laterite, more sand and partial vegetation cover of bushes and grass.

The use of field data provided order of magnitude estimations of sedimentation rates. Firstly the discharges estimated using a yearly average and daily hydrograph reference station method and using Manning equation were reasonably close, providing some confidence in their value, with consideration of the errors estimates. The TSS values were validated with turbidity measurements. Both these observations were validated qualitatively and roughly quantitatively by visual observations during the sample collection phase. These estimated sedimentation rates

also reflected the physical processes that could be observed. The watershed predominantly covered by primary forest had very low sedimentation rates, in spite of the steep slopes, which compared well to results in a steep tropical catchment in Trinidad (Jaramillo, 2007). The increase in the sedimentation rates were similar for the other two field sites, showing that both slope and vegetation cover are important parameters affecting sedimentation rates.

The use of GeoWEPP to estimate the sedimentation rates showed that it is essential to validate any simulation model before using it as a predictive tool. In spite of GeoWEPP having been used for forested areas as documented in the literature, it was incapable of predicting the very low sedimentation rate for the steep primary forest watershed using the forest cover index from the literature. This shows the importance of correctly defining the vegetation index. It also shows the importance that slope has once in contributing to high sedimentation rate in a watershed no longer covered with a protective primary forest. This is well known to be particularly problematic for areas underlain by laterite soils.

GeoWEPP was used to propose mitigative measures for the three field sites, in spite of the uncertainty in its value as a predictive tool when unvalidated. Although there is great uncertainty in the estimations from the simulations, the investigation did show the potential to use this model as a tool for mitigative designs.

Regardless, a number of recommendations can be made based on observations of the activities and their consequences for the areas affected by the pipeline construction. Firstly, it is very important to protect the primary forest in the steeply sloped mountain areas on laterite soils. Secondly it is important to try to revegetate by replanting trees in all areas that have previously been deforested. Lastly the civil works need to be designed to minimize the areas affected and also minimize the extent of affected areas with high slopes by judicious route choice.

REFERENCES

Achankeng, 2003. *Globization, Urbanisation and Municipal Solid Waste Management in Africa: African Studies Association of Australasia and the Pacific 2003 Conference Proceedings.*

Arulanandan J. K., J. K. Mitchell, 1968, *Electrical dispersion in relation to soil structure: Soil Mec. Fndns. Div., ASCE, 94, SM2, Proc. Paper 5853, March, pp. 447–471.*

Arnold, J.G, Santhi, C., Williams, J.R., Dugas, W.A., Srinivasan, R., Hauck, 1998, *Validation of the SWAT model on a large river basin with point and nonpoint sources*, Journal of the American Water Resources Association, Volume 37, Issue 5, 2001, pp 1169-1188.

Aubert G., 1954, Laterite soil on granite. *Observations sur la dégradation des sols et la formation de la cuirasse latéritique dans le Nord-Ouest du Dahomey*, C.R 4^e con. int. sci. Sol, Amsterdam, **Vol 3**, pp 123-8.

Beasley, D.B., L.F. Huggins, and E.J. Monke. 1980. *ANSWERS: A model for watershed planning*. Trans. ASAE 23:pp 938-944.

Beven K. & Freer J., 1 August 2001, *Equifinality, data assimilation, and uncertainty estimation in mechanistic modelling of complex environmental systems using the GLUE methodology*, Journal of Hydrology, **Volume 249**, Issues 1–4 , pp. 11-29.

Beven, K., Mwakalila, S., Campling, P., Feyen, J., Wyseure, G., 2001, *Application of a data-based mechanistic modelling (DBM) approach for predicting runoff generation in semi-arid regions*, Hydrological Processes 15 (12) , pp. 2281-2295.

Beven K.J., Younger P.M., Freer J.E., 2009, *Detecting the effects of spatial variability of rainfall on hydrological modelling within an uncertainty analysis framework*, Hydrological Processes 23 (14), pp. 1988-2003.

Bouraoui, F., Silgram, M., Anthony, S.G., Collins, A.L., Stromqvist, J., Schoumans, O., Lo Porto, A., Groenendijk, P., Arheimer, B., Mimikou, M. et al., 2005, *Application of the SWAT model on the Medjerda river basin (Tunisia) Evaluation of diffuse pollution model applications in EUROHARP catchments with limited data*, Journal of Environmental Monitoring, **Volume 11**, Issue 3, 2009, pp 554-571.

Chaperon P., Danloux J., 1993, *Fleuves et Rivières de Madagascar*, IRD Editions, pp 874.

Davis P.A, S. Mietz N., Kohl K.A., Rosiek K.R., Gonzales F.M, M. F. Manone M.F., Hazel J.E., Kaplinski M.A., 2002, *Evaluation of lidar and photogrammetry for monitoring volume changes in riparian resources within the grand canyon Arizona, Pecora 15/Land Satellite Information IV/ISPRS Commission I/FIEOS Conference Proceedings, 2002.*

De Roo A.P.J., Jetten, V.G., 1999, *Modelling soil erosion by water at the catchment scale: Preface*, Catena 37 (3-4), pp. 275-276.

De Vente J., Poesen J., Verstraeten G., Van Rompaey A., Govers G., 2008, *Spatially distributed modeling of soil erosion and sediment yield at regional scales in Spain.* Global and Planetary Change 60(3-4): pp 393-415.

Desmet P.J.J., Govers, G., 1996, *A GIS procedure for automatically calculating the USLE LS factor on topographically complex landscape units*, Journal of Soil and Water Conservation 51 (5) , pp. 427-433.

Donigian A.S., Jr., Imhoff, J.C., Bicknell, Brian, Kittle, J.L., Jr., 1984, *Application guide for Hydrological Simulation Program--Fortran (HSPF)*: U.S. Environmental Protection Agency, Environmental Research Laboratory, Athens, Ga., EPA-600/3-84-065, 177 p.

Donigian Jr., Anthony S., Patwardhan, Avinash S., 1992, *Modeling nutrient loadings from croplands in the Chesapeake Bay watershed, Water Resources Planning and Management: Saving a Threatened Resource - In Search of Solutions*, Proceedings of the Water Resources Sessions at Water Forum, pp. 817-822.

Dynatec Corp., 2006, *Etude d'Impact Environnemental. Projet Ambatovy, Vol I.* 1375p

Ewen J., Zhang, X, 2000, *Efficient method for simulating gravity-dominated water flow in unsaturated soils*, Water Resources Research 36 (9), pp. 2777-2780.

Favis-Mortlock D.T., Boardman, J., Parsons, A.J., Lascelles, B., *Emergence and erosion: A model for rill initiation and development*, Hydrological Processes 14 (11-12), pp. 2173-2205.

Ferencevic M. V., Ashmore P., 2012, *Creating and evaluating digital elevation model-based stream-power map as a stream assessment tool*, River Research and Applications 28 (9), pp. 1394-1416.

Fosberg, M. A, 1963, *A warm sea breeze*, U.S. Forest Service research note PSW, Pacific Southwest Forest and Range Experiment Station (Berkeley, Calif.). pp. 18-23.

Gentile A.R., 2002, *Assessment and reporting on soil erosion*, Technical report, EEA, 131p.

Gidigas M.D., 1972, *Mode of formation and geotechnical characteristics of laterite materials of Ghana in relation to soil forming factors*, Engineering Geology, **Volume 6**, Issue 2, August 1972, pp. 79-150.

Gidigas M.D, 1976, *Laterite soils engineering. Textbook. Developments in geotechnical engineering*, International Journal of Rock Mechanics and Mining Sciences & Geomechanics Abstracts, **Volume 13**, Issue 1, January 1976, Pages A1.

Gobin A., Jones, R., Kirkby, M., Campling, P., Govers, G., Kosmas, C., Gentile, A.R., 2004, *Indicators for pan-European assessment and monitoring of soil erosion by water*, Environmental Science and Policy 7 (1), pp. 25-38.

Hebel B., 1997, *Measured vs. WEPP simulated runoff and erosion from differently tilled plots*, Paper - American Society of Agricultural Engineers. **Volume 2**, 11p.

Jaramillo F., 2007, *Estimating and modeling soil loss and sediment yield in the Maracas-St-Joseph River catchment with empirical models (RUSLE and MUSLE) and a physically based model (EROSION 3D)*, M.Eng. Thesis, Civil Engineering, McGill University.

Kerstesz, 2007, *Hungarian Geographical Bulletin*, Food Chemistry 71 (4), pp. 563-566.

Kliment Z, Kadlec J., 2008, *Evaluation of suspended load changes using AnnAGNPS and SWAT semi-empirical erosion models*. Catena 73, pp. 286–299.

Krysanova V., Post J., Suckow F., Mirschel W., Rogasik, J., Merbach, I, *Integrated eco-hydrological modelling of soil organic matter dynamics for the assessment of environmental change impacts in meso to macro-scale river basins*, Ecological Modelling 206 (1-2) , pp. 93-109.

Lambe J., Kikuchi, C., 1960, *Paramagnetic resonance of CdTe: Mn and CdS: Mn*, Physical Review 119 (4), pp. 1256-1260.

Lin Q., 1980, *Monitoring and analyzing the soil erosion changes in northern china during the latest twenty years a field site in upper Chao River basin of China*, Journal of Hydrology, pp. 3127 - 3130

Lumb P., 1966, *The variability of natural soils*, Journal of Terramechanics, **Volume 6**, Issue 2, 1969, pp. 64–65.

Mahalinga-Iyer, Williams D.J, *Consolidation and shear strength properties of a lateritic soil*, Engineering Geology 38 (1-2), pp. 53-63.

Maignien, 1966, *Compte rendu de recherches sur les latérites*. Unesco Paris. Geoderma. **Volume 1**, Issue 2, pp. 139-158.

Mandimbiharison A.J., Randrianja R., 2002, *Evolution minéralogique et géochimique du profil latéritique nickélique d'Ambatovy*. Madamines, ISSN 2220-0681, **vol. 4**. 20p.

Melluso L., Morra V., 2005, *Geochronology and Petrogenesis of the Cretaceous Antampombato–Ambatovy Complex and Associated Dyke Swarm, Madagascar*. Journal of petrology. **Volume 46**. Number 10. pp. 1963–1996.

Minkowski M., Dr. Chris Renschler, 2008, *GeoWEPP for ArcGIS 9.x. Full Version Manual*, Department of Geography The State University of New York at Buffalo, 129p.

Moehansyah H., Maheshwari B.L., Armstrong J., 2004, *Field evaluation of selected soil erosion models for catchment management in Indonesia*, Biosystems Engineering, **Volume 88**, Issue 4, pp. 491-506.

NSERL [Internet]. 2002. Washington DC; updated on Nov. 2013. Available from: http://www.ars.usda.gov/main/site_main.htm?modecode=36-02-15-00.

Parton W.J, 1997, *Simulating trends in soil organic carbon in long-term experiments using the century model*; Geoderma. **Volume 81**, Issues 1–2, pp. 75–90.

Pohlert T., Huisman J.A., Breuer L., Frede H.-G., 2003, *Integration of a detailed biogeochemical model*

into SWAT for improved nitrogen predictions-Model development, sensitivity, and GLUE analysis, *Ecological Modelling*. **Volume 203**, Issue 3-4, pp. 215-228.

Quinton, 1997, *The influence of vegetation species and plant properties on runoff and soil erosion: Results from a rainfall simulation study in south east Spain*, IAHS-AISH Publication (290) , pp. 186-194.

Rakoto A., 2007, *Modélisation des paramètres hydrologiques d'un bassin versant*, ESPA, 205p.

Refsgaard J.C and Storm, 1995, *MIKE SHE: Computers model of watershed hydrology*, *Journal of Hydrology*, **Volume 198**, Issues 1–4, 1 November 1997, pp. 69-97.

Remillon, A., 1955, *Stabilization of laterite soils*. High. Res. Board. Bull. No. 108: pp.96-101

Renschler C., 2003, *Designing geo-spatial interfaces to scale process models: the GeoWEPP approach*. *Hydrological processes*. 17, pp. 1005–1017.

Renschler, C. S., 2006, *Spatial and temporal model validation: Representing landscape properties and processes across scales. Proceedings of the iEMSS, 2006, 3rd Biennial Meeting," Summit on Environmental Modelling and Software, Serbia"*.

Ryu J. H, 2009, *"Application of HSPF to the distributed model intercomparison project: Field site."* *Journal of Hydrologic Engineering* 14(8): pp. 847-857.

Sang M. K., Benham B.L., 2007, *Comparison of hydrologic calibration of HSPF using automatic and manual methods*. *Water resources research*, **VOL. 43**, W01402.

Schmidt, Schindewolf M, 1999, *Parameterization of the EROSION 2D/3D soil erosion model using a small-scale rainfall simulator and upstream runoff simulation*, *Catena*. **Volume 91**, pp. 47–55.

Sherman G., 1949, *Factors influencing the Development of Lateritic and Laterite Soils in the Hawaiian Islands*, *Pacific science*, **Vol III**, pp. 307-314.

Smith J.A, Miller J.A, Baeck M.L, Nelson P.A, Fisher G.T, Meierdiercks K.T, 2005, *Extraordinary Flood Response of a Small Urban Watershed to Short-Duration Convective Rainfall*, *Hydrometeor*, **6**, 599–617.

Takken, 1999, *MODSIM05 - International Congress on Modeling and Simulation: Advances and Applications for Management and Decision Making*, *Proceedings*, pp. 2672-2678.

Thiebes B., Bell R., Glade T., Jäger S., Anderson M., Holcombe L., 24 May 2012, *A WebGIS decision-support system for slope stability based on limit-equilibrium modelling*, *Engineering Geology*, Volume 158, pp. 109-118.

USGS, 2007, *Evaluation of LiDAR-Acquired Bathymetric and Topographic Data Accuracy in Various Hydrogeomorphic Settings in the Deadwood and South Fork Boise Rivers, West-Central Idaho*, *Scientific Investigations Report* 2011–5051, 40p.

Vallerga B. A., Shuster J. A., Love A. L. and Van Til C. J., 1969. *Engineering study of laterite and lateritic*

soils in connection with construction of roads, highways and airfields. Phase I - Southeast Asia (Thailand). Final Report for U.S. Agency for International Development. Contract AID/csd- 18 10. Soil and Pavement Consultants, Oakland, Calif.: 165p. and Appendices.

Watts J. L., 2007, *Geo-spatial HSPF model creation: Toward a digital watershed. Restoring Our Natural Habitat - Proceedings of the 2007 World Environmental and Water Resources Congress, Tampa*. 5p.

Wischmeier, W. H., and D. D. Smith, 1960. "A universal soil-loss equation to guide conservation farm planning." *Trans. Int. Congr. Soil Sci.*, 7th, pp. 418-425.

Whitmore T.J., 1975, *Tropical rain forests in the far east*, Oxford University Press, Oxford, 2nd, revised edn., pp 289-292.

Wu Q. and Wang M., 2007, "A framework for risk assessment on soil erosion by water using an integrated and systematic approach." *Journal of Hydrology* 337p.

Yoder D. & Lown J., 1995, *The Future of RUSLE: inside the new revised universal soil loss equation*, *Journal of Soil and Water Conservation*, **50 (5)**, pp. 484–489.

APPENDIXES

I. Appendix A

Table 18. 1st site physical hydrology parameters data sampling results: pH, temperature, conductivity and TDS

Date	Hour	pH	Temp (°C)	Conductivity (µS/cm)	TDS (ppm)
30/08/2008	9h48	6.22	11.3	80.2	40.4
30/08/2008	9h44	6.66	10.9	78.3	39.4
07/08/2008	9h15	6.81	19	84.3	42.4
30/09/2008	13h11	7.74	20.8	92.9	46.1
25/11/2009	16h45	6.94	20.6	91.4	45.7
19/05/2010	09h57	7.25	26	78	39
15/11/2010	16h00	6.7	22.2	95.3	47.8
10/01/2011	13h40	6.74	28.28	97.69	48.85
14/04/2011	08h10	7.63	24.4	88.9	44.5
23/05/2011	14h12	7.62	23.4	89.8	

Table 19. 1st site physical hydrology parameters data sampling results: TSS and turbidity

Date	Hour	Turbidity (NTU)	TSS (mg/l)	Rainfall (mm)	Remarks
30/08/2008	9h48	2.9		0.4	Drizzles, upstream
30/08/2008	9h44	4.96	0.7	0.4	Drizzles, downstream
07/08/2008	9h15	321	226.7	0.4	
30/09/2008	13h11	5.36		0.4	
25/11/2009	16h45	392	338	2.2	Cut and fills works
19/05/2010	09h57	90.2	51	0.4	√
15/11/2010	16h00	10.5			
10/01/2011	13h40	5.99			
14/04/2011	08h10	3.21			
23/05/2011	14h12	44.9	2.76		
24/08/2011	16h16	6.06	0.98		
24/10/2011	14h52	5.56	0.87		
05/12/2011	17h05	16.68	3.72		
17/01/2012	08h34	4.01	0.55		
17/04/2012	09h55	3.36	0.43		
21/05/2012	10h26	3.78	0.51		
04/06/2012	11h23	3.38	0.44		
16/07/2012	11h43	2.48	0.28		

20/08/2012	13h00	5.17	0.79		
20/09/2012	15h40	3.53	0.46		
15/10/2012	11h27	4.08	0.51		
26/11/2012	13h37	6.21	0.97		
18/12/2012	16h30	10.5	2.15		
29/01/2013	09h23	197	164.65		
12/02/2013	09h35	57	50.49		
27/03/2013	13h41	31	28.25		

Table 20. 2nd site physical hydrology parameters data sampling results: TSS and turbidity

Date	Hour	pH	Temp (°C)	Conductivity (µS/cm)	TDS (ppm)
05/05/2010	15h46	6.51	22.7	35.3	17.7
22/09/2010	13h57	6.43	24.5	35.5	17.7
19/01/2011	09h35	6.46	27.8	36.4	18.1
18/05/2011	13h35	6.65	20.5	32.2	16.1

Table 21. 2nd site physical hydrology parameters data sampling results: TSS and turbidity

Date	Hour	Turbidity (NTU)	TSS (mg/l)
05/05/2010	15h46	12.5	7
22/09/2010	13h57	13.1	4
19/01/2011	09h35	31	8
18/05/2011	13h35	7.9	5.3
18/08/2011	14h30	23.3	6.5
27/10/2011	09h30	14.1	7
07/12/2011	15h57	44.6	22
18/01/2012	16h56	15.7	9.59
19/04/2012	08h20	10.9	6.32
17/05/2012	08h53	9.8	5.59
07/06/2012	07h44	9.93	5.68
17/07/2012	10h00	11.5	6.72
23/08/2012	10h17	11.7	6.85
18/09/2012	09h55	11.8	6.92
18/10/2012	09h14	9.75	5.56
29/11/2012	08h54	8.57	4.8
20/12/2012	08h40	9.1	5.14
19/02/2013	10h29	10.7	6.18
25/03/2013	15h45	8.1	4.5

Table 22. 3rd site physical hydrology parameters data sampling results: pH, temperature, conductivity and TDS

Date	Hour	pH	Temp (°C)	Conductivity (µS/cm)	TDS (ppm)
25/01/2010	17h30	5.83	29.5	56	28
06/05/2010	16h35	6.67	25.5	58.4	29.2
29/09/2010	15h12	6.64	25.6	49.7	24.8

Table 23. 3rd site physical hydrology parameters data sampling results: TSS and turbidity

Date	Hour	Turbidity (NTU)	TSS (mg/l)	Rainfall (mm)
25/01/2010	17h30	19.9		
06/05/2010	16h35	58.3	30	0.3
29/09/2010	15h12	15.9	7	4.3
25/01/2011	17h30	19.9	10	
06/04/2011	10h24	31.2	19	3
11/08/2011	14h15	3.6	2.91	
02/11/2011	16h43	2.75	2.46	0.1
23/01/2012	13h05	14.7	9.84	0.7
24/04/2012	10h57	12.3	8.49	
24/05/2012	14h30	10.4	7.39	
27/06/2012	15h40	8.2	6	
25/07/2012	11h07	13.75	9.21	
24/08/2012	11h50	2.57	2.3	
25/09/2012	16h14	2.41	2.18	
24/10/2012	16h04	4.63	3.74	
06/12/2012	11h37	95	45.65	
26/12/2012	14h10	20.1	12.61	
21/02/2013	13h48	4.4	3.59	
20/03/2013	12h02	6.8	5.14	

Table 24. Wash load calculations from the full year hydrograph

	Case 1	Case 2	Case 3
<i>January</i>	128.04	3.78	4.80
<i>February</i>	205.57	7.85	10.02
<i>March</i>	195.56	7.30	8.30
<i>April</i>	130.01	3.66	5.70
<i>May</i>	124.14	3.45	5.04
<i>June</i>	112.00	2.66	4.60
<i>July</i>	135.58	3.97	4.50

<i>August</i>	129.70	3.64	4.10
<i>September</i>	119.97	3.10	3.30
<i>October</i>	101.37	2.07	2.50
<i>November</i>	118.40	3.02	3.90
<i>December</i>	141.67	4.31	5.15
<i>Annual average</i>	136.83	4.07	5.16

II. Appendix B: Ambatovy standards for TSS

The following protocol presents the table of the TSS standards applied for the Ambatovy project. These procedures were certified and assigned to be applied for the entire project with the participation of the ONE (Office national pour l'Environnement), an entity related to the Environmental Ministry of Madagascar.

The protocol was applied for the following goals, on the entire pipeline route of the Ambatovy project:

- Manage the TSS effects in the rivers during the construction
- Reduce TSS effects in the rivers during and after the construction calendar and not pass the 50ppm value of TSS.

Criteria have been established in terms of season, the stream sensitivity and the duration of the rain event.

The following document is presented in French, and validated in March 2009.

PROPOSITION DE TAUX LIMITES DES MES EN FONCTION DES CRITERES DE BASE

Conditions météorologiques	Taux limite de conformité	Actions obligatoires au cas où non respect des taux limites
Saison sèche	<p>Le taux limite de conformité sera fixé en fonction de la valeur de MeS de base du site en question, ainsi :</p> <ul style="list-style-type: none"> ➤ <i>Pour le secteur Ouest du pipeline</i> <ul style="list-style-type: none"> ▪ une augmentation maximale de 15 % autorisée durant 24 heures ▪ 7.5 % pour une période de 30 jours ➤ <i>Pour le secteur Est du pipeline</i> <ul style="list-style-type: none"> ▪ une augmentation maximale de 30% autorisée durant 24 heures ▪ 15% pour une période de 30 jours 	<p>Notifier immédiatement le contractant. Effectuer immédiatement des travaux de réparation dans le cours d'eau en parallèle à la réalisation des travaux.</p> <p>L'entrepreneur a une période moyenne de huit heures (08) journalières pour accomplir toutes les activités de construction prévues.</p> <p>Si après ces 08 heures d'activités, et compte tenu des réparations qui s'effectuent en parallèle, le taux de TSS dans la rivière n'a pas encore atteint le taux limite de conformité, tous travaux au niveau du cours d'eau doivent être arrêtés jusqu'à ce que les niveaux de MeS reviennent aux limites acceptables.</p> <p>Quoique, au cas de dépassement de n'importe quel taux limite de conformité pendant 2 heures ou plus, il faut rédiger un rapport d'incident.</p>
Saison de pluies (Evènements pluvieux de 2 à 4h et/ou pendant X jours	<p>Le taux limite de conformité sera fixé en fonction de la valeur de MeS de base du site en question, ainsi :</p> <ul style="list-style-type: none"> ➤ <i>Pour le secteur Ouest pipeline</i> <ul style="list-style-type: none"> ▪ une augmentation maximale de 10% autorisée durant 24 heures ▪ 5% pour une période de 30 jours ➤ <i>Pour le secteur Est du pipeline</i> <ul style="list-style-type: none"> ▪ une augmentation maximale de 20% autorisée durant 24 heures ▪ 7.5% pour une période de 30 jours 	<p>Quoique, au cas de dépassement de n'importe quel taux limite de conformité pendant 2 heures ou plus, il faut rédiger un rapport d'incident.</p>

(Source: Ambatovy Project, 2009)

Type de cours d'eau	Distance limite de conformité au point de prélèvement Aval (1)	Distance limite de conformité au point de prélèvement Aval (2)	Distance limite de conformité au point de prélèvement Aval (3)
Systèmes de bassins tels que lacs, étangs, marécages, et les autres plans d'eau où les vitesses sont moins de 0.5 m/s	Les échantillons doivent être pris à intervalles de 30 m autour de la circonférence de la barrière de la turbidité.	Les échantillons doivent être pris à intervalles de 30 m autour de la circonférence de la barrière de la turbidité.	Les échantillons doivent être pris à intervalles de 30 m autour de la circonférence de la barrière de la turbidité.
Cours d'eau permanent moins de 10 mètres de largeur	1 distance égale à la largeur du cours, en aval	2 distances égales à 2 fois la largeur du cours, en aval	3 distances égales à 3 fois la largeur du cours, en aval
Cours d'eau permanent entre 10 à 30 mètres de largeur	30 mètres en aval	60 mètres en aval	90 mètres en aval
Cours d'eau permanent plus de 30 mètres mais moins de 60 mètres de largeur	60 mètres en aval	120 mètres en aval	180 mètres en aval
Cours d'eau permanent plus de 60 mètres de large	90 mètres en aval	180 mètres en aval	270 mètres en aval

Distance limite de conformité = Distance à partir de laquelle le taux de valeur de base de MeS doit revenir à la valeur initiale, c'est-à-dire, au taux en amont du point de franchissement

Point de prélèvement aval (1) : pour les cours d'eau *de haute sensibilité*

Point de prélèvement aval (2) : pour les cours d'eau *de moyenne sensibilité*

Point de prélèvement aval (3) : pour les cours d'eau *de sensibilité faible*

(Source: Ambatovy Project, 2009)

- **Laboratory procedures for the TSS estimation**

- ✓ Filters will have to be washed prior to use, by rinsing the filter with deionized (DI) water three times and they will be placed in a drying oven with a temperature of $110 \pm 5^\circ\text{C}$ for a minimum of one hour.
- ✓ The weight of the pre-washed and prepped filter will be recorded.
- ✓ The filtering apparatus will be assembled by placing the filter paper in a cleaned Buchner funnel and begin suction.
- ✓ The filter will have to be wet with a small volume of reagent-grade water to seat it.
- ✓ For obtaining of a more uniform (preferably homogeneous) aliquot for analysis, the contents will be shaken, stirred and mixed in a sample container.
- ✓ Immediately after homogenizing the sample, the required aliquot will be collected in a clean graduated cylinder and recorded on an appropriate worksheet.
- ✓ The volume will be poured slowly onto the seated glass microfiber filter until the entire aliquot has been filtered. If residue lingers in the cylinder, rinse the cylinder with DI water and filter this rinse water.
- ✓ Dry filters for a minimum of 1 hour at $110 \pm 5^\circ\text{C}$ in drying oven.
- ✓ After drying is complete, the filters will be reweighted and the dry filter and residue weight will be recorded.
- ✓ The following calculation to determine TSS will be used:

$$TSS \left[\frac{mg}{L} \right] = \frac{(residue+filter)-filter}{sample\ filtered} \times 1000 \quad (12)$$

III. Appendix D: Models details

III.1. HSPF details

HSPF uses continuous rainfall and other meteorological records to compute streamflow hydrographs and pollutographs. HSPF simulates interception soil moisture, surface runoff, interflow, base flow, snowpack depth and water content, snowmelt, evapotranspiration, ground-water recharge, dissolved oxygen, biochemical oxygen demand (BOD), temperature, pesticides, conservatives, fecal coliforms, sediment detachment and transport, sediment routing by particle size, channel routing, reservoir routing, constituent routing, pH, ammonia, nitrite-nitrate, organic nitrogen, orthophosphate, organic phosphorus, phytoplankton, and zooplankton. Program can simulate one or many pervious or impervious unit areas discharging to one or many river reaches or reservoirs. Frequency-duration analysis can be done for any time series. Any time step from 1 minute to 1 day that divides equally into 1 day can be used. Any period from a few minutes to hundreds of years may be simulated. HSPF is generally used to assess the effects of land-use change, reservoir operations, and point or nonpoint source treatment alternatives, flow diversions. (Ref: USGS.gov).

The model was developed in the early 1960's as the Stanford Watershed Model. In the 1970's, water-quality processes were added. Development of a FORTRAN version incorporating several related models using software engineering design and development concepts was built by the Athens, Ga., Research Lab of EPA in the late 1970's. In the 1980's, preprocessing and post-processing software, algorithm enhancements, and the use of the USGS WDM system were developed jointly by the USGS and EPA.

The HSPF is a mathematical model developed under EPA sponsorship for use on digital computers to simulate hydrologic and water quality processes in natural and man-made water systems. It is an analytical tool which has application in the planning, design, and operation of water resources systems. The model enables the use of probabilistic analysis in the fields of hydrology and water quality management. HSPF uses such information as the time history of rainfall, temperature, evaporation, and parameters related to land use patterns, soil

characteristics, and agricultural practices to simulate the processes that occur in a watershed. The initial result of an HSPF simulation is a time history of the quantity and quality of water transported over the land surface and through various soil zones down to the groundwater aquifers. Runoff flow rate, sediment loads, nutrients, pesticides, toxic chemicals, and other quality constituent concentrations can be predicted. The model uses these results and stream channel information to simulate in stream processes. From this HSPF produces a time history of water quantity and quality at any point in the watershed.

HSPF is an extension and improvement of three previously developed models: 1) The EPA Agricultural Runoff Management Model (ARM), 2) The EPA Nonpoint Source Runoff Model (NPS), and 3) The Hydrologic Simulation Program (HSP, including HSP Quality), a privately-developed proprietary program. EPA recognized that the continuous simulation approach contained in these models would be valuable in solving many complex water resource problems. Thus, a fairly large investment was devoted to developing a highly flexible non-proprietary FORTRAN program which contains the capabilities of these three models, plus many extensions.

HSPF simulates for extended periods of time the hydrologic water quality, processes on pervious and impervious land surfaces and in streams and well-mixed impoundments.

HSPF is a valuable tool to water resource planners. Because it is more comprehensive than most systems, it permits effective planning. User's benefits include:

- Flexibility in solving a wide range of water quantity and quality problems using a single model
- Convenient data management features that save time and money
- Modular program structure which facilitates program changes and additions for special applications

HSPF is currently the most comprehensive and flexible model of watershed hydrology and water quality available. It is the only available model that can simulate the continuous, dynamic event or steady-state behavior of both hydrologic/hydraulic and water quality processes in a

watershed. The model is also unusual in its ability to represent the hydrologic regimes of a wide variety of streams and rivers with reasonable accuracy. Thus, the potential applications and uses of the model are comparatively large including:

- Flood control planning and operations
- Hydropower studies
- River basin and watershed planning
- Storm drainage analyses
- Water quality planning and management
- Point and non-point source pollution analyses
- Soil erosion and sediment transport studies
- Evaluation of urban and agricultural best management practices
- Fate, transport, exposure assessment, and control of pesticides, nutrients, and toxic substances
- Time-series data storage, analysis, and display

There have been hundreds of applications of HSPF all over the world. The largest application is the 62,000 square mile tributary area to the Chesapeake Bay. The smallest application has been experimental plots of a few acres near Watkinsville, Ga. The most significant applications within the USGS have been in the Seattle area, Chicago area, Patuxent River, Md., Truckee-Carson Basins, Nev., and watersheds in Pennsylvania.

III.1.1. Data requirements

Meteorological records of precipitation and estimates of potential evapotranspiration are required for watershed simulation. Air temperature, dew point temperature, wind, and solar radiation are required for snowmelt. Air temperature, wind, solar radiation, humidity, cloud cover, tillage practices, point sources, and (or) pesticide applications may be required for water-quality simulation. Physical measurements and related parameters are required to describe the land area, channels, and reservoirs. (USGS.gov)

III.2. GeoWEPP details

The model has been parameterized for a large number of soils across the U.S. and model performance has been assessed under a wide variety of land-use and management conditions. In addition, WEPP can generate long-term daily climatic data with CLIGEN, an auxiliary stochastic climate generator. The CLIGEN database contains weather statistics from more than 2,600 weather stations in the United States. The WEPP climate database is supplemented by the PRISM (Parameter-elevation Regressions on Independent Slopes Model) database, which further refines the climatic data based on longitude, latitude, and elevation. WEPP can provide daily runoff, subsurface flow, and sediment output categorized into five particle-size classes: primary clay, primary silt, small aggregates, large aggregates, and primary sand, allowing calculation of selective sediment transport, and enrichment of the fine sediment sizes.

Data input required are the National Elevation Dataset 30 Meters (DEM), the National Land Cover Dataset by State (Landcov), and the Soil Survey Geographic (SURGO 2.1) DB (Soilsmap)

Enhanced Digital Raster Graphics 1:24,000 (Topo Images).

The Geo-spatial interface for the WEPP model (GeoWEPP) ArcX 2004.3 uses the Geographic Information System (GIS) ArcView software and its Spatial Analyst Extension - both developed by the Environmental Systems Research Institute (ESRI) - as a platform to apply the erosion prediction model (WEPP) and the Windows interface (WEPPWIN) with geospatial datasets for topography, land use and soils.

The interface accesses databases, organizes WEPP simulations, creates all necessary input files for WEPP including the climate files. The current version of GeoWEPP allows delineation of larger watersheds beyond the recommended watershed size for WEPP watershed simulations (<500 hectare). Note that only the dominant land use and soil is delineated for each representative hillslope of a contributing area (subcatchment) to a channel.

The U.S. Forest Service has developed a suite of internet interfaces, the Forest Service WEPP (FS WEPP) interfaces, for easier applications by stakeholders in forest and rangeland management

(forest engineers, rangeland scientists, federal and state regulatory personnel) and the general public^[20]. The interfaces can be readily accessed and run through the internet (<http://forest.moscowfsl.wsu.edu/fswpepp/>), and do not require any in-depth understanding of the hydrology, hydraulic and erosion principles embedded in the WEPP model. The FS WEPP interfaces include:

- Cross Drain - to predict sediment yield from a road segment across a buffer
- Rock:Clime - to create and download a modified WEPP climate file
- WEPP:Road - to predict erosion from a forest road segment
- WEPP:Road Batch - to predict erosion from multiple forest road segments
- Disturbed WEPP - to predict erosion from rangeland and forest disturbances (wildfire, harvest operations)
- Tahoe Basin Sediment Model (under construction) - to predict runoff and erosion for the Lake Tahoe Basin
- WEPP FuME (Fuel Management) - to predict erosion from fuel management practices
- ERMiT (Erosion Risk Management Tool) - to predict the probability of sediment delivery with various mitigation treatments in each of five years following wildfire.

III.3. SWAT (Soil and Water Assessment Tool) details

SWAT is the acronym for Soil and Water Assessment Tool, a river basin or watershed model developed by Dr Jeff Arnold for the USDA Agricultural Research Service (ARS). SWAT was developed to predict the impact of land management practices on water, sediment and agricultural chemical yields in large complex watersheds with varying soils, land use and management conditions over long period of time. (USDA-ARS, 1995).

SWAT, a physically based model, requires specific information about topography, vegetation and land management practices occurring in the watershed. The physical processes associated with water movement, sediment movement, crop growth are directly modeled by SWAT. SWAT is a continuous time model, a long-term yield model. The model is not designed to simulate detailed, single-event flood routing.

SWAT incorporates features of several ARS models and is a direct outgrowth of the SWRRB model (Simulator for Water Resources in Rural Basins- Willams et al., 1985; Arnold et al., 1990). Specific models that contributed significantly to the development of SWAT were CREAMS (1980), GLEAMS (Leonard et al., 1987) and EPIC (Williams et al., 1984).

Since SWAT was created in the early 1990s, it was continuously reviewed with more expansion of capabilities such as multiple hydrologic response units incorporated (SWAT94.2), canopy storage of water integrated, the Penman-Monteith potential evapotranspiration equation and the waterflow in the soil based on kinematic storage model assimilated (SWAT96.2); the tile flow drainage added as management option and model modified for use in Southern Hemisphere (SWAT98.1); the infiltration, the daily solar radiation, the relative humidity parameter parameters added, the wind speed to be read in or calculated, potential ET methods calculated and reviewed, the modified dormancy calculations for proper simulation in tropical areas (SWAT2000); weather forecast scenarios added, sub-daily precipitation generator added (SWAT2009).

In addition to the changes listed above, interfaces for the model have been developed in Windows (Visual Basic), GRASS and ArcView.

SWAT allows a number of different physical processes to be simulated in a watershed. For modeling purposes, a watershed may be partitioned into a number of sub-watersheds or sub-basins. The use of the sub-basins in a simulation is particularly beneficial when different areas of the watershed are dominated by land uses or soil dissimilar enough in properties to impact hydrology. By partitioning the watershed into sub-basins, it is able to refer to different areas of the watershed to one another spatially.

Water balance is the driving force behind everything that happens in the watershed. To predict the movement of sediments or nutrients accurately, the hydrologic cycle as simulated by the model must conform to what is happening in the watershed. Simulation of the watershed's hydrology can be separated into two major divisions. The first division is the land phase of the hydrologic cycle. The land phase of the hydrologic cycle controls the amount of water, sediment, nutrient and pesticide loadings to the main channel in each sub-basin. The second

division is the water or routing phase of the hydrologic cycle which can be defined as the water movement, the sediments through the channel network of the watershed to the outlet.

The hydrologic cycle as simulated by SWAT is based on the water balance equation:

$$SW_t = SW_0 + \sum_{i=1}^t (R_{day} - Q_{surf} - E_a - W_{weep} - Q_{gw}) \quad (4)$$

SW_t : final soil water content [mm H₂O]

SW_0 : initial soil water content on day i [mm H₂O]

t : time [days]

R_{day} : the amount of precipitation on day i [mm H₂O]

E_a : amount of evapotranspiration on day i [mm H₂O]

W_{seep} : the amount of water entering the vadose zone from the soil profile on day i [mm H₂O]

Q_{gw} : amount of return flow on day i [mm H₂O]

The subdivision of the watershed enables the model to reflect differences in evapotranspiration for various crops and soils. Runoff is separated for each HRU and routed to obtain the total runoff for the watershed. This increases accuracy and gives a much better physical description of the water balance.

The climate of the watershed provides the moisture and energy inputs that control the water balance and determine the relative importance of the different components of the hydrologic cycle. The climatic variables required by SWAT consist of daily precipitation, maximum/minimum air temperature, solar radiation, wind speed and relative humidity. The model allows values for daily precipitation, maximum/minimum air temperatures, solar radiation, wind speed and relative humidity to be input from records of observed data or generated during the simulation.

As precipitation descends, it may be intercepted and held in the vegetation canopy or fall to the soil surface. Water on the soil surface infiltrates into the soil profile or flow overland as runoff. Runoff moves relatively quickly toward a stream channel and contributes to short term stream

response. Infiltrated water may be held in the soil and later evapotranspired or it may slowly make its way to the surface-water system via underground paths.

Erosion and sediment yield are estimated for each HRU with the (MUSLE) (Williams, 1975). While the USLE uses rainfall as an indicator of erosive energy, MUSLE uses amount of runoff to simulate erosion and sediment yield. The substitution results in a number of benefits: the prediction accuracy of the model is increased, the need for a delivery ratio is eliminated, and single storm estimates of sediment yields can be calculated. The hydrology model supplies estimates of runoff volume and peak runoff rate which, with the sub-catchment area, are used to calculate the runoff erosive energy variable. The crop management factor is recalculated every day that runoff occurs. It is a function of above-ground biomass, residue on the soil surface, and the minimum C factor for the plant. Other factors of the erosion equation are evaluated as described by Wischmeier and Smith (1978).

IV. Appendix E:

IV.1. Soil's characteristics

The soil type used in the GeoWEPP model is required to provide the geotechnical information about the laterite soil's characteristics. For the study, the following parameters have been used; some of them have been calculated by the model itself.

Table 25. Wash load calculations from the full year hydrograph

Parameter	1 st case	2 nd case	3 rd case
Albedo	0.3	0.3	0,3
Initial saturation level	50%	40%	35%
Interrill erodibility	Have model calculated		
Rill erodibility	Have model calculated		
Critical shear stress	Have model calculated		
Hydraulic conductivity	Have model calculated		

IV.2. Cross- section pictures

Each cross section has been compared to the cross section from Chaudhry, 2008 in the way to estimate the n Manning. Values for n = 0.049, 0.050 and 0.070 are presented from Chaudhry, 2008.

n = 0.049: with banks composed of gravel, with trees and brushes and steep banks.



Fig 56. From Chaudhry, 2008 Fig 57. From the 1st field site

n = 0.050: creek with angular boulders.



Fig 58. From Chaudhry, 2008



Fig 59. From the 3rd field site

$n = 0.070$: with a fine sand and silt bottom, with irregular banks with heavy grow of grass, shrubs and trees.



Fig 60. From Chaudhry



Fig 61. From the 2nd field site

V. Appendix F

V.1. Sedimentation of the first field site

Table 26. Wash load calculations from the full year hydrograph

Date	1	2	3	4	5	6	7	8	9	10	11	12	13	14	15	16
janv.-12	33463	42473	25740	24453	23166	23166	21878	21878	21878	19562			19304	19304	19304	20591
févr.-12		20591	19562	19562	19562	19562	20591	33463	20591	19562			20720	19304		20591
mars-12	19304	302476	258713	217524	20591	19562	19562	19304	19562	19562	20591	19562		36037	38611	
avr.-12	20591	30888	42473	19304	25740	19562	29601	19304	19562	19562	19562	37324	37324	36037	36037	36037
mai-12	21878	28314	28314	37324	19304	37324	18017	37324	20591	36037	20591	19304	19304	18017		
juin-12	19562	19562		14413	18017	19304	19304	19304	23166	18017		20591	19304	19304	19304	19562
juil.-12	19304	19304	37324	21878		18017	18017	19562	18017	205940	37324	37324	19562	21878	18017	14156
août-12	23166	19562	23166	25740	24453		19562	25740	20591	20591	20591	20591	19304	19304	37324	42473
sept.-12	20591	19562	19562	19304	21878	20591	37324	19304	25740	21878	19562	19562	20591	21878	19562	36037
oct.-12	20591	19304	21878	21878	19304	19562									14413	19562
nov.-12	19562	20591	21878	37324	19562	24453	19562	19304	20591	20591	18017	19304	19304	19562	19562	19304
déc.-12	19562		128711	18017	19562	19562	19304	19562	19562	19304	19304	37324	37324	18017	20591	19562

Date	17	18	19	20	21	22	23	24	25	26	27	28	29	30	31	Total for 30 mins/months
janv.-12	18017	18017	19304	19304	42473	19304	146731			19562	77226	25740	25740	25740		38079143.12
févr.-12	19562		16730	37324	36037	19304	33463	140296	128711	128711	27027	351387	459507			79282462.81
mars-12		19562	19562			205940	19304	36037	30888	30888	30888	36037	19304	19304	36037	73666100.43
avr.-12	18017	19304	21878	18017	18017	33463	19304	29601	25740	21878	18017	24453	21878	29601		36867606.68
mai-12	18017		19304	19562	128711	19562	18017			23166	23166	23166	23166	23166	23166	34742865.87
juin-12	19304	36037	24453	24453	24453	20591	19304		19304	19304	23166	19562	19304	19562		26760365.80
juil.-12	19562	19562	19562	19304	25740	21878	20591	23166	19562	19304	21878	19304	19304	19562	19304	39993822.03

août-12	23166	25740	20591	102968	37324	18017	36037	19562	21878		19304	19304	19304	19562	19562	36694762.37
sept.-12	19304	37324	20591	14413	19304	20591	19304	19562	19304	19562	20591	19304	19304	19304		31233005.11
oct.-12	19304	19562	19304	19304	20591	19304	19562		19562	19562	42473	19304		19562	19304	20793023.54
nov.-12	19304	19562	19304	18017	20591	20591	20591	21878	23166	14413	21878	19304	36037	19304		30355687.76
déc.-12	18017	218811	19304	19304	18017	19304		19562	19562		19562	23166	19304	18017	37324	43416891.03
																36,891,430,240.32

V.2. Sedimentation of the second field site

Table 27. Wash load calculations from the full year hydrograph

Date	1	2	3	4	5	6	7	8	9	10	11	12	13	14	15	16
janv.-12	17400	16139	9783	9294	8805	8805	8316	8316	8316	7436	4697	4697	7338	7338	7338	7827
févr.-12	6521	7827	7436	7436	7436	7436	7827	12716	7827	7436	4697	5217	8769	14437	11735	11735
mars-12	120016	117314	98284	82637	56568	10771	10771	10735	10771	10771	10915	10771	8033	13694	14672	9268
avr.-12	7827	11738	16139	7338	9783	10771	11249	10735	10771	10771	10771	14183	14183	13694	13694	13694
mai-12	10887	11787	11787	13048	10526	14183	11481	14183	11841	13694	7827	7338	7338	6849	4327	4327
juin-12	10562	7436	4697	5480	6849	7338	7338	7338	8805	6849	4945	7827	7338	7338	7338	7436
juil.-12	10526	7338	14183	12022	8959	6849	6849	7436	6849	56052	14183	14183	7436	8316	6849	5382
août-12	11067	5217	8805	9783	9294	5871	5871	5871	5871	5871	5871	5871	5871	5871	14183	8805
sept.-12	10706	5217	5217	5217	5217	5217	5217	7338	5871	5871	5871	5871	5871	5871	5871	5871
oct.-12	7827	7338	8316	8316	7338	7436	5217	7824	7824	7824	7824	7824	7824	6521	7827	7827
nov.-12	7436	7827	8316	14183	7436	8120	7436	7338	7827	7827	6849	10526	10526	10562	10562	10526
déc.-12	7436	30885	48899	6849	7436	7436	7338	7436	7436	7338	7338	14183	14183	6849	7827	7436
Date	17	18	19	20	21	22	23	24	25	26	27	28	29	30	31	Total for 30 mins/months
janv.-12	6849	6849	7338	7338	16139	7338	55744	26073	4697	7436	29341	9783	9783	9783	6180	352512

févr.-12	11735	11735	11735	11735	11735	11352	12716	53300	56954	88093	114162	133488	11735			676965
mars-12	9268	7436	7436	4697	4697	58659	7338	13694	11738	11738	11738	13694	7338	7338	13694	786495
avr.-12	6849	7338	8316	6849	6849	12716	7338	11249	9783	8316	6849	9294	8316	11249		308655
mai-12	6849	4636	7338	7436	48899	7436	6849	5562	5562	5562	5562	5562	5562	5562	5562	295363
juin-12	7338	13694	9294	9294	9294	7827	7338	4636	7338	7338	8805	7436	7338	7436		229318
juil.-12	7436	7436	7436	7338	9783	8316	7827	8805	7436	7338	8316	7338	7338	7436	7338	310324
août-12	8805	9783	7827	7827	14183	11481	7827	7827	7827	8650	7338	7338	7338	7436	7436	248913
sept.-12	7338	7338	7827	5480	7338	7338	7338	7338	7338	7338	7338	7338	7338	7338		197680
oct.-12	7827	7827	7827	7827	7827	7827	7827	7827	7827	7827	7827	7827	7827	7436	7338	237429
nov.-12	10526	10562	10526	6849	7827	7827	7827	8316	8805	5480	8316	7338	7338	7338		258175
déc.-12	54664	85088	7338	7338	6849	7338	4636	7436	7436	4697	7436	8805	7338	6849	14183	433731
																15,608,021,660

V.3. Sedimentation of the third field site

Table 28. Wash load calculations from the full year hydrograph

Date	1	2	3	4	5	6	7	8	9	10	11	12	13	14	15	16
janv.-12	14701	18659	11308	10743	10177	10177	9612	9612	9612	8594	8594	8594	8481	8481	8481	9046
févr.-12	11932	9046	8594	8594	8594	8594	9046	14701	9046	8594	8594	9546	9546	10739	10739	10739
mars-12					14701	14701	14701	14701	14701	14701	14701	14701	14701	15832	16963	16963
avr.-12	9046	13570	18659	8481	9546	9546	13004	11932	11932	14701	14701	16397	16397	15832	15832	15832
mai-12	14319	14319	14319	14319	14319	16397	16397	16397	16397	15832	9046	8481	8481	7915	7915	7915
juin-12	8594	8594	8594	6332	7915	8481	8481	8481	10177	7915	9046	9046	8481	8481	8481	8594
juil.-12	8594	8481	8481	6219	6219	6219	6219	6219	6219	6219	6219	6219	6219	6219	6219	6219
août-12	14319	8594	10177	11308	10743	10743	8594	8594	8594	9046	9046	9046	8481	8481	8481	8481
sept.-12	14319	14319	14319	14319	14319	14319	14319	8481	11308	9612	8594	8594	13126	13126	8481	8481

oct.-12	9046	8481	9612	9612	8481	8594	21479	14319	14319	14319	14319	14319	14319	11932	11932	14319
nov.-12	8594	9046	9612	16397	8594	8594	8594	8481	9046	9046	7915	7915	14319	14319	14319	14319
déc.-12	8594	56544	56544	7915	8594	8594	8481	8594	8594	8481	8481	16397	16397	7915	9046	8594

Date	17	18	19	20	21	22	23	24	25	26	27	28	29	30	31	Total for 30 mins/months	
janv.-12	7915	7915	8481	8481	18659	8481			8594	8594	33926	11308	11308	11308	11308	321150.48	
févr.-12	21479	21479	21479	16397	15832	15832	14701									283844.05	
mars-12	16963	8594	8594	8594	8594	8594	8481	15832	13570	13570	13570	15832	8481	8481	8481	348293.52	
avr.-12	7915	8481	9612	7915	7915	7915	8481	8481	11308	9612	7915	10743	9612	13004		344318.85	
mai-12	7915	8481	8481	8594	8594	8594	7915	10177	10177	10177	10177	10177	10177	10177	10177	342763.08	
juin-12	8481	8481	10743	10743	10743	9046	8481	8481	8481	8481	10177	8594	8481	8594		263700.30	
juil.-12	6219	6219	6219	6219	11308	9612	9046	10177	8594	8481	9612	8481	8481	8594	8481	232147.58	
août-12	10177	11308	9046	9046	16397	16397	15832	15832	15832	15832	8481	8481	8481	8594	8594	331058.33	
sept.-12	8481	8481	9046	6332	8481	13126	13126	13126	13126	13126	13126	13126	13126	13126		348989.68	
oct.-12	14319	14319	14319	14319	14319	14319	14319	14319	14319	14319	14319	14319	14319	14319	8594	8481	402627.38
nov.-12	14319	14319	14319	7915	9046	9046	9046	9612	10177	6332	9612	8481	15832	8481		315650.71	
déc.-12	95465	96125	8481	8481	7915	8481	8481	8594	8594	8594	8594	10177	8481	7915	16397	558542.22	
																14,735,110,265	

